Uropathogenic *Escherichia coli* cause resistance to apoptotic cell death of infected cells by epigenetically suppressing BIM expression

Inaugural Dissertation

submitted to the

Faculty of Medicine

in partial fulfillment of requirements

for the PhD-Degree

of the Faculty of Medicine

of the Justus Liebig University Giessen

by

Zhengguo Zhang

from

Chongqing, China.

Giessen 2015

From the Department of Anatomy and Cell Biology
Director/Chairman: Prof. Dr. Andreas Meinhardt
Faculty of Medicine
Justus-Liebig-University of Giessen, Germany.

First Supervisor and Committee Member: Prof. Andreas Meinhardt

Second Supervisor and Committee Member: Prof. Martin Bergmann

Committee Members: Prof. Friedemann Weber

Prof. Artur Mayerhofer

Date of Doctoral Defense: 21-12-2015

CONTENTS

ABBREVIATIONS

APS	Ammonium persulfate
bp	Base pair
BSA	Bovine serum albumin
°C	Degree Celsius
cDNA	Complementary DNA
DAPI	4', 6'-diamino-2-phenylindole,
DNA	Deoxyribonucleic acid
DNase	Deoxyribonuclease
dNTPs	2'-deoxynucleoside-5'-triphosphate
DTT	Dithiothreitol
E. coli	*Escherichia coli*
et al	And others
EDTA	Ethylene diamine tetraacetic acid
FADD	Fas-associated death domain
FCS	Fetal calf serum
FOXO	Forkhead box O
HRP	Horseradish peroxidase
IL-6	Interleukin 6
JNK	c-Jun N-terminal kinase
kb	Kilo base pair
kD	Kilo Dalton
LPS	Lipopolysaccharide
M	Molar
MAPK	Mitogen activated protein kinase
mg	Milligram
min	Minute
ml	Milliliter
mM	Milimolar
MOI	Multiplicity of infection
MW	Molecular weight
NaCl	Sodium chloride
NGS	Normal goat serum
NF-κB	Nuclear factor-κB
NP-40	Nonidet P-40
OD	Optical density
PAGE	Polyacrylamide gel electrophoresis
PAMP	Pathogen associated molecular pattern
PBS	Phosphate buffered saline
PCR	Polymerase chain reaction
PMSF	Phenylmethylsulfonyl fluoride

PRR	Pattern recognition receptor
RIP	Receptor interacting protein
RNA	Ribonucleic acid
RNase	Ribonuclease
rpm	Revolutions per minute
RT	Room temperature
SDS	Sodiumdodecylsulphate
sec	Second
TAE	Tris acetate EDTA
TGFβ	Transforming growth factor β
TLR	Toll like receptor
TNFα	Tumor necrosis factor alpha
Tris	Tris(hydroxymethyl) amino methane
U	Unit
UPEC	Uropathogenic *E. coli*
UV	Ultraviolet
V	Volt
v/v	Volume per volume
w/v	Weight per volume
wt	wild type
µ	Micro
µg	Microgram
µl	Microliter
µM	Micromolar

1 INTRODUCTION

1.1 Epidemiology and etiology of male infertility

According to WHO definition, infertility is the inability of a sexually active, non-contracepting couple to achieve spontaneous pregnancy in 1 year (WHO, 2000). About 15% of couples cannot achieve pregnancy within 1 year and seek medical treatment. In approximately 50% of these couples, a male infertility-associated factor was found together with abnormal semen parameters. Idiopathic infertility remains the most common diagnostic category of male infertility. The known causes of male infertility include varicocele, male genital tract infection, genetic causes such as chromosomal aberrations and Y chromosome deletions, endocrine disease, as well as post-testicular disorders such as obstruction (Bhushan et al., 2009a).

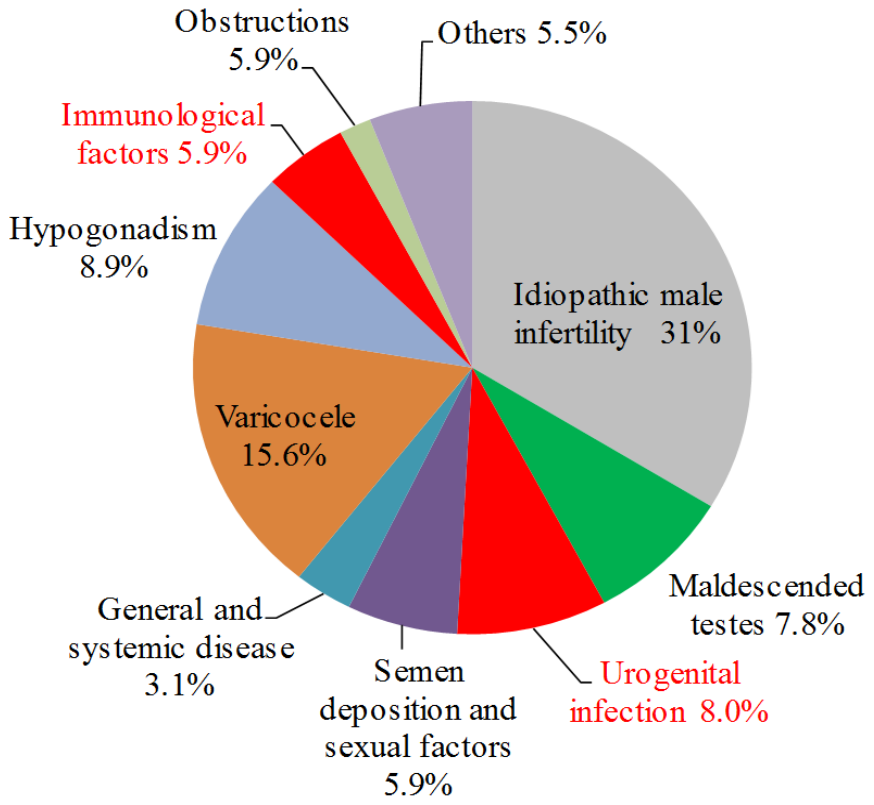

Figure 1: Male infertility-associated factors and percentage of distribution (Jungwirth et al., 2012).

Figure 1 summarizes the etiology and percentage of distribution of male infertility. Urogenital infection and immunological factors account for 13% to 15% of all cases of male infertility (Jungwirth et al., 2012). The percentage may be still underestimated as idiopathic infertility may include part of these cases.

1.1.1 Infection and inflammation associated male infertility

Infection and inflammation of the male reproductive tract are common and also potentially correctable causes of male infertility (Organization, 2000; Weidner et al., 1999). Infections of the male genital tract comprise urethritis, prostatitis, epididymitis, and epididymo-orchitis. Most of these diseases have a potential negative influence on spermatozoa at different levels of their development, maturation, transport, and function, and are thereby considered as male sub- or infertility (Bhushan et al., 2009a; Rusz et al., 2012; Weidner et al., 2013). Testicular inflammation could be induced by local or systemic infection of microorganisms, neoplastic processes (like seminoma, carcinoma in situ), chemical insults, physical factors such as trauma beside pre-existenting testicular disorders of other origin (Schuppe and Meinhardt, 2005; Schuppe et al., 2008). Testicular infection and inflammation are detrimental for spermatogenesis. Osegbe (Osegbe, 1991) has reported that bacterial gonadal infection causes persistent azoospermia or oligospermia and leads to impairment of both testes as assessed by testicular biopsy and follicle-stimulating hormone examination, even though the infection is clinically confined in one testis. This clinical observation, suggesting persistent testicular inflammation and impairment of spermatogenesis after genital infection in spite of antibiotic treatment, is further supported by animal experiments (Demir et al., 2007; Ludwig et al., 2002; Pilatz et al., 2015). The prevalence of infection and inflammation in infertile males is difficult to determine due to subacute or chronic asymptomatic inflammation of the testis, and is therefore likely to be ignored (Schuppe et al., 2008). In addition, lymphocyte infiltration of the testis was found in more than 50% in asymptomatic patients with impaired fertility

(Schuppe et al., 2008). Therefore, infection- and inflammation-induced male infertility is likely to be underestimated, and further investigations need to be performed.

1.1.2 Pathogens involved in genital tract infection

A plethora of microbes have been implicated to cause male genital tract infections, including a variety of bacteria, viruses, fungi, as well as protozoa (Keck et al., 1998; Ochsendorf, 2008). Urethritis is mainly caused by *Chlamydia trachomatis*, *Ureaplasma urealyticum,* and *Neisseria gonorrhea* (Schiefer, 1998), whilst the most common causes of bacterial prostatitis are Gram-negative bacteria, mainly strains of *Escherichia coli* (Naber and Weidner, 2000). It is a general agreement that epididymitis in men younger than 35 years is most likely caused by sexually transmitted pathogens such as *Chlamydia trachomatis* and *Neisseria gonorrhea*, while in men older than 35 years the disease is most commonly caused by enteric pathogens like *Escherichia coli*. This classification has been challenged recently by a study using state-of-the-art methods to investigate the etiology of acute epididymitis, suggesting that *Escherichia coli* is the predominant etiologic pathogen regardless of the patients' age (Pilatz et al., 2014). Orchitis is not only caused by canalicular ascending pathogens, but also may be developed as a complication of systemic, predominantly viral infections such as mumps virus, due to hematogenous dissemination of the pathogen (Hviid et al., 2008; Rubin et al., 2015). Other viruses associated with the development of orchitis consist of Coxsackie virus types, Epstein-Barr, influenza, varicella, and human immunodeficiency viruses (HIV) (Bachir and Jarvi, 2014; Schuppe et al., 2008). Uropathogenic *Escherichia coli* (UPEC) has been identified as the most frequently isolated pathogen in urinary tract infections, one of the most common bacterial infections of humans (Barber et al., 2013; Ulett et al., 2013). This pathovars also accounts for epididymitis or epididymo-orchitis (Bhushan et al., 2009a; Pilatz et al., 2014).

1.1.3 Pathogenicity of uropathogenic *Escherichia coli*

UPEC strains possess a variety of virulence factors that enable them to cause diseases, including fimbrial adhesions, toxins, iron acquisition systems, and flagella amongst others (Emody et al., 2003; Nielubowicz and Mobley, 2010). The prototype RTX pore-forming toxin α-hemolysin (HlyA), frequently encoded by strains of UPEC, has distinct effects on host cells aside from outright lysis (Dhakal and Mulvey, 2012; Wiles and Mulvey, 2013). It has been demonstrated that a sublytic concentration of HlyA can inhibit the AKT survival signaling pathway and activate the downstream transcription factor FOXO1 (Wiles et al., 2008). In addition, UPEC also utilize HlyA to attenuate immune response by inhibition of pro-inflammatory cytokine production (Hilbert et al., 2012). HlyA is associated with bacteria elicited thrombocytopenia by inducing degradation of Bcl-xL, a survival protein, in platelets (Kraemer et al., 2012). Moreover, HlyA triggers proteolysis of a number of host proteins to facilitate bacterial dissemination as well as to attenuate the host immune response (Dhakal and Mulvey, 2012). Recently, Gur *et al* showed HlyA-dependent NK cell killing is a strategy for UPEC to fight against NK cell-mediated host defense (Gur et al., 2013). Of note, HlyA also could induce inflammasome formation and pyroptosis of urothelial cells, which served as the first line of immune defense against intracellular UPEC (Nagamatsu et al., 2015). Collectively, apart from other virulence factors, HlyA is associated with various biological processes including bacterial dissemination, immune response suppression as well as inflammasome formation.

1.2 Structure and function of the male reproductive system

1.2.1 Structure and functions of the testis

The testis is comprised of two compartments, the seminiferous tubules and the

interstitium. Spermatogenesis takes place in the seminiferous epithelium where the spermatogonia undergo mitosis, followed by meiosis, ultimately divided into haploid round spermatids, and then transformed into spermatozoa. The later process termed spermiogenesis is characterized by removal of most cytoplasm of spermatid, condensation of DNA in the sperm head, tail formation, as well as the establishment of the acrosome. Apart from maturing germ cells, the seminiferous tubules also contain Sertoli cells surrounded by one or more layers of peritubular myoid cells. Sertoli cells not only play a key role in the regulation of spermatogenesis (Chen and Liu, 2015; Griswold, 1998), but also maintain immune tolerance primarily by forming the blood-testis-barrier (BTB) (Jiang et al., 2014; Kaur et al., 2014; Meinhardt and Hedger, 2011). Sertoli cells also engulf residual bodies from spermiogenesis as well as degenerated germ cells (Johnson et al., 2008). Peritubular myoid cells as smooth-muscle-cell-like cell type surrounding the seminiferous tubular are responsible for tubular contractility and transport the immotile sperm (Albrecht, 2009; Mayerhofer, 2013). The interstitial space is composed of Leydig cells, blood vessels, as well as immune cells. Leydig cells are a prominent cell type within the interstitium and produce androgens. Testosterone, the predominant androgen produced in testis, plays an important role in both spermatogenesis and the development and maintenance of male secondary sex characteristics. The immune cells in the interstitial space include macrophages, lymphocytes, mast cells, natural killer cells as well as dendritic cells, but no B cells.

1.2.2 The epididymis, vas deferens and accessory sex glands

Spermatozoa released from seminiferous tubules reach the epididymis via the rete testis and a series of efferent ducts. Sperm maturation takes place in the epididymis, which is a long single highly coiled tubule (Eddy et al., 1985; Hinton and Palladino, 1995). Sperm are stored prior to ejaculation in the cauda region of the epididymis. During ejaculation the sperm pass through the vas deferens, a muscularized duct, and

the urethra into the female reproductive tract. A genetic disease named congenital bilateral absence of the vas deference (CBAVD) is associated with male infertility due to the lack of both vas deferens and epididymis (Bombieri et al., 2011; Chan et al., 2009). CBAVD as a genital phenotype of cystic fibrosis (CF) is caused by cystic fibrosis transmembrane conductance regulator (CFTR) gene mutations (Claustres, 2005; Yu et al., 2012). In humans, the accessory sex glands include seminal vesicles, the prostate and bulbourethral glands. However, disparity is observed among different species. In cats and dogs, the seminal vesicles are not present, whereas rodents have well-developed seminal vesicles, coagulating glands, and prostate glands. Approximately 90% of semen originate from the accessory glands, the seminal vesicles in particular.

1.3 Testicular immunology

During spermatogenesis, a plethora of autoantigens are expressed, which are tolerated by the testis. Hence, testes function as immune privileged organ to protect developing germ cells from a systemic autoimmune attack. The characteristic immune privilege of the testis is further supported by transplantation studies, in which histoincompatible allo- and xenografts transplanted into the interstitial space of the rat testis survived and prospered for indefinite periods of time (Bobzien et al., 1983; Head and Billingham, 1985; Head et al., 1983; Setchell, 1990). The BTB plays an important role in testicular immune tolerance by limiting the entry of leukocytes or immunoglobulins into the luminal compartment, thus preventing the contact between immune cells with auto-antigens. The BTB is formed by neighboring Sertoli cells via tight junctions (TJ), basal ectoplasmic specializations, gap and desmosome-like junctions, which divide the seminiferous tubule into a basal and apical (adluminal) compartment (Arck et al., 2014; Jiang et al., 2014). Other than the formation of the BTB, Sertoli cells also have inherent immune suppressive properties (Doyle et al., 2012; Kaur et al., 2014). Numerous studies have shown that Sertoli cells protect co-

transplanted grafts, such as adrenal glands, neurons, heart and pancreatic islets (xeno- or allo-transplantation) (Korbutt et al., 1997; Lim et al., 2009; Mital et al., 2010; Sanberg et al., 1996; Selawry and Cameron, 1993). As transplants are placed into the individual space, this protection cannot be attribute to the existence of a physical barrier (BTB) between neighboring Sertoli cells, but is mediated by Sertoli cell-secreted factors, including anti-inflammatory proteins such as TGFβ, activin, complement, and proteinase inhibitors as well as indolamin-2,3-dioxygenase (IDO) (Fallarino et al., 2009; Lee et al., 2007; O'Bryan et al., 2005; Sipione et al., 2006; Suarez-Pinzon et al., 2000). In addition, Sertoli cells also influence B and T cell-mediated cellular immune responses (Dal Secco et al., 2008; Mital et al., 2011).

Although the testis is an immune privileged organ, it is still able to initiate an effective immune response or inflammatory reaction against bacteria or viral infection. Sertoli cells and testicular macrophages express Toll-like receptors (TLRs), which play an important role in activation of NF-κB or mitogen activated protein kinases (MAPKs) signaling pathways to mount a proinflammatory response (Bhushan et al., 2009b; Bhushan et al., 2008; Riccioli et al., 2006). Macrophages and NK cells in the testis are also involved in the innate immune response against bacterial or viral infection. In conclusion, the testis needs to maintain a delicate balance between suppression of the immune response to protect germ cells from auto-immune attack and the ability to mount an immune response against invading pathogens.

1.4 Cell death pathways and immune response

The immune system responds to infection using various pathways, ranging from activation of pathways promoting survival to those eliciting cell death. The cell death pathways can be categorized into two classes i.e. regulated cell death (RCD) as well as accidental cell death (ACD) (Galluzzi et al., 2015). ACD is triggered by a variety of stimuli such as trauma, shearing, and potent detergent. ACD does not involve a

specific molecular machinery, and therefore cannot be prevented or modulated, revealing the structural disassembly of cells exposed to extremely harsh physicochemical conditions. On the contrary, the RCD involves a genetically encoded molecular machinery, and can be prevented or altered by the means of pharmacologic or/and genetic interventions targeting the key components of the machinery (Galluzzi et al., 2015). Caspases are a family of endoproteases, which play an essential role in the regulated cell death pathway (McIlwain et al., 2013). Therefore, regulated cell death pathways can be further categorized as caspase-dependent including apoptosis and pyroptosis or caspase-independent pathways such as necroptosis, mitochondria permeability transition-mediated regulated necrosis (MPT-RN), parthanatos, ferroptosis as well as NET release-associated cell death (NETosis) (Figure 2). Each pathway leads to different consequences (Galluzzi et al., 2015).

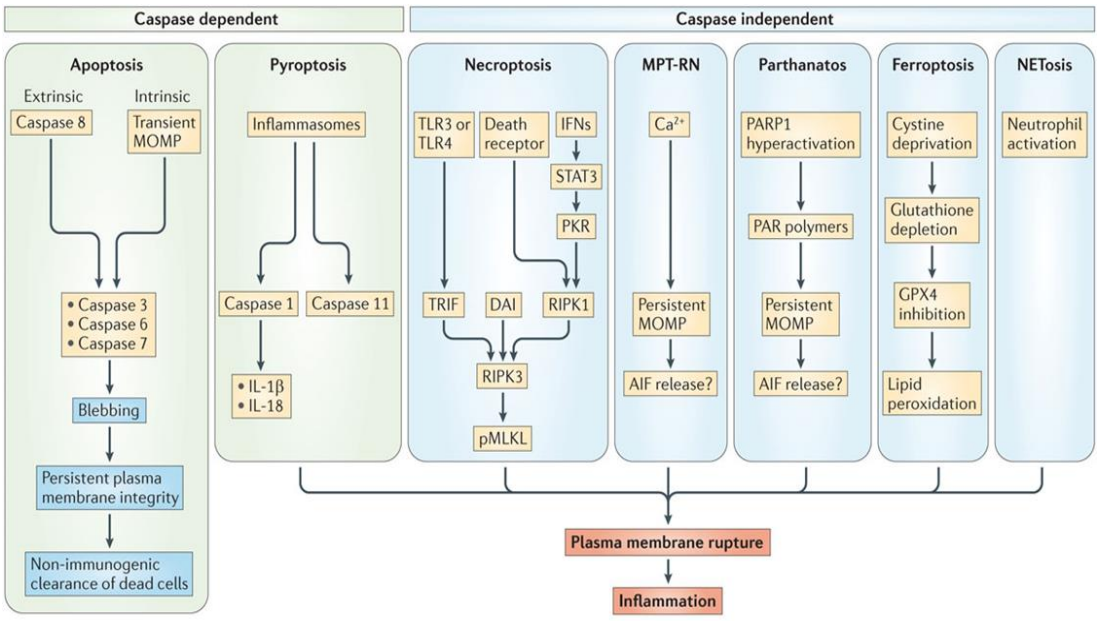

Figure 2: Signaling pathways of regulated cell death(Linkermann et al., 2014).

1.4.1 Apoptosis

The term apoptosis is derived from the ancient Greek word meaning “falling off”, and was coined by the Australian pathologist Kerr and colleagues in 1972 (Kerr et al.,

1972). The morphological characteristics of apoptosis have been well established as cytoplasmic shrinkage, chromatin condensation initiating at the nuclear membrane (marginalization), which is then extending to the entire nucleus (pyknosis), followed by nuclear fragmentation (karyorrhexis). Moreover, little or no ultrastructural modifications of cytoplasmic organelles are seen, yet, plasma membrane blebbing (without losing its integrity until the final stages of the process), and cell membrane-enclosed cell fragment formation (apoptotic bodies) are evident. The apoptotic cells are further engulfed by resident phagocytes *in vivo* (Kroemer et al., 2009). Apoptosis could be initiated by intrinsic and extrinsic stimuli (Favaloro et al., 2012), which are further illustrated in Figure 3.

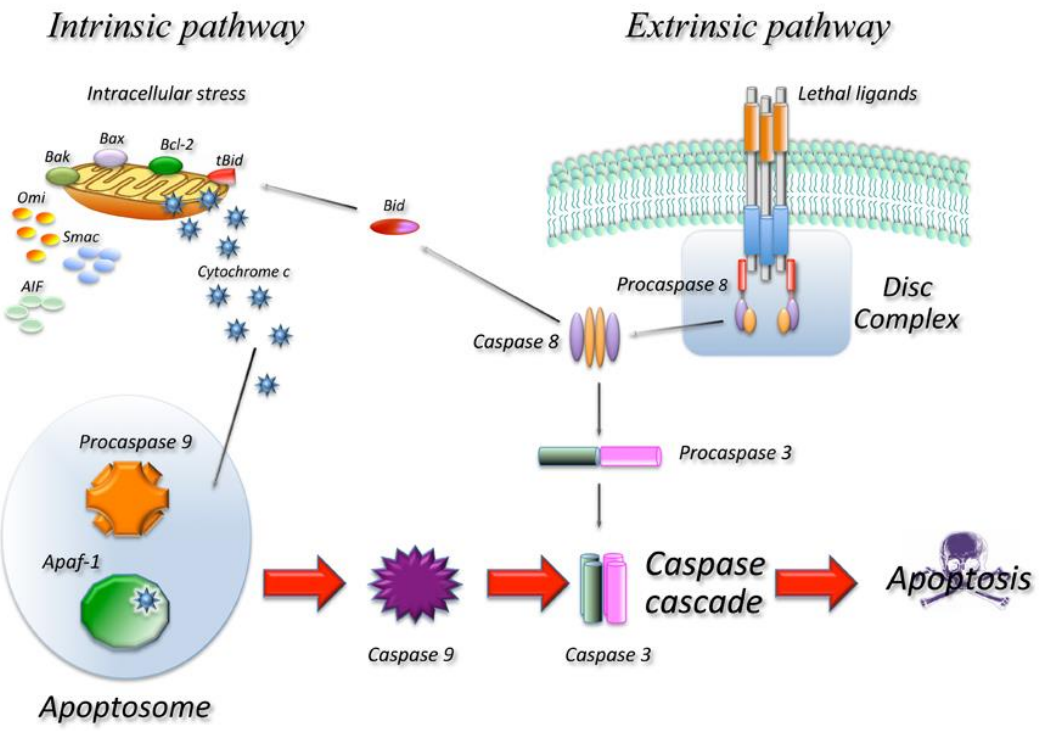

Figure 3: Schematic representation of the extrinsic and intrinsic pathways leading to apoptosis (Favaloro et al., 2012).

1.4.1.1 Intrinsic apoptotic pathway

A variety of intracellular stresses such as oxidative stress, DNA damage, and

endoplasmic reticulum (ER) stress, can trigger intrinsic apoptotic cell demise. All these stresses converge at the mitochondria to induce mitochondria outer membrane permeabilization (MOMP), which further triggers the caspase activation cascade to cause apoptosis (Tait and Green, 2012). MOMP is stringently controlled by the B cell lymphoma-2 (BCL-2) family of proteins via protein-protein interactions (Westphal et al., 2014). The BCL-2 family is comprised of three groups of proteins based on their structure and function. The executioner proteins BCL-2 antagonist killer (BAK), and BCL-2 associated X protein (BAX) oligomerize in the mitochondria and permeabilize the mitochondria outer membrane to evoke MOMP. The anti-apoptotic members consist of BCL-2, BCL-w, BCL-XL, myeloid cell leukemia 1 (MCL-1) as well as BCL2 related gene A1. The BCL-2 homology (BH) 3 only proteins including BCL-2 interacting domain death agonist (BID), BCL-2 interacting mediator of cell death (BIM), p53 upregulated modulator of apoptosis (PUMA), BCL-2 antagonist of cell death (BAD), BCL-2 interacting killer (BIK), BCL-2 modifying factor (BMF), harakiri (HRK) and Noxa can directly or indirectly activate the effector BCL-2 family members (Table 1) (Shamas-Din et al., 2013; Volkmann et al., 2014; Westphal et al., 2014).

Anti-apoptotic proteins	Anti-apoptotic protein binds to		
	BAX/BAK/BID	BH3 proteins	
		Activator	Sensitizer
BCL-2	BAX, BID	BIM, PUMA	BMF, BAD
BCL-XL	BAX, BAK, BID	BIM, PUMA	BMF, BAD, BIK, HRK
BCL-w	BAX, BAK, BID	BIM, PUMA	BMF, BAD, BIK, HRK
MCL-1	BAK, BID	BIM, PUMA	Noxa, HRK
A1	BAK, BID	BIM, PUMA	Noxa, BIK, HRK

Table 1: Binding profiles within BCL-2 family members (Shamas-Din et al., 2013).

BID, BIM, and PUMA can directly activate the effector BAX, BAK to induce MOMP, whereas the sensitizers or derepressors containing BMF, BAD, BIK, HRK, Noxa, indirectly cause MOMP by disrupting the existing anti-apoptotic complex or occupying the protein binding sites in anti-apoptotic proteins (Moldoveanu et al., 2014). Moreover, it has been reported that BIM preferentially activates BAX, whilst BID preferentially activates BAK (Sarosiek et al., 2013). The release of intermembrane space proteins including cytochrome c, second mitochondria-derived activator of caspases (SMAC), as well as high temperature requirement protein A2 (HTRA2) into the cytosol, resulting from MOMP, activates the caspase cascade, ultimately causing apoptosis.

1.4.1.2 Extrinsic apoptotic pathway

Extrinsic apoptosis can be induced by the binding of lethal ligands including Fas ligand (FasL), TNFα as well as TNF-related apoptosis inducing ligand (TRAIL), to the corresponding receptors such as Fas, TNFα receptor 1 (TNFR1) and TRAIL receptor (TRAILR) 1-2(Strasser et al., 2000; Wajant, 2002). Fas aggregation responding to the FasL binding recruits receptor interacting kinase 1 (RIP1), Fas associated protein with a death domain (FADD), cellular inhibitor of apoptosis proteins (cIAPs), c-FLIPs as well as pro-caspase 8 (or caspase 10). This supramolecular complex at the inner leaflet of the plasma membrane known as death-inducing signaling complex (DISC) constitutes a platform to regulate caspase 8 or caspase 10 activation. The active caspase 8 can either catalyze and activate the downstream executor caspases (caspase 3, 6, 7) to induce apoptosis in a mitochondria-independent way or truncate BID, which in turn causes MOMP and apoptosis, acting as a link between the intrinsic and extrinsic pathways.

1.4.2 Pyroptosis

Pyroptosis was first introduced to describe *Salmonella typhimurium*-induced macrophage peculiar death by Brennan and Cookson in 2000 (Brennan and Cookson, 2000). Pyroptosis is not limited to macrophages or as a result of bacterial infection (Bergsbaken et al., 2009). Pyroptosis shares the characteristics of both apoptosis and necrosis. Similar to necrosis, pyroptosis leads to cytoplasmic swelling, plasma membrane rupture, as well as release of the intracellular contents into the extracellular space. However, nuclear condensation and internucleosomal DNA fragmentation are also observed during pyroptosis, which is similar to apoptosis but not necrosis (Bergsbaken et al., 2009). Pyroptosis can be initiated by activation of caspase 1 or caspase 11, referred to as canonical and noncanonical inflammasomes, respectively, to combat infection (Lamkanfi and Dixit, 2014). Canonical inflammasomes convert procaspase 1 into active caspase 1 to mediate the maturation and secretion of proinflammatory cytokines IL-1β and IL-18. The noncanonical inflammasomes are triggered by activated caspase 11, inducing pyroptosis and release of IL-1α. The activation of caspase 11 can be induced by acylated lipid A, a component of the *Escherichia coli* lipopolysaccharide (LPS), as well as *Salmonella typhimurium* LPS, independent of the LPS receptor TLR4 (Hagar et al., 2013; Kayagaki et al., 2013). LPS is a key virulence factor of Gram-negative bacteria. Therefore, caspase 11 activation is mainly provoked by Gram-negative bacteria (Broz et al., 2012; Case et al., 2013; Casson et al., 2013; Rathinam et al., 2012), but not by Gram-positive bacteria (Rathinam et al., 2012). Recently, it has been demonstrated that the UPEC virulence factor HlyA can trigger caspase 1- and caspase 11- (caspase 4 in human) mediated pyroptosis and release of IL-1α and IL-1β, indicating that caspase 1/caspase 4-mediated pyroptosis plays a role in host defense against intracellular UPEC (Nagamatsu et al., 2015). The molecular mechanism underlying pyroptosis is still largely unknown.

1.4.3 Necroptosis

Necrosis has been considered as accidental cell death for a long time. Until recently, increasing evidence indicates that necrosis can occur in a regulated manner, referred to as necroptosis, and has a predominant role in inflammation and infections. Necroptosis could be triggered by multiple stimuli such as alkylating DNA damage and ligation of death receptors. A plethora of key molecular components of necroptosis has been identified, including receptor interacting kinase 3 (RIPK3), receptor interacting kinase 1 (RIPK1), as well as mixed lineage kinase domain like protein (MLKL). Upon TNFα binding to its receptor, the adaptor protein, tumor necrosis factor receptor type 1-associated death domain protein (TRADD) was recruited, further leading to an interaction between RIPK1 and RIPK3 via RIP homotypic interaction motif (RHIM). The formation of RIPK1 and RIPK3 complex, called necrosome, leads to activation of these kinases. The cellular inhibitor of apoptosis protein 1 (cIAP1) and cellular inhibitor of apoptosis protein 2 (cIAP 2) negatively regulate necroptosis by inhibiting RIPK1 and RIPK3 activation (McComb et al., 2012), whereas cyclindromatosis (CYLD) promotes necroptosis via deubiquitylation of RIPK1 (O'Donnell et al., 2011). MLKL was identified as a key RIPK3 downstream protein in necroptotic pathway. The phosphorylation of MLKL by RIPK3 is critical for necroptosis (Sun et al., 2012; Zhao et al., 2012). Of note, cells derived from MLKL-deficient mice are resistant to TNF-induced necroptosis, whereas a mutant of MLKL that mimics its active form directly induces cell death even in RIPK3 deficient cells. This study strongly suggested modification of MLKL is essential for propagation of the necroptosis pathway downstream of RIPK3 (Murphy et al., 2013). However, the mechanism of necroptosis execution is still controversial.

1.4.4 The influence of cell death pathway on inflammation

Regulated cell death plays an essential role in immune responses against infections. The different death pathways have different outcomes. The cytoplasmic constituents include a variety of danger associated molecular patterns (DAMPs) such as ATP, high mobility group box 1 (HMGB1), heat shock protein (hsp) 70 as well as hsp90, which can elicit inflammation by binding to the pattern recognition receptors (PRRs) of immune cells (Linkermann et al., 2014). In general, apoptotic cell death has been considered as non- or anti-inflammatory cell death pathway (Fadok et al., 1998; Voll et al., 1997). First of all, the cellular components are packaged into plasma-membrane-bound vesicles, namely apoptotic bodies, therefore restricting DAMPs release. Secondly, phagocytes are attracted to engulf the apoptotic cells, leading to effective clearance of the apoptotic cells *in vivo*. In contrast, pyroptosis and necroptosis are pro-inflammatory death pathways (Bergsbaken et al., 2009; Pasparakis and Vandenabeele, 2015; Vanden Berghe et al., 2014). The release of DAMPs from cells undergoing pyroptosis and necroptosis can activate neighboring immune cells by binding to PRRs. Furthermore, pro-inflammatory cytokines including IL-1β, IL-33, and IL-18 secreted by cells undergoing pyroptosis or necroptosis can also trigger immune cell activation.

1.5 FOXO transcriptional factors

The forkhead box O (FOXO) transcription factors consists of FOXO1 (also known as FKHR), FOXO3 (also known as FKHRL1), FOXO4 (AFX1), and FOXO6, which are homologs of the *Caenorrhabditis elegans* transcription factor DAF-16 (abnormal dauer formation-16) and Drosophila melanogaster dFOXO (Kenyon et al., 1993; Weigel et al., 1989). FOXOs mainly act as transcription factor by binding to the conserved consensus core recognition motif TTGTTTAC to regulate specific gene

expression programs (Furuyama et al., 2000; Obsil and Obsilova, 2011). All the FOXO members share the same DNA-binding element. Therefore, they may play a redundant role in the regulation of target gene expression.

1.5.1 Functions of FOXO transcription factors

The FOXO transcription factors regulate diverse gene expression programs, which are involved in multiple important biological processes, such as apoptosis, reactive oxygen species (ROS) detoxification, cell cycle arrest, as well as metabolism (Calnan and Brunet, 2008; Eijkelenboom and Burgering, 2013).

1.5.1.1 Inducing Apoptosis

Apoptosis is a programmed death mode that includes intrinsic and extrinsic death pathways. It has been demonstrated that FOXOs induce apoptosis of hematopoietic cells deprived of growth factors by upregulation of BIM (Dijkers et al., 2000a; Essers et al., 2004). Gilley et al have found that FOXO3 directly activates the BIM promoter via two conserved FOXO binding sites to upregulate BIM expression and induce neuron apoptosis (Gilley et al., 2003). In addition to elevate BIM expression, PUMA, another BH3 only protein of the BCL2 family, is also under the control of FOXO3. FOXO-mediated PUMA upregulation is responsible for lymphoid cell apoptosis upon growth factor or cytokine withdrawal (You et al., 2006). Recently, it has been demonstrated that FOXO3 directly upregulates PUMA expression and cooperates with BIM to induce neuron death in response to toxic β-amyloid 1-42 (Akhter et al., 2014). FasL, inducing extrinsic apoptosis, is also transcriptionally regulated by FOXO3 (Brunet et al., 1999). Moreover, *TRAIL* is a FOXO-regulated gene, which can initiate extrinsic apoptosis. The TRAIL promoter contains a FOXO binding site, and overexpression of FOXO1 and FOXO3 results in TRAIL upregulation and apoptosis

in prostate cancer cells, suggesting TRAIL is a direct target of FOXO3 (Modur et al., 2002). Collectively, FOXO could induce apoptosis both in intrinsic and extrinsic pathways by increasing different sets of target gene expression.

1.5.1.2 Cell cycle arrest and DNA repair

The cell cycle comprises the interphase phase that includes the G1 (gap phase 1), S (DNA synthesis), G2 (gap phase 2), and cell division or M phases (mitosis). The phase transitions of the cell cycle are under stringent control by the cooperative activity of specific cyclin-dependent kinases (CDKs), cyclins, and CDK inhibitors (CKIs) (Malumbres and Barbacid, 2009). CKIs can be divided into two classes, i.e., the Cip/Kip family including p21Cip1, p27Kip1, and p57Kip2, and the INK4 family containing p15INK4B, p16INK4A, p18INK4C, as well as p19INK4D. The association between the Cip/Kip family or the INK4 family with CDKs prevents the progression of the cell cycle. FOXOs primarily control the G1/S phase transition by regulation of cell cycle associated gene expression. p27Kip1 could be transcriptionally activated by FOXO4 to induce G1 cell cycle arrest (Medema et al., 2000). Beside FOXO4, the activation of FOXO3 has also been shown to upregulate p27Kip1 (Dijkers et al., 2000b). In addition to upregulation of p27Kip1 expression, the expression of p21Cip1 is also increased through the activation of FOXOs and the TGF-β signaling pathway (Seoane et al., 2004). Other CKIs, the INK4 family, p15INK4B and p19INK4D are associated with FOXO-mediated G1cell cycle arrest. FOXOs can bind to promoter regions to induce transcription of p15INK4B and p19INK4D (Katayama et al., 2008). Additionally, FOXOs have also been demonstrated to impede cell cycle progression through regulating the expression of cyclin D, cyclin G, as well as the retinoblastoma protein family member p130 (Chen et al., 2006; Schmidt et al., 2002). Taken together, FOXOs are associated with G1 cell cycle arrest via regulating the expression of a set of genes involved in cell cycle progression.

DNA damage can activate the G2-M checkpoint, which triggers cell cycle arrest providing time for repair. FOXO3 directly increases Gadd45a expression via two FOXO binding sites in its promoter region. FOXO3 induces a delay in the G2-M phase in response to stress stimuli during which FOXO3 upregulate Gadd45a to repair damaged DNA (Tran et al., 2002).

1.5.1.3 Oxidative stress resistance

Reactive oxygen species (ROS), including hydrogen peroxide (H_2O_2), superoxide ($O_2^{\bullet-}$) as well as hydroxyl radicals (•OH), are normal byproducts of cell metabolism or are generated to facilitate intracellular signaling (Storz, 2011). Oxidative stress occurs within cells when ROS are generated over the capability of antioxidants, or when cells are exposed to an extracellular source of ROS. FOXOs have been shown to play an important role in ROS detoxification (Droge and Kinscherf, 2008). Superoxide dismutase 2 (SOD2) is directly upregulated by FOXO3, which is an enzyme to detoxify ROS. The protection of cells from ROS by FOXO3-mediated SOD2 upregulation antagonizes apoptosis caused by glucose deprivation (Kops et al., 2002). Catalase, which is another target gene of FOXO3, hydrolyzes hydrogen peroxide to water. It has been shown that FOXO3-mediated catalase upregulation results in an increase in both hydrogen peroxide scavenging and oxidative stress resistance (Nemoto and Finkel, 2002). Thus, FOXOs are able to detoxify ROS and thereby increase cell survival via cooperative regulation of both SOD2 and catalase.

1.5.2 Posttranslational control of FOXOs

The activity of FOXOs is dynamically regulated in response to numerous intracellular or extracellular stimuli such as cytokine stimulation, growth factor withdrawal, and oxidative stress. Due to the functional importance of FOXO

transcription factors, their activity must be tightly regulated. One of the most important strategies is post-translational modification, including phosphorylation, acetylation, ubiquitination, methylation, and glycosylation.

1.5.2.1 Phosphorylation of FOXOs

Like the homolog of the *C. elegans* transcription factor DAF-16 under the control of DAF-2, the FOXO transcription factors are also negatively regulated by the phosphatidylinositol-3-kinase (PI3K) and protein kinase B (PKB, also known as AKT) signaling pathway. AKT dependent phosphorylation of FOXOs on distinct threonine and serine residues promotes their interaction with 14-3-3 chaperone proteins and relocalization from nucleus to the cytosol as illustrated in Figure 3. The cytoplasm retention of FOXOs is dependent on 14-3-3-mediated masking of the FOXO nuclear localization signal (NLS) and reduction of their flexibility (Obsilova et al., 2005).

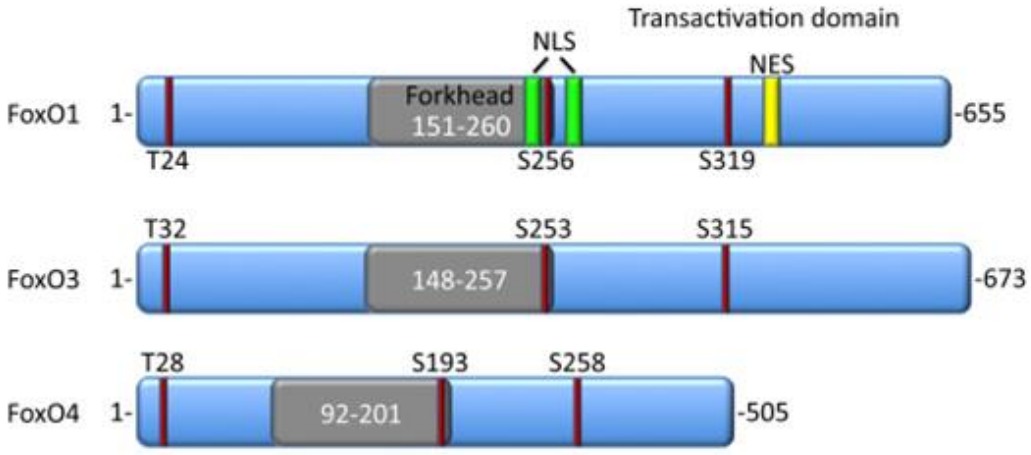

Figure 4: Conserved AKT phosphorylation sites in FOXO proteins (Tzivion et al., 2011).

FOXOs are also substrates for other kinases. In contrast to the AKT signaling pathway, JNK-mediated phosphorylation of FOXOs drive their nuclear localization. It has been reported that FOXO4 can be phosphorylated by JNK at two different sites (threonine 447 and threonine 451) under oxidative stress, which causes its nuclear localization and activation (Essers et al., 2004). ERK has been reported to

phosphorylate FOXO3 resulting in its nuclear exclusion and degradation (Yang et al., 2008). However, the AMP-activated protein kinase (AMPK) dependent phosphorylation of FOXO3 leads to its activation without influencing the subcellular localization (Greer et al., 2007).

1.5.2.2 Other posttranslational modifications of FOXOs

The FOXOs are also subject to acetylation to regulate their transcriptional activity, a process controlled by histone acetyltransferases (HATs) and histone deacetylases (HDACs). The DNA binding activity of FOXOs are decreased after acetylation by CBP/P300, whilst the deacetylation of FOXOs by Sirtuin 1 (SIRT1) increases the ability of inducing cell cycle arrest as well as resistance to oxidative stress but inhibits the ability of triggering cell death (Brunet et al., 2004; Daitoku et al., 2004; van der Heide and Smidt, 2005). Nonetheless, Wang et al reported that deacetylation of FOXO3 by SIRT1 or SIRT2 causes Skp2-mediated FOXO3 polyubiquitination and proteasomal degradation (Wang et al., 2011). Polyubiquitination of FOXOs leads to their degradation (Huang et al., 2005), whereas monoubiquitination of FOXO4 has been demonstrated to induce its nuclear translocation and increase its transcriptional activity (van der Horst et al., 2006). Moreover, FOXO1 could be methylated by the protein arginine methyltransferase 1 (PRMT1) at arginine residues within a consensus site for AKT phosphorylation, thereby blocking AKT-mediated phosphorylation of FOXO1 (Yamagata et al., 2008). Recently, it has been demonstrated that FOXO3 can be methylated by the methyltransferase Set9 at lysine 270, resulting in the inhibition of its DNA binding activity and transactivation. This lysine methylation of FOXO3 is associated with FOXO3-mediated BIM expression and apoptosis in neurons under oxidative stress (Xie et al., 2012).

1.5.3 Regulation of FOXO transcriptional output by binding partners

The transcriptional output of FOXOs is highly context-dependent and cell- or tissue-specific, which was proven by gene analysis of different cell types in FOXO1, FOXO3, and FOXO4 knockout mice (van der Vos and Coffer, 2011). To ensure cell type- or tissue-specific transcriptional outcomes, FOXOs utilize a number of binding partners to control the transcription specificity and activity, besides posttranslational modifications.

Androgen receptor (AR) is a member of the steroid/thyroid hormone receptor superfamily, which could be activated by androgens including testosterone and dihydrotestosterone (DHT) (Evans, 1988; Matsumoto et al., 2013). AR is comprised of an N-terminal domain (A/B domains), a DNA binding domain, a short hinge region, and a C-terminal ligand-binding domain. The activated AR inhibits FOXO1 DNA-binding activity, thereby impairs the FOXO-mediated FasL expression, apoptosis as well as cell cycle arrest in prostate cancer cells. These effects are achieved by the interaction between the carboxyl terminus of FOXO1 and A/B domains as well as the ligand-binding domain of AR (Li et al., 2003). Meanwhile, the association between FOXO1 and AR suppresses the interaction of AR and p160 coactivators and also inhibits AR-dependent gene expression (Ma et al., 2009). Moreover, androgens induce increased activity of an acidic cysteine protease, resulting in proteolysis of FOXO1, to protect prostate cancer cells from FOXO-mediated cell death (Huang et al., 2004). FOXOs have also been shown to interact with another proteins such as PPARγ coactivator 1(PGC-1α), estrogen receptor α (ERα) and β-catenin (Daitoku et al., 2011; van der Vos and Coffer, 2008). In conclusion, by interaction with other binding partners, FOXOs crosstalk with other pathways to integrate upstream signals and affect its own activity.

1.6 Epigenetic regulation of gene expression

In order to control target gene expression, the transcription factors need to bind specific DNA sequence elements. However, only the presence of a consensus DNA element is not sufficient to direct transcription factor binding to chromatin (Guertin and Lis, 2013). In eukaryotes, 145-147 base pairs of DNA are wrapped around a histone octamer consisting of two copies each of histone 2A (H2A), histone 2B (H2B), histone 3, and histone 4 to form the nucleosome, which restrict transcription factors access (Kornberg and Lorch, 1999; Luger et al., 1997). Therefore, dynamic chromatin remodeling processes are required for the initial steps in gene expression, and these processes are further regulated by epigenetic mechanisms such as DNA methylation, histone modifications, and small non-coding RNAs (microRNA) (Figure 5) (Relton and Davey Smith, 2010).

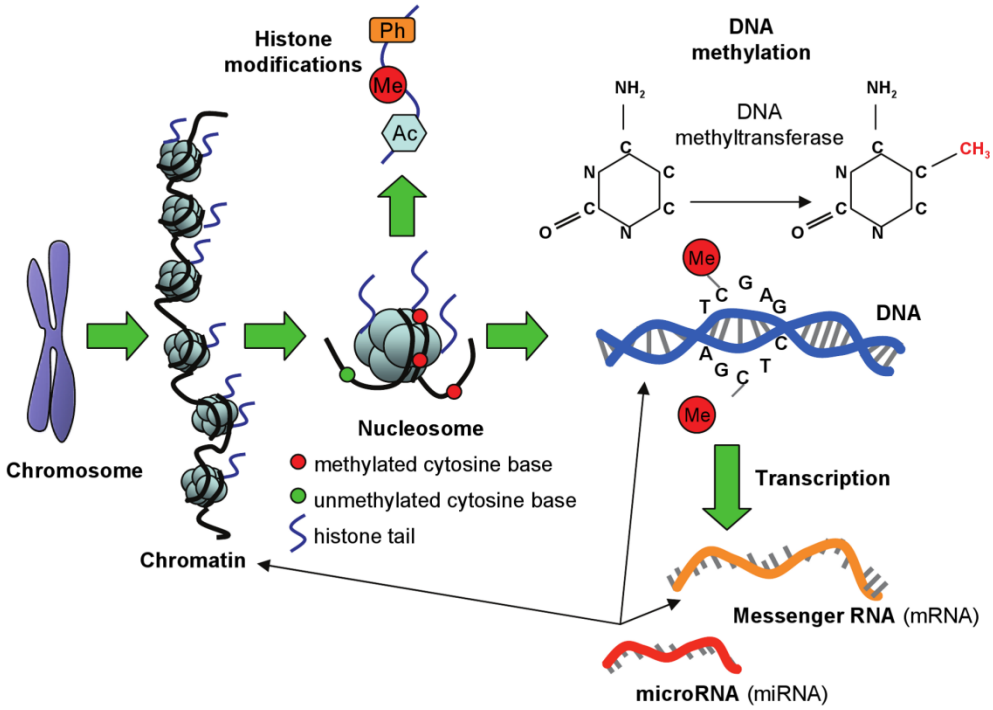

Figure 5: Types of epigenetic modifications (Relton and Davey Smith, 2010).

1.6.1 Histone acetylation

In 1964, Allfrey and colleagues reported that histones can be modified by adding acetyl and methyl groups and their possible role in regulation of RNA synthesis (Allfrey et al., 1964). Since then, it has been well documented that histone acetylation facilitates the access of transcription factors to the DNA, and is thereby associated with actively transcribed genes (Khan and Khan, 2010; Shahbazian and Grunstein, 2007; Verdin and Ott, 2014). Increased DNA accessibility to transcription factors is achieved by acetylation of histones through neutralizing the positive charge of lysine residues by acetyl groups, thereby weakening the charge-dependent interaction between histones and nucleosomal DNA as well as linker DNA or adjacent histones (Grunstein, 1997; Zentner and Henikoff, 2013). The lysine acetylation in histone tails is a dynamic reversible process controlled by two groups of enzymes: histone acetyltransferases (HATs) and histone deacetylases (HDACs) (Lee and Workman, 2007). HATs can be categorized into three major families: the MYST family (named after its four founding members MOZ, Ybf2 (Sas3), Sas2, and Tip60), the Gcn5 related N-acetyltransferase (GNAT) family, and CBP/p300 family (Berndsen and Denu, 2008), whilst HDACs can be classified into four classes (Barneda-Zahonero and Parra, 2012). More than 20 HATs have been identified, which acetylate histones via utilizing acetyl-coenzyme A (acetyl-CoA) as an essential cofactor to provide an acetyl group to the target lysine residue (Choudhary et al., 2014). Class I HDACs are comprised of 4 members HDAC1-3 and HDAC8, class II HDACs include HDAC4-7, HDAC 9 and 10, while class IV HDACs only consists of HDAC11. The class III HDACs, also known as Sirtuins, are comprised of Sirtuin 1-7. The class I, II, and IV HDACs are Zn^{2+}-dependent enzymes, whereas class III HDACs need NAD^{+} as a cofactor (Marks and Xu, 2009).

1.6.2 Other histone modifications

Histone 3 lysine 4 tri-methylation (H3K4me3) is enriched at the promoter region of actively transcribed genes (Barski et al., 2007; Heintzman et al., 2007; Koch et al., 2007), a step considered as a hallmark of actively transcribed promoters (Hon et al., 2009). Histone 3 lysine 36 tri-methylation (H3K36me3) is located in the body of genes and associated with actively transcribed genes (Kolasinska-Zwierz et al., 2009). In contrast, both histone 3 lysine 9 tri-methylation (H3K9me3) and histone 3 lysine 27 tri-methylation (H3K27me3) are associated with epigenetic gene repression (Kooistra and Helin, 2012). The gene repression by H3K9me3 is involved in the recruitment of heterochromatin protein 1 (HP1) to induce heterochromatin formation (Fischle et al., 2003), while H3K27me3 is catalyzed by the Polycomb repressive complex 2 (PRC2) and associated with repressed gene expression (Margueron and Reinberg, 2011).

1.6.3 DNA methylation

DNA methylation is a biochemical process in which a methyl group from S-adenosylmethionine is added to the C_5 position of the pyrimidine ring of a cytosine base. In mammals, 60% to 90% of cytosines from cytosine-guanine (CpG) dinucleotides are methylated (Tucker, 2001), whereas the remaining unmethylated CpGs are clustered at certain regions, called CpG islands. In human and mice, CpG islands are present in the promoter regions of approximately 60% of genes (Antequera, 2003). DNA methylation is a silencing epigenetic mark involved in a number of key biological processes such as genomic imprinting, X-chromosome inactivation, tissue specific gene repression, as well as carcinogenesis (Jones, 2012). In mammals, DNA methylation is catalyzed by a family of enzymes termed DNA methyltransferases (DNMTs) such as DNMT1, DNMT3A, and DNMT3B. DNMT1 is associated with maintenance of the pattern of DNA methylation after DNA replication (Hermann et

al., 2004), whilst DNMT3A and DNMT3B are involved in the establishment of *de novo* DNA methylation pattern during early development and gametogenesis (Okano et al., 1999). Aberrant DNA hypermethylation at the promoter region of tumor suppressor genes is associated with tumorigenesis.

1.7 Aim of study

UPEC is the causative pathogen in the vast majority of both acute and chronic urinary tract infections in humans (Barber et al., 2013; Ulett et al., 2013). Due to the anatomical connection of the urinary tract to the genital tract in the male, UPEC can invade the ductal system of the male genital tract and cause urethritis, prostatitis, epididymitis or combined epididymo-orchitis.(Bhushan et al., 2009b; Ludwig, 2008). UPEC strains possess a plethora of virulence factors, which enable them to colonize and manipulate the host innate immune response. In recent years, the UPEC virulence factor α-hemolysin (HlyA) has been shown to deviate host survival signaling pathways including MAP kinases, NF-κB, AKT and inflammasome activation, as a strategy to escape the host immune response (Bhushan et al., 2008; Nagamatsu et al., 2015; Wiles et al., 2008). It has been reported previously that HlyA can activate AKT/FOXO signaling, but the occurrence of apoptosis in bladder cells was not observed (Wiles et al., 2008). This is in agreement with *in vivo* studies from our group using an experimental epididymo-orchitis model indicating that UPEC infection causes death of testicular cells predominantly by necrosis instead of apoptosis (Lu et al., 2013). Furthermore, in our previous study it has been found HlyA is associated with long term impairment of semen parameters in genitourinary tract infection patients (Lang et al., 2013).

Therefore, the objective of this study was to investigate the molecular mechanism of UPEC mediated suppression of apoptotic cell death pathways as a means to facilitate bacterial propagation and silent chronification of disease.

2 MATERIALS AND METHODS

2.1 Materials

2.1.1 Chemicals

Acetic acid	Merck, Darmstadt
Acrylamide 30% (w/v)	Roth, Karlsruhe
Agarose	Invitrogen, Karlsruhe
Bromophenol blue sodium salt	Sigma-Aldrich, Steinheim
Calcium chloride	Merck, Darmstadt
Dimethylsulfoxide	Merck, Darmstadt
Dithiothreitol (DTT)	Roth, Karlsruhe
D-Glucose	Sigma-Aldrich, Steinheim
Ethanol	Sigma-Aldrich, Steinheim
Ethidium bromide	Roth, Karlsruhe
Ethylene diaminetetraacetic acid disodium salt	Merck, Darmstadt
Formamide	Merck, Darmstadt
37% Formaldehyde solution	Sigma-Aldrich, Steinheim
Glycerol	Merck, Darmstadt
Glycine	Sigma-Aldrich, Steinheim
Glycogen	Invitrogen, Karlsruhe
4-(2-hydroxyethyl)-1-piperazineethanesulfonic acid	Roth, Karlsruhe
Halt Phosphatase Inhibitor Cocktail	Thermo Fisher Scientific, Waltham
Igepal CA-630 (NP-40)	Sigma-Aldrich, Steinheim
Magnesium chloride	Merck, Darmstadt
Magnesium sulfate	Sigma-Aldrich, Steinheim
LY294002	Cell Signaling Technology, Danvers

β-Mercaptoethanol	AppliChem, Darmstadt
Methanol	Sigma-Aldrich, Steinheim
Non-fat dry milk	Roth, Karlsruhe
Paraformaldehyde	Merck, Darmstadt
Ponceau S	Roth, Karlsruhe
Potassium chloride	Merck, Darmstadt
Proteinase inhibitor cocktail	Sigma-Aldrich, Steinheim
Roti®-Phenol	Roth, Karlsruhe
Sodium acetate	Roth, Karlsruhe
Sodium chloride	Sigma-Aldrich, Steinheim
Sodium deoxycholate	Roth, Karlsruhe
N, N, N', N'-Tetramethylethylenediamin	Roth, Karlsruhe
Tris (hydroxymethyl) aminomethane	Roth, Karlsruhe
Triton X-100	Sigma-Aldrich, Steinheim
Tween-20	Roth, Karlsruhe

2.1.2 PCR reagents

DNase I	Invitrogen, Carlsbad
EDTA	Invitrogen, Carlsbad
dNTP	Promega, Mannheim
SuperScript® II Reverse Transcriptase	Invitrogen, Carlsbad
Oligo dT	Promega, Mannheim
RNase A	Invitrogen, Karlsruhe
Taq polymerase	Promega, Mannheim
SYBR green	Bio-Rad, Munich

2.1.3 Enzymes for Sertoli cell and peritubular cell isolation

Enzyme	Company	Catalogue No.
Collagenase A	Roche Diagnostics, Mannheim	103586
DNase I	Sigma-Aldrich, Steinheim	DN25
Hyaluronidase	Sigma-Aldrich, Steinheim	H3506
Trypsin	Sigma-Aldrich, Steinheim	T5226
Trypsin inhibitor	Sigma-Aldrich, Steinheim	T6522

Table 2: The list of enzymes used for Sertoli and peritubular cell isolation from rat testis.

2.1.4 Antibodies

Primary Antibody	Manufacturer	Catalogue No.	Dilution (application)
Rabbit anti p-AKT	Cell Signaling Technology, Danvers, USA	5012	1:1000 (WB)
Rabbit anti AKT	Santa Cruz, Dallas, USA	sc-8312	1:500 (WB)
Rabbit anti cleaved caspase 3	Cell Signaling Technology, Danvers, USA	9661	1:1000 (WB)
Rabbit anti p-FOXO1 (Thr24)/FOXO3a (Thr32)	Cell Signaling Technology, Danvers, USA	9464	1:1000 (WB)
Rabbit anti p-FOXO1 (Thr24)/FOXO3 (Thr32)/FOXO4 (Thr28)	Cell Signaling Technology, Danvers, USA	2599	1:1000 (WB)
Rabbit anti p-FOXO1 (Ser256)	Cell Signaling Technology, Danvers, USA	9461	1:1000 (WB)

Rabbit anti p-FOXO3 (Ser253)	Cell Signaling Technology, Danvers, USA	13129	1:1000 (WB)
Rabbit anti FOXO1	Cell Signaling Technology, Danvers, USA	2880	1:1000 (WB) 1:100 (IF)
Rabbit anti FOXO3a	Cell Signaling Technology, Danvers, USA	2497	1:1000 (WB) 1:100 (IF)
Rabbit anti FOXO4	Cell Signaling Technology, Danvers, USA	9472	1:1000 (WB)
Rabbit anti catalase	Cell Signaling Technology, Danvers, USA	8841	1:1000 (WB)
Rabbit anti BIM	Cell Signaling Technology, Danvers, USA	2933	1:1000 (WB)
Rabbit anti p27Kip1	Cell Signaling Technology, Danvers, USA	2552	1:1000 (WB)
Rabbit anti p15INK4B	Cell Signaling Technology, Danvers, USA	4822	1:1000 (WB)
Rabbit anti cyclin D1	Cell Signaling Technology, Danvers, USA	2926	1:1000 (WB)
Rabbit anti cyclin D3	Cell Signaling Technology, Danvers, USA	2936	1:1000 (WB)
Rabbit anti SOD2	EMD Millipore, Billerica, USA	AB10346	1:2000 (WB)
Rabbit control IgG	Abcam, Cambridge, UK	Ab46540	1:100 (ChIP)

Rabbit anti-acetyl-histone 4	EMD Millipore, Billerica, USA	06-866	1:2500 (WB) 1:100 (ChIP)
Rabbit anti-acetyl-histone 3	EMD Millipore, Billerica, USA	06-599	1:2500 (WB) 1:100 (ChIP)
Rabbit anti-vimentin	Santa Cruz, Dallas, USA	sc-7557	1:100 (IF)
Mouse anti β-actin	Sigma-Aldrich, Steinheim, Germany	A5441	1:2500 (WB)

Table 3: Information for primary antibodies used for Western blotting (WB), immunofluorescence staining (IF) and chromatin immunoprecipitation (ChIP).

Secondary antibody	Manufacturer	Catalogue No.	Dilution
Donkey anti rabbit IgG-Cy3	Chemicon, Hampshire, UK	AP182C	1:1000
Goat anti rabbit IgG -HRP	Cell Signaling Technology, Danvers , USA	7074	1:10,000
Horse anti mouse IgG-HRP	Cell Signaling Technology, Danvers , USA	7676	1:10,000

Table 4: Secondary antibodies for Western blotting and immunofluorescence staining.
IgG: Immunglobulin G
HRP: Horseradish peroxidase

2.1.5 Cell culture reagents

Dulbecco ́s PBS (1×) w/o Ca^{2+} & Mg^{2+}	Gibco, Darmstadt
Fetal bovine serum	Gibco, Darmstadt
Penicillin/Streptomycin (100×)	Gibco, Darmstadt
RPMI 1640 medium	Gibco, Darmstadt
Trypsin/EDTA	Gibco, Darmstadt

2.1.6 Equipments

Cell culture CO_2 incubator	Binder, Tullingen
Confocal laser scanning microscope TCS SP2	Leica, Wetzlar

Desktop centrifuge Biofuge Fresco	Heraeus, Hanau
Electronic balance SPB50	Ohaus, Giessen
Fluorescent microscope Axioplan 2 Imaging	Carl Zeiss, Göttingen
FUSION-FX7 Advance	PEQLAB, Erlangen
Gel Jet Imager 2000 documentation system	Intas, Göttingen
Heat block DB-2A	Techne, Cambridge
Horizontal mini electrophoresis system	PEQLAB, Erlangen
Magnetic particle concentrator	Invitrogen, Karlsruhe
Microwave oven	Samsung, Schwalbach
Mini centrifuge Galaxy	VWR International
Mini-rocker shaker MR-1	PEQLAB, Erlangen
Mixer Mill MM 300	Retsch, Haan
MyiQ^{TM}2 two-color real-time PCR detection system	Bio-Rad, Munich
NanoDrop ND 2000	Thermo Fisher Scientific, Waltham
PCR thermocycler	Biozyme, Oldendor
Potter S homogenizer	B. Braun, Melsungen
Power supply units	PEQLAB, Erlangen
Pre-cast gel system	Invitrogen, Karlsruhe
SDS gel electrophoresis chambers	Consurs, Reiskirchen
Semi-dry-electroblotter	PEQLAB, Erlangen
Thermo Shaker	PEQLAB, Erlangen
Vertical electrophoresis system	PEQLAB, Erlangen
Ultrasonic homogenizer Bandelin Sonopuls	Bandelin, Berlin
UV visible spectrophotometer Ultrospec 2100 Pro	Biochrom, Cambridge

2.1.7 Miscellaneous

Bio-Rad Protein Assay	Bio-Rad, Munich
DNA Ladder (100 bp)	Promega, Mannheim

DAPI	Vector, Burlingame
Enhanced chemiluminescence (ECL) reagents	Thermo Fisher Scientific, Waltham
Hybond ECL nitrocellulose membrane	Amersham, Freiburg
Protein size markers	Thermo Fisher Scientific, Waltham
Sterile plastic ware for cell culture	Sarstedt, Nümbrecht

2.1.8 Primers

All primers were designed by using "Primer BLAST", which is available online at http://www.ncbi.nlm.nih.gov/tools/primer-blast/. Primer sequences and annealing temperatures for PCR analysis are listed in Table 4. All primers were purchased from MWG-Biotech (Ebersberg, Germany) and diluted in 1 × Tris-EDTA (pH 8.0) buffer to achieve 100 pmol/µl and stored as stock solution at -20 ℃.

Gene	**Primer Sequences**	**Annealing Temperature**	**Accession No.**	**Amplicon Size (bp)**
β2M-fw	5 ́CCGTGATCTTTC TGGTGCTT3 ´	60 ℃	NM_012512	109
β2M-rv	5 ́AAGTTGGGCTT CCCATTCTC3 ´			
BIM-fw	5 ́AGATACGGATC GCACAGGAG3 ´	59.6 ℃	NM_171989	148
BIM-rv	5 ́ACCAGACGGAA GATGAATCG3 ´			
SOD2-fw	5 ́ACCGAGGAGAA GTACCACGA3 ´	59.6 ℃	NM_017051	148
SOD2-rv	5 ́TGGGTTCTCCAC CACCCTTA3 ´			

Catalase-fw	5´GCTCCGCAATCCTACACCAT3´	59.6 ℃	NM_012520	104
Catalase-rv	5´GTGGTCAGGACATCGGGTTT3´			
Gadd45α-fw	5´GGAGTCAGCGCACCATAACT3´	59.6 ℃	NM_024127	108
Gadd45α-rv	5´GGTCGTCATCTTCATCCGCA3´			

Table 5: Information on sequences of forward (fw) and reverse primers (rv) used in quantitative real-time PCR, annealing temperatures, gene accession numbers and amplicon sizes.

2.2 Methods

2.2.1 Animals

19-day old male Wistar rats (249~270 g) were purchased from Charles River Laboratories (Sulzfeld, Germany) and kept at 22°C with 12 h light: 12 h dark schedule and fed with standard food pellets and water *ad libitum*. This study was carried out in strict accordance with the recommendations in the Guide for the Care and Use of Laboratory Animals of the German law of animal welfare. The protocol was approved by the Committee on the Ethics of Animal Experiments of the Regierungspraesidium Giessen, Giessen, Germany (permit number GI 20/23 –No. 16/2009 and GI 20/23–No. A31/2012). The rats were scarified by CO_2 inhalation, and all efforts were made to minimize suffering.

2.2.2 Bacterial strains and propagation

UPEC pyelonephritic strain prevalent in urinary tract infections: strain 536 (NCBI: NC_008253, CP000247) and the mutant with deletion of both α-hemolysin (*hlyA*) genes in the UPEC 536 strain (*hlyA* double mutant = UPEC 536 HDM) were obtained from

Prof. Ulrich Dobrindt (University of Muenster, Germany).

Uropathogenic *E. coli* strain UPEC 536 was propagated overnight on Columbia blood agar plates (Oxoid, Wesel, Germany). Fresh cultures were inoculated in LB medium and grown to early exponential phase (OD600 = 0.4~0.8) at 37 ℃ in a shaker incubator. The concentration of viable bacteria was calculated using growth curves. Bacteria (2×10^9 cfu) were centrifuged at 4,500 × g for 8 min at room temperature. The pellet was washed once at room temperature with PBS and diluted again in 10 ml saline or RPMI 1640 medium.

2.2.3 UPEC induced epididymo-orchitis model

The bacterial induced epididymo-orchitis model in male Wistar rat was previously established in our laboratory (Bhushan et al., 2008; Lu et al., 2013). Briefly, after successfully anaesthetizing the adult male Wistar rats (250~275g) with 50 mg/ml Ketamine and 2% Xylazine (v:v=7:3), the testis, epididymis and vas deferens were exposed by scrotum incision. One hundred µl of saline containing ~ 4×10^6 bacteria were injected into the vas deferens, close to the distal end of the epididymis. Sham operated rats were injected with saline. The rats were scarified and the testes were removed aseptically seven days post infection. Testes were snap frozen in liquid nitrogen and kept at -80°C for immunofluorescence and Western blot analysis.

2.2.4 Isolation of Sertoli cells

Medium

PBS-A

500 ml PBS Dulbecco's without Ca^{2+} and Mg^{2+}

750 mg D-Glucose

5 ml 100 × Penicillin & Streptomycin

Trypsin-DNase-solution in PBS-A

10 ml PBS-A

25 mg Trypsin

200 µg DNase I

Trypsin inhibiter-solution A in PBS-A

5 ml PBS-A

50 mg Trypsin inhibiter

Trypsin inhibiter-solution B in PBS-A

10 ml PBS-A

25 mg Trypsin inhibitor

Collagenase-Hyaluronidase-DNase-solution in PBS-A

10 ml PBS-A

10 mg Collagenase

10 mg Hyaluronidase

200 µg DNase I

Hyaluronidase-DNase-solution in PBS-A

10 ml PBS-A

10 mg Hyaluronidase

200 µg DNase I

All enzyme solvents above were sterilized by passing through a 0.20 µm filter (SARSTEDT, Nuembrecht, Germany).

Sertoli cell culture medium

500 ml RPMI-1640 medium with L-glutamine

5 ml 100 × Penicillin & Streptomycin

Sertoli cells were isolated from 19-day old Wistar rats. Ten rats were killed by CO_2 inhalation. The abdomen was disinfected with 70% ethanol and twenty testes were collected aseptically via abdominal incision. Testes were rinsed by equal volume of 1% (w/v) iodine alcohol, and immediately washed two times with PBS. Next, testis was decapsulated by grasping one end with forceps, and cutting a small incision into the tunica albuginea at the other end of testis. The tubules were squeezed out by using closed forceps.

Seminiferous tubules were digested with 10 ml Trypsin-DNase-solution at 32°C in ashaking water bath (120 oscillations/min) for 3-6 min. When seminiferous tubules were properly separated, trypsin digestion was terminated by adding Trypsin inhibitor solution A (10 mg/ml) and B (2.5 mg/ml) sequentially. Seminiferous tubules were washed 9 times for 10 min with PBS-A to remove contaminating interstitial cells, followed by digestion with Collagenase-Hyaluronidase-DNase-solution at 32°C in a shaking water bath (120 oscillations/min) for 8-10 min. The digested tubules were observed under the microscope to check the length of tubules and smoothness of the surface of the tubules. If tubules shortened in length and edges appeared rough, the enzymatic digestion was stopped immediately. The rough edge and shortened length of tubules are both indicative of peritubular cell release. After digestion, tubular fragments were allowed to settle for 8 min. The supernatant with enriched peritubular cells was discarded. After 3-5 times washing with PBS-A, the remaining tubular fragments were further digested with 10 ml of Hyaluronidase-DNase-solution at 32°C in a shaking water bath (120 oscillations/min) for 3-5 min. The digestion of tubules was stopped when tubular fragments became very short and started to disintegrate to individual cells. The fragmented tubules were allowed to settle for 8 min, and washed 3 times with PBS-A to get rid of contaminating germ cells and peritubular cells. The Sertoli cell enriched fraction was dispersed by passing through an 18G needle 10 times using a 20 ml syringe, followed by spinning the cells down by centrifugation at 300 × g for 10 min. The cell pellet was resuspended in 40 ml RPMI 1640 medium, which was further passed through 70 µm nylon filter (BD Biosciences, Heidelberg, Germany) to remove the undigested

tubular fragments. 4×10^6 cells/well were seeded in 6-well plates and incubated at 32°C with 5% CO_2. Cell numbers were adjusted accordingly for culture in 12-well and 24-well plates. The hypotonic shock treatment was performed on the 3rd day of culture to eliminate contaminating germ cells. Briefly, Sertoli cells were rinsed two times with PBS and incubated with 20 mM Tris-HCl (pH 7.5) for 1 min. Subsequently, cells were washed twice with PBS and cultured for at least 1 day in RPMI 1640 medium. On the 4th day, Sertoli cells were ready for experiments.

Purity of Sertoli cell preparation was estimated > 95% by immunofluorescence using antibody directed against vimentin.

2.2.5 cDNA synthesis and quantitative real-time PCR

2.2.5.1 Isolation of RNA

Total RNA was extracted from Sertoli cell samples by using the PureLink® RNA Mini Kit (Invitrogen, Carlsbad, USA). After the indicated time periods of UPEC infection, Sertoli cells were collected in 600 µl RLT buffer (containing 1% β-Mercaptoethanol) by using cell scrapers. The cell lysates were passed through a 21G needle with a 1 ml syringe for 5~10 times to avoid cell clumps, subsequently frozen in liquid nitrogen and then stored at -80°C for the day of isolation. Otherwise, the lysate was directly mixed thoroughly with 1 volume of 70% ethanol. Up to 700 µl of the mixture was transferred to spin cartridge (with the collection tube) for centrifugation at 12,000 × g for 15 sec. The flow-through was discarded and the spin cartridge was reinserted into the collection tube. This process was repeated until the entire sample was processed. Wash buffer 1 (700 µl) was added to the spin column to wash column membrane by centrifugation at 12,000 × g for 15 sec. The collection tube was replaced with a new collection tube and wash buffer 2 (500 µl) was added to the column. The spin column was centrifuged for 15 sec at 12,000 × g and the flow through was discarded. This process was repeated

again followed by a centrifugation at 12,000 × g for 2 min to dry the membrane. The RNeasy spin column was placed in a new 1.5 ml collection tube, and 30~40 µl RNase-free water was directly added to the column membrane. After incubation for 1 min, the RNA was eluted by centrifugating at 16,060 × g for 2 min. RNA concentration of each sample was measured by NanoDrop.

2.2.5.2 DNA digestion

Prior to RT-PCR amplification, putative contamination of genomic DNA from each RNA sample was eliminated by DNase I (Invitrogen, Carlsbad, USA) treatment. RNA from each sample (2.5 µg) was treated with 2 µl DNase I at room temperature for 15 min in the reaction mixture given below. Two µl of 25 mM EDTA (pH 8.0) solution was added to each sample and subsequently heated at 65℃ for 10 min to inactivate DNase I.

DNase digestion reaction mix:

Component	**Volume**
2.5 µg RNA	X µl
DNase I (1 U/µl)	2.0 µl
10 × DNase I buffer	2.0 µl
RNase free water	to 20 µl

Each DNase I digested RNA sample was amplified by standard PCR to detect the expression of a housekeeping gene (β-actin). The absence of PCR product was verified by agarose gel electrophoresis and ethidium bromide (EB) staining to confirm the samples were free of DNA contamination.

2.2.5.3 Reverse transcription

The DNase I digested RNA sample was reverse transcribed by using SuperScript® II Reverse Transcriptase (Invitrogen, Carlsbad, USA). For each reaction, 2.5 µg of RNA

was mixed with 2 µl of Oligo (dT) 15 Primer and 2 µl dNTP (10 mM), subsequently denatured at 65 ℃ for 5 min.

Denaturation of RNA and primer annealing:

Component	Volume
2 µg of DNase I digested RNA	20 µl
Oligo dT_{15}	2 µl
dNTP Mix (A,C, G and T, each 10 mM)	2 µl

The denatured samples were snap chilled on ice. The RT mix was prepared as below prior to mix with the denatured RNA samples.

RT mix:

Component	Volume
5 × first strand buffer buffer	8 µl
DTT (0.1M)	4 µl
RNase-free water	4 µl

The samples were preheated at 42 ℃ for 2 min, and 1 µl of reverse transcriptase (SuperScript® II Reverse Transcriptase, 200 U/µl) was added to each sample. The reaction mix was incubated at 42 ℃ for 50 min, followed by inactivation of reverse transcriptase by heating samples at 70 ℃ for 15 min. And cDNA samples were stored at -20 ℃.

2.2.5.4 Quantitative real-time RT PCR (qRT-PCR)

qRT-PCR is a widely used laboratory technique based on the standard polymerase chain reaction (PCR) to amplify and simultaneously detect or quantify a targeted cDNA molecule. Besides the general principle of PCR, the key feature of qRT-PCR is that the amplified product is detected and measured as the reaction progresses, which is in "real time". The real-time quantitative detection of PCR products can be achieved by adding to the reaction a fluorescent molecule, which reports an increase in the amount of DNA with

a proportional increase in fluorescence signal. The fluorescent molecule could be non-specific fluorescent dyes (such as SYBR green used in this project) that intercalate with double-stranded DNA or fluorescently labeled sequence-specific DNA primers or probes. The fluorescence signal can be monitored and recorded in a thermocycler, which is used to measure the threshold cycle (Ct) value. The Ct value is inverse proportional to the initial amount of cDNA.

To measure SOD2, BIM, catalase, and Gadd45α expression, primer pairs were designed by "Primer BLAST" and synthesized by Eurofins MWG Operon. The appropriate annealing temperatures were determined by gradient PCR. A typical 25 µl qRT-PCR reaction mix was used as follows.

Component	**Volume per reaction**
cDNA	1 µl
2 ×iQ SYBR green supermix	12.5 µl
Forward and reverse primer mix (10 pM/µl)	1 µl
DNase/RNase free water	10.5 µl
Total volume	**25 µl**

Real-time PCR was performed in duplicate to measure the expression of target genes by using the iCycler iQ® System (Bio-Rad, Munich, Germany) according to the manufacturer's procedure. PCR amplification was carried out at 95℃ for 8 min, and then cycled 45 times at 95℃ for 20 sec, at annealing temperature (see Table 4) for 30 sec, and at 72℃ for 30 sec.

The specificity of the PCR product was confirmed by melt curve examination. Real-time RT PCR results were analyzed with the delta delta threshold cycle method using β-microglobulin as an internal standard to normalize the amount of mRNA. Data were presented as relative expression (RE): $RE= 2^{\Delta Ct\ UPEC-\Delta Ct\ Ctrl}$, $\Delta Ct=Ct_{target\ gene}-Ct_{\beta 2M}$.

2.2.5.5 Agarose gel electrophoresis

6 × gel loading buffer with Bromophenol blue

0.25% (w/v) Bromophenol blue

30% Glycerol in H_2O

50 × TAE electrophoresis buffer (1L, pH 8.0)

242 g of Tris base

57.1 ml of Glacial acetic acid

100 ml of 0.5 M EDTA

1 × TE buffer

10 mM Tris-HCl pH 8.0

1 mM EDTA

2.2.6 Immunoblotting

2.2.6.1 Buffers and solutions

30% Acrylamide solution

Acrylamide/Bisacrylamide = 37.5:1

RIPA buffer

10 mM Tris-HCl pH 7.4

150 mM NaCl

0.25% NP-40

1% Triton X-100

2 mM EDTA

1 mM PMSF *

1 × Proteinase inhibitor cocktail (Sigma-Aldrich, Steinheim, Germany)*

1 × Halt Phosphatase Inhibitor Single-Use Cocktail (Thermo Fisher Scientific, Waltham, USA)*

* Added fresh just before cell lysis

Protein gel sample loading buffer

50 mM Tris-HCl; pH 6.8

2% SDS

10% Glycerol

1% β-Mercaptoethanol

12.5 mM EDTA

0.02% (w/v) Bromophenol blue

10 × Phosphate buffered saline (PBS)

4 g KCl

4 g KH_2PO_4

160 g NaCl

23 g $Na_2HPO_4 * H_2O$

Dissolved in 1L H_2O, pH to 7.4 with HCl

10 × Tris buffered saline (TBS)

24.2 g Tris base

80 g NaCl

Dissolved in 1L water, pH to 7.4 with HCl

Washing buffer TBS/T

1 × TBS

0.1% (v/v) Tween-20

Blocking buffer

100 ml 1 × TBS

0.1 ml Tween-20

5 g Non fat dry milk

10 × Electrophoresis buffer (pH 8.3)

30.3 g Tris base

144 g Glycine

10 g SDS

Dissolved in 1L water, set pH to 8.3 with HCl

Stripping buffer

6.25 ml 1 M Tris-HCl (pH 6.8)

2 ml 10% SDS

700 µl β-Mercaptoethanol*

Make volume up to 100 ml with water

* added freshly just before stripping of membrane

Cathode buffer

25 mM Tris

40 mM 6-amino-hexanoic acid

20% (v/v) Methanol

10 × Anode buffer

300 mM Tris

20% (v/v) Methanol

1 × Anode buffer

30 mM Tris

20% (v/v) Methanol

Separating gel:

	7.5%*	10%*	12.5%*	15%*
Water	4.85 ml	4.01 ml	3.17 ml	2.35 ml
1.5 M Tris-HCl pH 8.8	2.5 ml	2.5 ml	2.5 ml	2.5 ml
10% (w/v) SDS	100 µl	100 µl	100 µl	100 µl
Acrylamid	2.5 ml	3.34 ml	4.17 ml	5 ml
10% (w/v) APS**	50 µl	50 µl	50 µl	50 µl
TEMED	5 µl	5 µl	5 µl	5 µl
Total	10 ml	10 ml	10 ml	10 ml

Stacking gel:

	4%*
Water	3 ml
0.5 M Tris-HCl pH 6.8	1.25 ml
10% (w/v) SDS	50 µl
Acrylamide	0.65 ml
10% (w/v) APS**	25 µl
TEMED	5 µl
Total	5 ml

* Separating gels with different percentages were used according to the molecular weight of target proteins (based on 37.5:1 acrylamide/bisacrylamide ratio). 7.5% gel: 250~120 kDa; 10% gel: 120~40 kDa; 12.5% gel: 40~15 kDa; 15% gel: < 20 kDa.

** Ammoniumpersulfate (APS) was prepared fresh before each experiment.

2.2.6.2 Western blotting

Following treatment as indicated in respective figures, Sertoli cells were washed twice with PBS and then collected into RIPA lysis buffer (10 mM Tris-HCl pH 7.4, 150 mM NaCl, 0.25% NP-40, 1% Triton X-100, 2 mM EDTA and 1 mM PMSF) supplemented with proteinase inhibitor cocktail and Halt Phosphatase Inhibitor Single-Use Cocktail. The concentrations of protein in cell lysates were determined by the Bradford Method (Bio-Rad, Munich, Germany). Twenty µg protein of each sample were fractioned on SDS-polyacrylamide gel and separated proteins were electrophoretically transferred onto a 0.2 µm pore size nitrocellulose membrane (Hybond™ ECL™, GE Healthcare, Cambridge, UK) by using a PerfectBlue™ semidry electroblotter. Following blocking in 5% non-fat milk in Tris-buffered saline (TBS) with 0.1% Tween (TBS-T) for 1 h at room temperature, the membranes were probed with primary antibodies (Table 2) diluted in BSA and incubated overnight at 4 ℃. After rinsing three times with TBS-T, membranes were incubated with HRP-conjugated anti-mouse or anti-rabbit antibody (Table 3) for 1 h at room temperature. Subsequently, the membranes were rinsed again for three times. The blots were developed by enhanced chemiluminescence (Thermo Fisher Scientific) and visualized by using Fusion Imaging system.

2.2.6.3 Reprobing of membrane

Membranes were incubated with stripping buffer at 60°C for 3 min. The membranes were washed again three times with a large volume of TBS/T and blocked with blocking buffer for 1 h at room temperature. Subsequently, the antibody decoration and visualization were performed as described above.

2.2.7 Immunofluorescence staining

Sertoli cells were grown on glass coverslips in 12-well cell culture plates (BD Biosciences, Heidelberg, Germany) and infected with UPEC for 4 h. Cells were then washed two times with ice cold PBS, fixed with 4% precooled paraformaldehyde for 30 min and subsequently permeabilized with 0.2% Triton X-100 in PBS for 15 min. After blocking the cells with 5% normal goat serum and 5% BSA solution for 1 h, cells were incubated overnight at 4℃ with the indicated primary antibodies. Next day, the samples were rinsed thoroughly and then incubated with Cy3-labeled secondary antibodies (Chemicon, Hampshire, UK) for 1 h. Nuclei were counterstained with Cy5-conjugated TO-PRO-3 dye (Invitrogen, Carlsbad, USA). Images were visualized using TCSSP2 confocal laser-scanning microscope.

Frozen tissue sections (10 μm) were fixed with ice cold methanol and then permeabilized with 0.2% Triton X-100 in PBS for 15 min. Following blocking with 5% BSA and 5% normal horse serum solution for 1 h, the sections were incubated with indicated primary antibodies overnight at 4°C. After three rinses, the sections were incubated with Cy3-labeled secondary antibodies for 1 h and mounted with Vectashield® mounting medium containing DAPI (Vector Laboratories, Burlingame, USA). Images were captured with the Fluorescence Microscope Axioplan 2 imaging system.

2.2.8 FOXO DNA-binding activity assay

Sertoli cells were treated with UPEC for 2 and 4 hours. Nuclear extracts were isolated using the Nuclear Extract Kit (Active Motif, La Hulpe, Belgium) according to the manufacturer's instruction. The cells were washed twice with ice-cold PBS and scraped into PBS containing proteinase inhibitor cocktail. The suspension was centrifuged at 500 rpm at 4℃ for 5 min. The cell pellet was resuspened in 100 μl hypotonic buffer, mixed

thoroughly, and incubated on ice for 15 min. Detergent (5 µl) was added and vortexed at the highest setting for 10 sec. The suspension was centrifuged at 14000 × g at 4 ℃ for 30 sec. The nuclear pellet was suspended in 30 µl complete lysis buffer and vortexed 10 sec at the highest setting. The samples were incubated on a rocking platform at 4 ℃ for 30 min. After vortexing for 30 sec at the highest setting, the samples were centrifuged at 14000 × g at 4 ℃ for 10 min. The protein concentration was determined by the Bradford Method. DNA-binding activity of nuclear FOXO1 was measured using the Trans-AM FKHR Kit (Active Motif) as instructed by the manufacturer. Nuclear protein (10 µl) and complete binding buffer (40 µl) were added to each well on the plate. Nuclear extract (5 µg, provided by the manufacture) was diluted in 10 µl of complete lysis buffer and used as positive control. Complete lysis buffer (10 µl) was used as blank. Following incubation for 1 h at room temperature with mild agitation, each well was washed three times with 200 µl of wash buffer. The FOXO1 antibody was added to each well and incubated for 1 h at room temperature. After three washes with wash buffer, 100 µl of HRP-conjugated secondary antibody were added. Following 1 h incubation at room temperature and 4 × wash with wash buffer, 100 µl of developing solution were added to each well. The plate was incubated for 2-10 min at room temperature in the dark. Stop solution (100 µl) was added to each well, and mixed properly by gentle tapping of the plate. The color of the solution in the wells should change from blue to yellow. The absorbance was recorded at 459 nm with a reference wavelength of 655 nm by using a BioSource International ELISA reader and corresponding software.

2.2.9 Chromatin Immunoprecipitation Assay

ChIP assay was performed using Chromatin Immunoprecipitation Assay Kit (EMD Millipore, Billerica, USA) according to the manufacturer's instruction. After UPEC or mock treatment, Sertoli cells were washed twice with ice cold PBS and incubated in RPMI 1640 medium containing 1% formaldehyde for 10 min at room temperature to cross link the protein with DNA. Glycine (1×) was added to quench unreacted

formaldehyde. Sertoli cells were washed two times with ice cold PBS, and cells were collected into PBS containing proteinase inhibitor cocktail. The cells were centrifuged at 800 × g at 4℃ for 5 min, supernatants were discarded and cell pellets were lysed with 0.5 ml cell lysis buffer containing proteinase inhibitor cocktail. The cells were incubated on ice for 15 min with vortexing at every 5 min. The cell suspension was centrifuged at 800 × g at 4℃ for 5 min. The cell pellet was resuspened in 0.5 ml nuclear lysis buffer for further release of chromatin. The extracted chromatin was sonicated in 0.5 ml nuclear lysis buffer for sixteen rounds for 10 s each with an interval of 2 min using an Ultrasonic homogenizer Bandelin Sonopuls at 50% intensity, to generate fragments of 200-1000 bp of DNA. The entire sonication procedure was performed in ice. The sonicated chromatin was spun at 1000 × g at 4℃ for 10 min to remove insoluble material. Five µl sheared chromatin were analyzed by agarose gel electrophoresis to confirm the size of the DNA fragments. One hundred µl sheared chromatin were diluted in 400 µl dilution buffer containing proteinase inhibitor cocktail, and immunoprecipitated using rabbit polyclonal IgG anti-acetyl-histone 3 and rabbit polyclonal IgG anti-acetyl-histone 4 antibodies. Anti-rabbit IgG antibody was used as negative control. Ten µl of each sheared chromatin and dilution buffer mixture were used as input and stored at 4℃. The sheared chromatin, indicated antibodies and protein A & G magnetic beads were mixed and incubated at 4℃ with rotation overnight. The beads were separated by using magnetic particle concentrator. The protein A & G beads-antibody/chromatin complex was resuspened in low salt immune complex wash buffer and incubated for 3-5 min on a rotating platform followed by magnetic clearance and removal of the supernatant fraction. The same procedure was repeated using high salt immune complex wash buffer, LiCl immune complex wash buffer and TE buffer in sequence. The washed protein A & G beads-antibody/chromatin complex was incubated in 100 µl ChIP elution buffer containing 1 µl proteinase K (100 mg/ml) at 62℃ for 2 h with shaking to elute and reverse cross-link DNA. The complex was heated at 95℃ for 10 min to inactivate proteinase K. The supernatant was collected after separation by magnetic particle concentrator. Two hundred µl phenol/chloroform/isoamylalchohol were added to each sample and vortexed for 1 min. The supernatant was then transferred

into a new Eppendorf tube after centrifugation at 16060 × g at 4 ℃ for 15 min. Next, 25 µl sodium acetate, 1 ml of 100% ethanol and 3 µl glycogen (20 mg/ml) were added and kept at -80 ℃ for 1 h to precipitate DNA. The DNA pellet was washed once with 70% ethanol and subsequently dried at 37 ℃ for 15 min. DNA was dissolved by adding 40 µl of water. The precipitated DNA was analyzed by iCycler real-time PCR system using the iQSYBR Green Supermix. The PCR conditions were 8 min at 95 ℃ and then 20 sec at 95 ℃, 30 sec at 59.6 ℃, 30 sec at 72 ℃ for 45 cycles. 2% of input was compared to the IP sample and the values from the IgG control were subtracted as background. The primers were purchased from MWG-Biotech (Ebersberg, Germany). Primers for BIM promoter region were as follows:

Forward: 5'-GGTGATGAAGAGTCCCGCTT-3'

Reverse: 5'-GGTGCAAGGATGGGTACTGT-3'

2.2.10 Bisulfite sequencing

For bisulfite sequencing Sertoli cells were infected with UPEC for 4 and 6 h, respectively. DNA was extracted using DNeasy Blood & Tissue Kit (Qiagen, Venlo, The Netherlands) according to the manufacturer's instruction. Briefly, after infection Sertoli cells were collected in 1.5 ml microcentrifuge tubes and washed two times with PBS by centrifugation at 300 × g at 4 ℃ to get rid of residual medium. After centrifugation, the supernants were decanted and pellets were resuspended in 200 µl PBS. Next, 20 µl proteinase K and 200 µl buffer AL were mixed thoroughly with Sertoli cell suspension and incubated at 59.6 ℃ for 10 min. Each mixture was transferred into a spin column (with the collection tube) and centrifuged at 6,000 × g for 1 min. The flow-through was discarded and the spin column was inserted into a new collection tube. AW 1 (500 µl) was added to the spin column to wash the column membrane by centrifugation at 6,000 × g for 1 min. The collection tube was replaced and AW 2 (500 µl) was added in a new collection tube and the spin column was centrifuged for 3 min at

20000 × g. The spin column was placed in a new 1.5 ml collection tube, 40-60 µl buffer AE were added directly to the column membrane. After incubation for 1 min at room temperature, the DNA was eluted by centrifugation at 16,060 × g for 1 min. DNA concentration of each sample was measured by NanoDrop. All the above steps were performed at room temperature if not indicated differently. A maximum of 2 µg Sertoli cell DNA or genomic rat DNA was used for bisulfite conversion with EpiTect Fast Bisulfite Conversion Kit (Qiagen) according to the manufacturer´s guide. Sodium bisulfite converts unmethylated cytosines to uracils, while methylated cytosines are unaffected. Converted DNA was amplified using different primer pairs (as follows) in standard PCR. The primers bind both methylated and unmethylated templates. PCR was performed in a 50 µl reaction volume containing 250 ng of bisulfite converted DNA, PCR buffer, 1.5 mM $MgCl_2$, 0.2 mM of each dNTP, 0.66 µM of each primer and 0.5 µl of GoTaq polymerase (Promega, Mannheim, Germany). After an initial 95 ℃ step for 2 min, DNA was amplified in 40-45 cycles for 30 sec each at 95 ℃, appropriate annealing temperature (indicated in Table 6) and 72 ℃ followed by final extension at 72 ℃ for 10 min. Each PCR-product underwent preparative agarose gel electrophoresis. Expected signals were excised from the gel and purified using GeneJET Gel Extraction Kit (Thermo Fisher Scientific, Waltham, USA) according to the manufacturer's protocol. As a positive control genomic testicular rat DNA was methylated *in vitro* using SssI methylase (New England Biolabs, Hertfordshire, UK) according to the manufacturer's guidelines and cleaned up using GeneJET PCR Purification Kit (Thermo Fisher Scientific). The eluated DNA was sequenced by Seqlab, Sequence Laboratories, Göttingen using corresponding forward primers. Sequencing results were analyzed using Chromas Lite 2.1.1, a free software tool downloadable from http://technelysium.com.au/. The comparison of peaks in the pyrogram for cytosine and thymine-signals within expected CpGs gives an indication of methylation status for each CpG within tested sequence.

Primer	Primer sequence (5´-3)	Annealing temperature (°C)	Amplified area (bp from TSS)	Product size (bp)
CpG1-fw	5’TTGTTTTAATTTTGTGAGGAAA3’	56,5	-2392/-2081	311
CpG1-rv	5’CCAAATCAAAACACAAATAAAA3’			
CpG2-fw	5’AGTTTGGGGTTTTGTTGTGTTA3’	62	-1317/-990	327
CpG2-rv	5’AAAATCCCCTAACCCTCCTAAA3’			
CpG3-A-fw	5’AATTTAGTTTTTTTGGTTTGGG3’	60	-459/-12	447
CpG3-A-rv	5’ACCCCAACCACTCTACTCTTAC3’			
CpG3-B-fw	5’TAAAGGGATGTTTTTGAAGGTT-’	58,7	+1891/+2281	390
CpG3-B-rv	5’TTCCTTCAAAACAAACTTAAATCA3’			

Table 6: Primer pairs for bisulfite sequencing.

fw = Forward, rv = reverse, bp = base pairs, TSS = transcription start site.

3 RESULTS

3.1 UPEC suppress the AKT survival signaling pathway in an experimental epididymo-orchitis model

Previous studies from our group have demonstrated that necrosis constitutes the predominant cell death pathway in UPEC infected rat testis (Lu et al., 2013). To determine whether UPEC impede the host's AKT survival signaling pathway and actively alter the ability of infected cells for cellular survival, Western blot analysis was performed in testicular homogenates collected 7 d post UPEC infection in the vas deferens. As compared to sham control, levels of phosphorylated AKT decreased or were not detectable in UPEC infected testis (Figure 6A). In agreement, immunofluorescence analysis of phosphorylated AKT in cryosections of infected testis revealed a strong staining of cells in the seminiferous epithelium and testicular interstitial space, whilst control testis sections showed only faint labeling (Figure 6B).

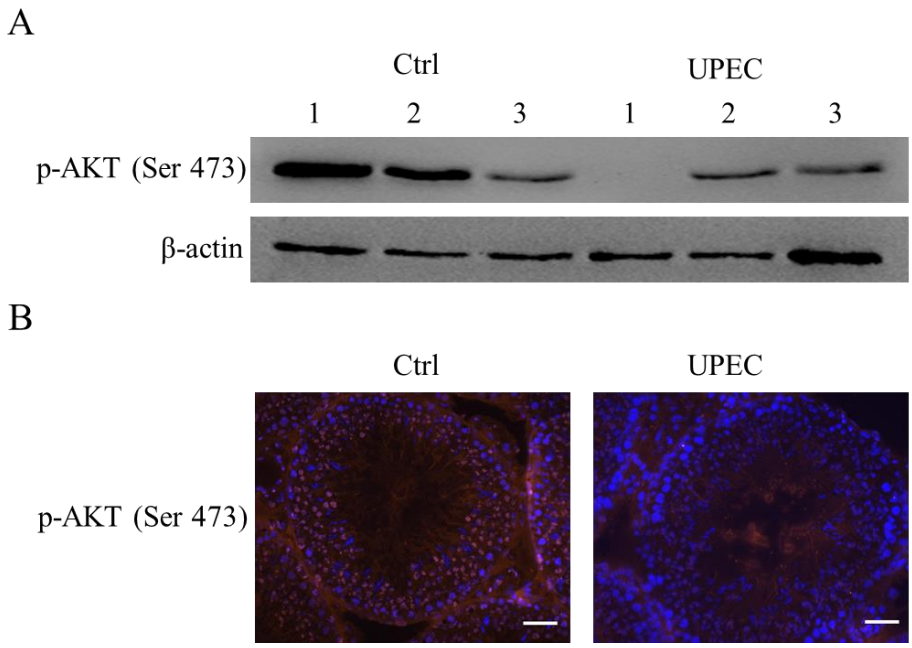

Figure 6: UPEC inactivate AKT survival signaling pathway *in vivo*. (A) Testicular homogenates of sham control (Ctrl) and UPEC treated groups were separated by SDS-PAGE (n=3, 50 µg) and immunoblots were probed with p-AKT (Ser 473), and β-actin as loading control. (B) Cryosections of

sham control testis (Crtl) and testis collected 7 d after UPEC infection were probed with p-AKT (Ser 473). Primary antibodies were visualized with Cy3-labeled secondary antibodies and nuclei were counterstained with DAPI. Micrographs were taken using an Axioplan 2 fluorescence microscope (Carl Zeiss, ×20 objective lens). Scale bars = 50 μm.

3.2 UPEC activate FOXO transcription factors following AKT dephosphorylation in the experimental epididymo-orchitis model

Dephosphorylation of AKT leads to activation of FOXOs. Hence, the phosphorylation status of FOXO1 (Thr 24) and FOXO3 (Thr 32) was determined in UPEC infected testes. Similar to AKT, phosphorylation of FOXO1 and FOXO3 was decreased or absent in UPEC infected testis as determined by Western blot (Figure 7A). Immunofluorescence of FOXO1 was very weak in sham control testis, whilst prominent labeling of FOXO1 was evident in meiotic germ cells, round spermatids and likely Sertoli cells of UPEC infected testis. In infected testis, fluorescence intensity increased and was visible in the nuclei of cells located at the base of the seminiferous epithelium with labeling in the peritubular cells mostly lost (Figure 7B, C). Taken together, these results indicate that UPEC infection leads to the suppression of AKT survival signaling pathway and consequently activation of FOXO transcription factors in UPEC infected testis.

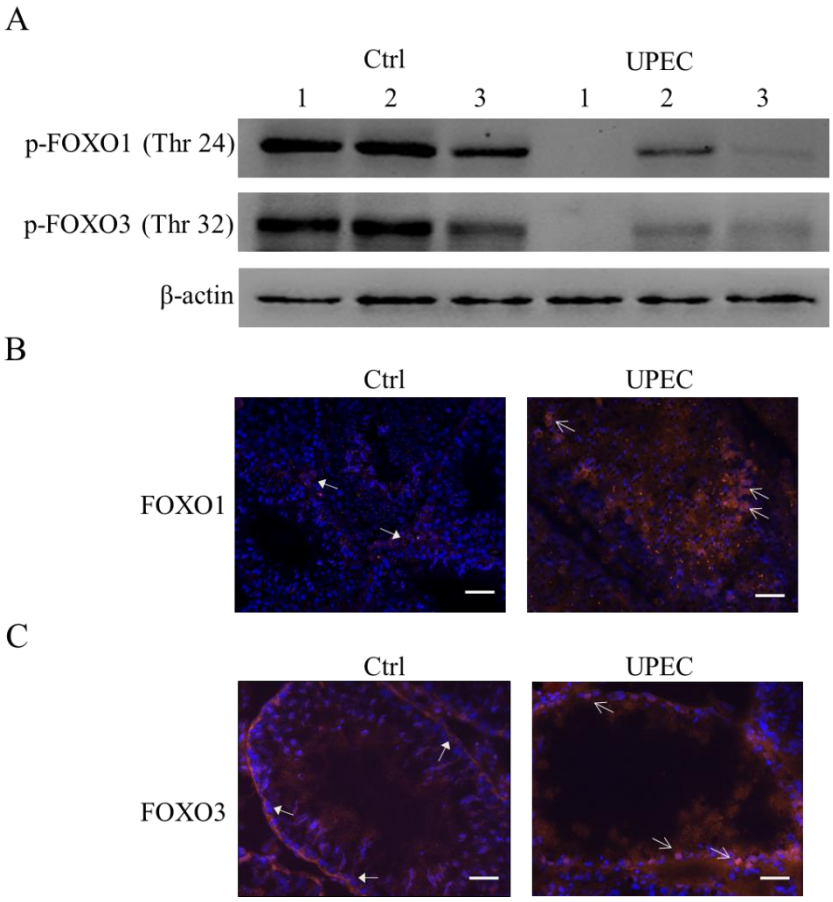

Figure 7: FOXOs were activated following AKT inhibition *in vivo*. (A) Testis homogenates of sham control (Ctrl) and UPEC treated groups were separated by SDS-PAGE (n=3, 50 µg) and immunoblots were probed with p-FOXO1 (Thr 24), p-FOXO3 (Thr 32) and ß-actin as loading control. (B, C) Cryosections of sham control testis (Crtl) and testis collected 7 d after UPEC infection were probed with (B) FOXO1 and (C) FOXO3 antibodies. Primary antibodies were visualized with Cy3-labeled secondary antibodies and nuclei were counterstained with DAPI. Micrographs were taken using an Axioplan 2 fluorescence microscope (Carl Zeiss, ×20 objective lens) and representative figures are shown. In control group, the arrowheads indicate cells with FOXO1 or FOXO3 cytoplasmic location; whilst the arrowheads indicate cells with positive nuclear staining of FOXO1 or FOXO3 in UPEC treated group. Scale bars= 50 µm.

3.3 UPEC virulence factor α-hemolysin suppresses the AKT survival signaling pathway in Sertoli cells

The fact that in our previous study substantial necrotic changes were seen in Sertoli cells in UPEC infected testis (Lu et al., 2013) and FOXO immunofluorescence was visible predominantly in the nuclei of Sertoli cells in this tissue (Figure 8A, B),

prompted to examine whether the UPEC pore forming virulence factor α-hemolysin is involved in Sertoli cell death by attenuation of the AKT survival pathway. Therefore, isolated rat Sertoli cells were infected *in vitro* with UPEC strains expressing α-hemolysin (UPEC 536) and a mutant with deletion of both α-hemolysin genes in UPEC 536 (HDM = hemolysin double mutant).

UPEC completely abrogated AKT phosphorylation (Ser 473) after 4 h post infection, whilst infection with HDM showed no change after 4 h and a marked increase of AKT phosphorylation 6 h post infection (Figure 9A, B). To verify the role of α-hemolysin in AKT dephosphorylation, Sertoli cells were challenged with UPEC in calcium free medium with the phosphorylation status of AKT remaining unchanged (Figure 9 C).

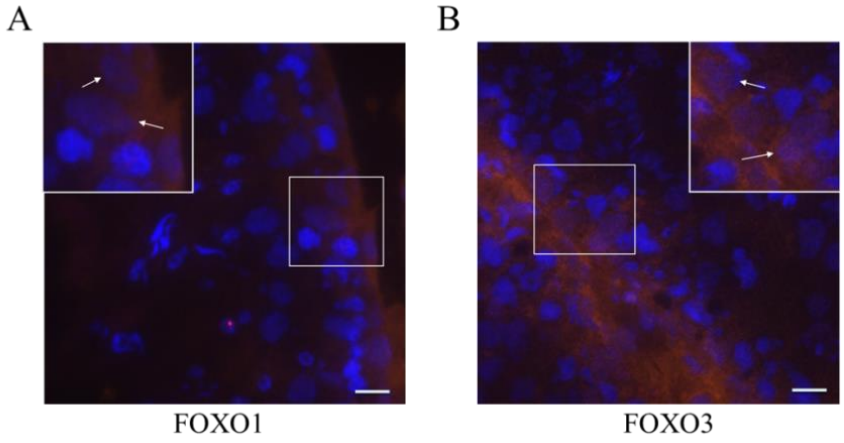

Figure 8: Localization of FOXO1 and FOXO3 in Sertoli cells using an *in vivo* acute bacterial orchitis model. UPEC infected testicular cryosections were probed with FOXO1 (A) and (B) FOXO3 antibodies followed by detection with Cy3-labeled secondary antibody. Nuclei were counterstained with DAPI. Sertoli cells were identified according to nuclear morphology and localization within the seminiferous epithelium. Images were taken using an Axioplan 2 fluorescence microscope (Carl Zeiss, ×40 objective lens) and representative figures are shown. Arrowheads indicate Sertoli cells with positive nuclear FOXO1 or FOXO3 staining. Scale bars =20 μm.

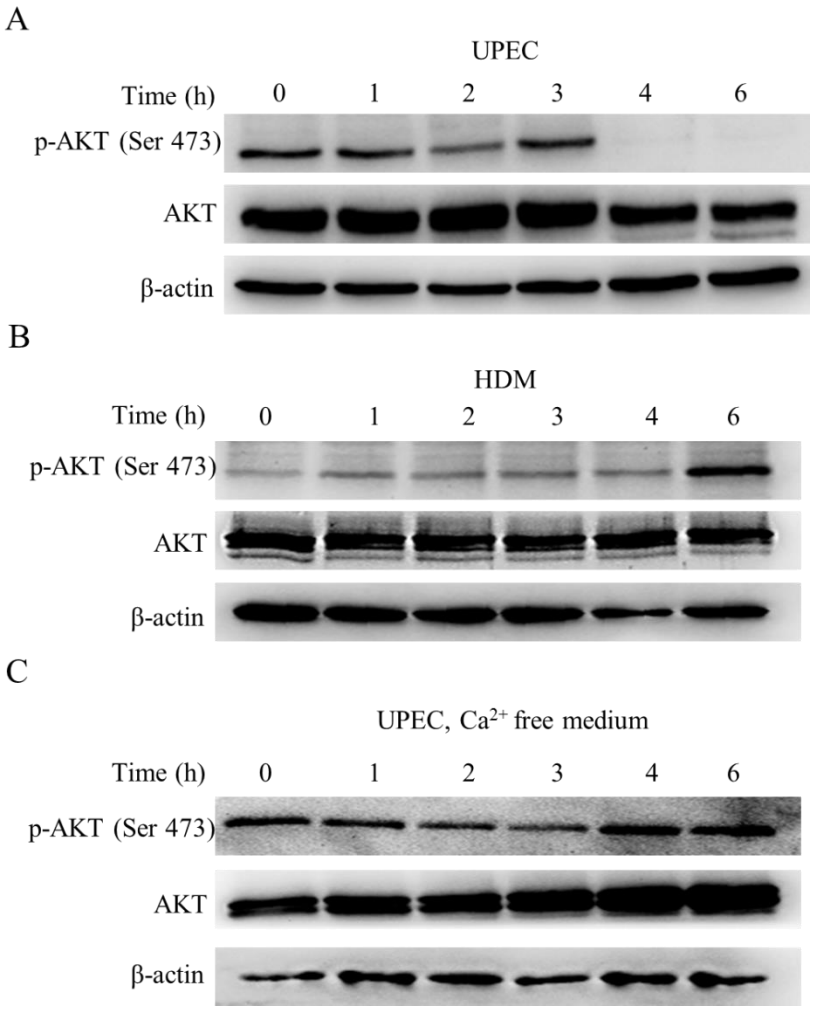

Figure 9: α-hemolysin is the responsible UPEC virulence factor for inactivation of the AKT signaling pathway in isolated Sertoli cells. (A) Sertoli cells were treated with UPEC MOI: 0.01 for the indicated time periods. Protein extracts (20 µg) were separated by SDS-PAGE and immunoblots were probed with p-AKT (Ser 473) and total AKT. (B) Sertoli cells were treated with HDM MOI: 0.01 for the indicated time points. Extracts of whole cell lysates (20 µg) were immunoblotted for p-AKT (Ser 473) and total AKT. (C) AKT dephosphorylation caused by UPEC infection is calcium dependent. Sertoli cells were incubated in calcium free medium 1 h prior infection with UPEC (MOI: 0.01) for the indicated time periods. Total cell lysates were subjected to Western blot analysis using antibodies against p-AKT (Ser 473) and total AKT. (A-C) Detection of β-actin served as loading control. Data are representative of three independent experiments.

3.4 UPEC virulence factor α-hemolysin suppresses the AKT survival signaling pathway in both peritubular myoid cells and 5637 cells

In order to determine whether AKT dephosphorylation represents a cell specific event or a more general phenomenon, testicular peritubular myoid cells and a uroepithelial cell line (5637) were treated with UPEC. Both cell types serve as models for UPEC target cells organs typically reached in infection (urinary tract, testis). In both cases UPEC infection ablated AKT activation, indicating a more general phenomenon (Figure 10A, B).

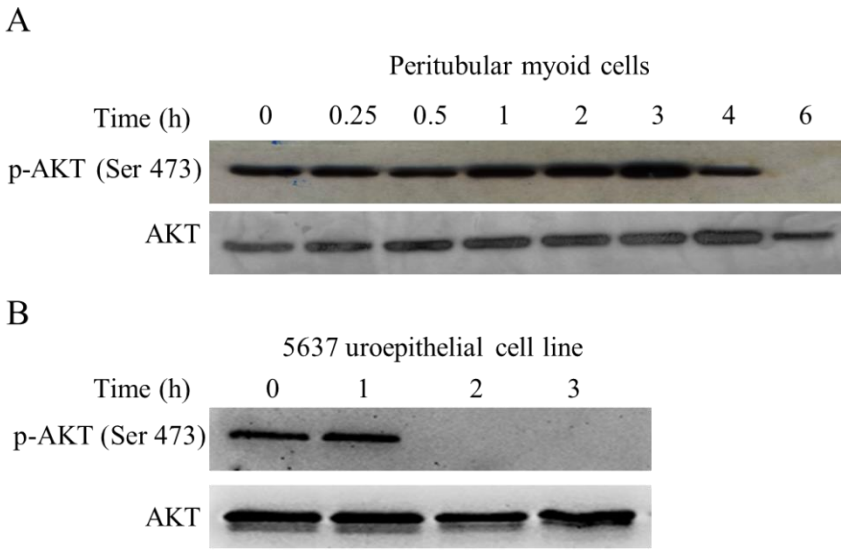

Figure 10: UPEC infection inhibits the AKT signaling pathway in isolated peritubular myeloid cells and 5637 cells. (A) Peritubular myeloid cells were treated with UPEC (MOI: 0.01) for the indicated time periods. Protein extracts (20 µg) were separated by SDS-PAGE and immunoblots were probed with p-AKT (Ser 473) and total AKT. (B) 5637 cells were treated with UPEC (MOI: 1) for the indicated time periods. Protein extracts were separated by SDS-PAGE and immunoblots were probed with antibodies against p-AKT (Ser 473) and total AKT. AKT detection served as loading control.

3.5 Dephosphorylation of FOXOs following AKT inhibition in Sertoli cells after UPEC infection

In order to investigate if FOXOs are also activated in testicular Sertoli cells following AKT suppression similar to the observation in testis, FOXO1 and FOXO3 levels were examined by Western blot analysis. Immunoblot data revealed that phosphorylation of FOXO1 (Thr 24), FOXO1 (Ser 253), FOXO3 (Thr 32), and FOXO3 (Ser 256) were barely detectable in isolated Sertoli cells 4 h after UPEC infection (Figure 11A, B). Analysis of the phosphorylation status of FOXO4 (Thr 28) demonstrated a similar result (Figure 12C).

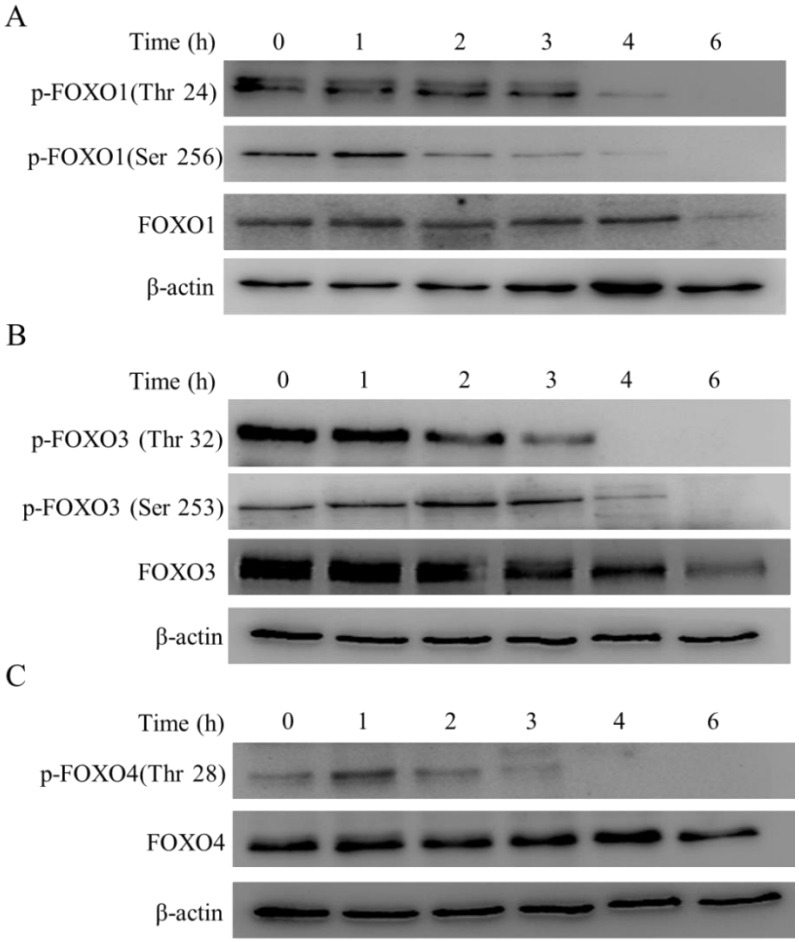

Figure 11: UPEC induce dephosphorylation of FOXO family proteins in isolated Sertoli cells. (A, B, C) Sertoli cells were challenged with UPEC for the indicated time periods. Extracts of whole cell lysates (20 µg) were subjected to Western blot analysis using antibodies against p-FOXO1 (Thr 24), p-FOXO1 (Thr 256) FOXO1, p-FOXO3 (Thr 32), p-FOXO3 (Thr 253), FOXO3, p-FOXO4 (Thr 28), and FOXO4. β-actin served as loading control.

3.6 Nuclear accumulation of FOXOs after UPEC treatment in Sertoli cells

In order to investigate the subcellular localization of FOXOs following dephosphorylation of AKT dependent lysine or serine sites, we have performed immunofluorescence analysis. As shown in Figure 12, FOXO1, FOXO3, and FOXO4 accumulated in nuclei of Sertoli cells 4 h after exposure to UPEC, indicating that they are transcriptionally active.

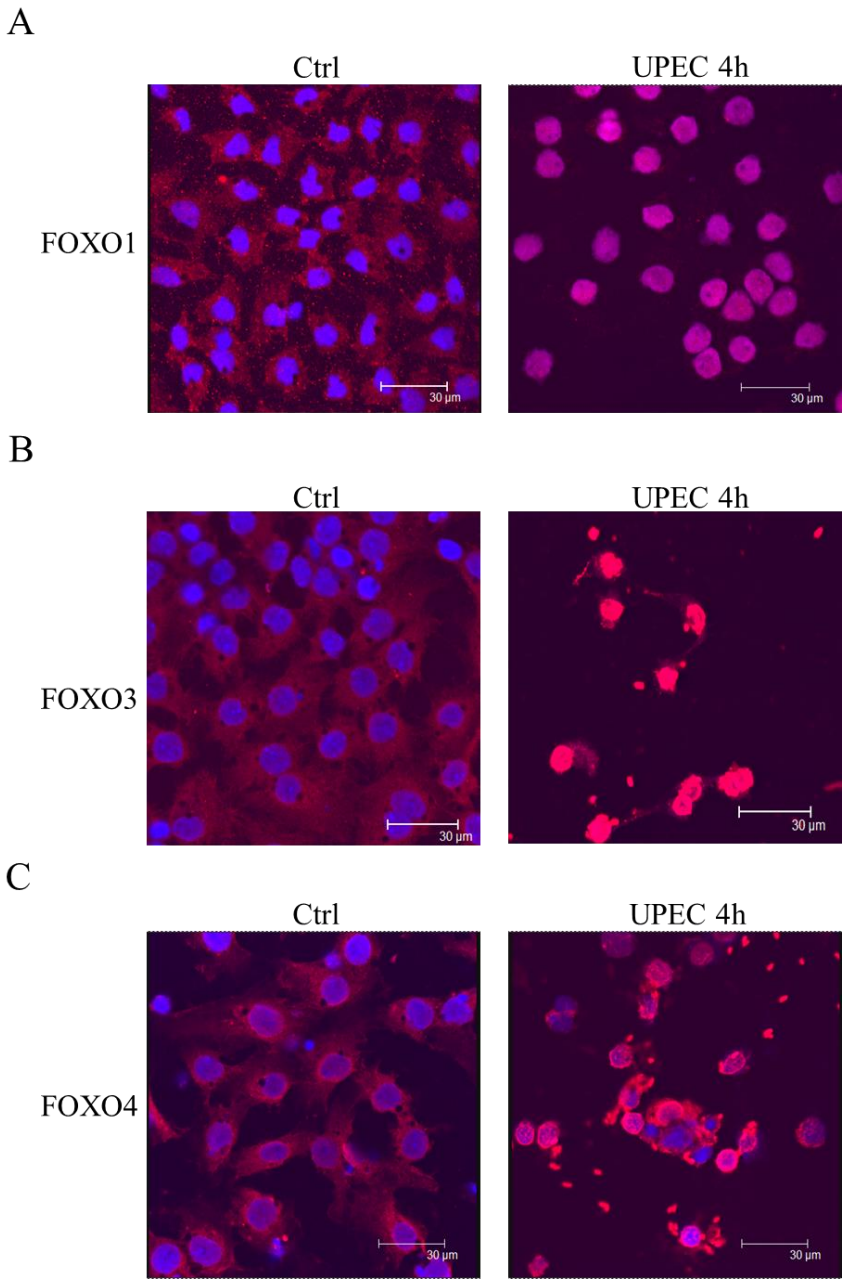

Figure 12: UPEC induce nuclear accumulation of FOXO family proteins. UPEC infection causes (A) FOXO1 (B) FOXO3 and (C) FOXO4 nuclear accumulation in Sertoli cells. Cells were incubated with UPEC or RPMI medium alone as control (Crtl) for 4 h. Immunofluorescence staining was performed for FOXO1, FOXO3 and FOXO4, and visualized using Cy3 labeled secondary antibodies. Nuclei were counterstained with Cy5-conjugated TO-PRO-3 dye. Images were visualized using TCS SP2 confocal laser-scanning microscope (Leica Microsystems, Germany). The representative images are shown.

3.7 The DNA binding activity of FOXO1 increases following UPEC treatment in Sertoli cells

To verify if FOXOs are indeed transcriptionally active following dephosphorylation and nuclear accumulation, the DNA binding activity was measured. FOXO1 DNA binding activity was significantly increased 4 h post UPEC infection in Sertoli cells, compared to control and 2 h UPEC infection.

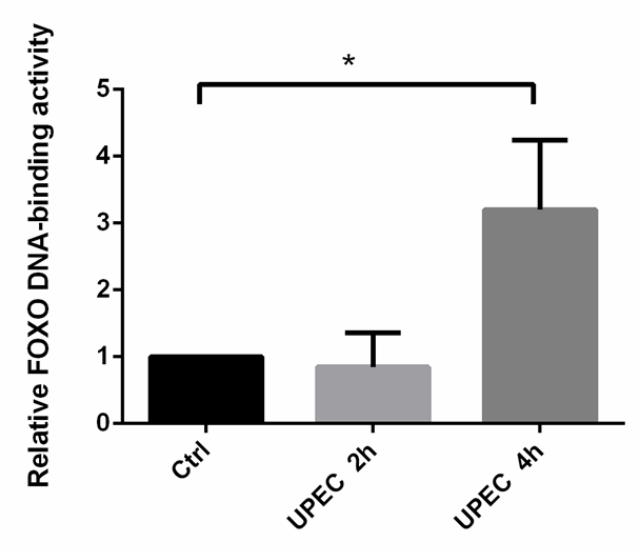

Figure 13: UPEC increase FOXO1 DNA binding activity. Sertoli cells were incubated with UPEC (MOI: 0.01) for the indicated time points or medium alone as control (Ctrl). DNA binding activity of FOXO1 was measured in nuclear extracts using the Trans-AM FKHR kit. Data are shown as mean ± SD of three independent experiments. Statistical analysis was performed using one-way ANOVA to determine the significant difference. *$p<0.05$.

3.8 FOXO signaling pathway is not activated by HDM infection

Next, we sought to determine whether the UPEC virulence factor HlyA is responsible for activation of FOXOs. Therefore, isolated rat Sertoli cell were incubated with HDM. Treatment with HDM failed to inactivate AKT signaling,

instead markedly increased the phosphorylation of AKT 6 h after infection. Consequently, an increase of phosphorylation of FOXO1 (Thr 24) and FOXO4 (Thr 28) was observed 6 h post HDM infection. Changes in the phosphorylation status of other AKT dependent sites including FOXO1 serine 256, FOXO3 threonine 32 and serine 253 were not visible. Together these results strongly propose a role for the UPEC virulence factor α-hemolysin in activation of FOXO transcription factors in Sertoli cells.

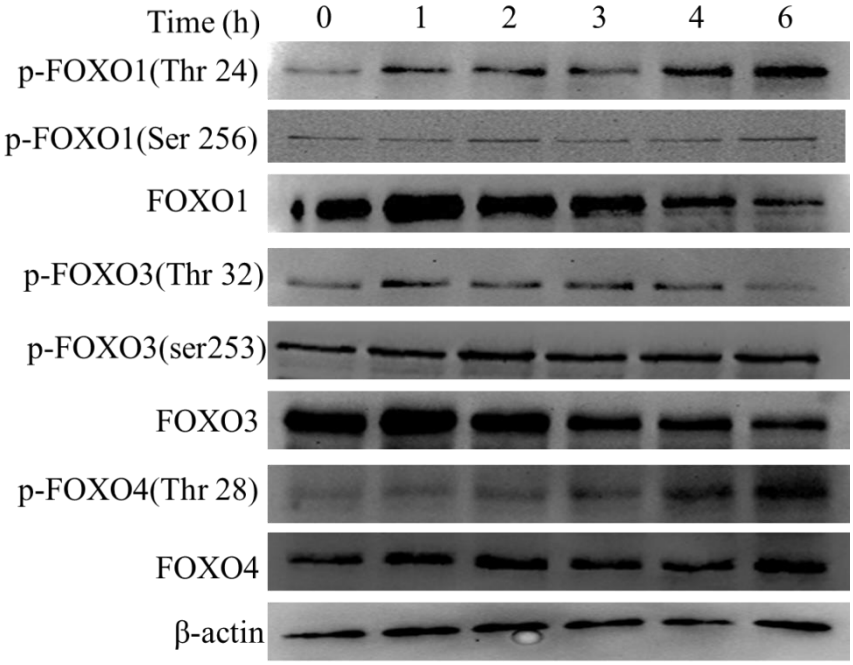

Figure 14: FOXOs remain phosphorylated after HDM infection. Sertoli cells were challenged with HDM (MOI: 0.01) for the indicated time periods. Whole cell lysates (20 µg) were subjected to Western blot analysis using antibodies against p-FOXO1 (Thr 24), p-FOXO1 (Ser 256), FOXO1, p-FOXO3 (Thr 32), p-FOXO3 (Ser 253), FOXO3, p-FOXO4 (Thr 28) and FOXO4. β-actin was probed to ensure equal protein loading.

3.9 SOD2 and catalase are not upregulated after UPEC treatment

FOXOs accumulated in the nucleus can bind to promoters or enhancers to regulate expression of genes involved in apoptosis, ROS detoxification, DNA repair and cell cycle arrest. It recently has been reported that *Porphyromonas gingivalis*, a prominent periodontal and emerging systemic pathogen, could activate FOXO transcription factors to control oxidative stress responses by upregulation of superoxide dismutase 2 (SOD2) and catalase (Wang et al., 2015). The upregulation of SOD2 and catalase by the FOXO family could detoxify ROS as a cell survival strategy (Kops et al., 2002; Storz, 2011). Therefore, as the next step, we investigated the expression levels of these enzymes by qRT-PCR and Western blot analysis. Surprisingly, protein and mRNA expression levels of FOXO target gene SOD2 and catalase were not regulated by UPEC infection at any of the investigated time points.

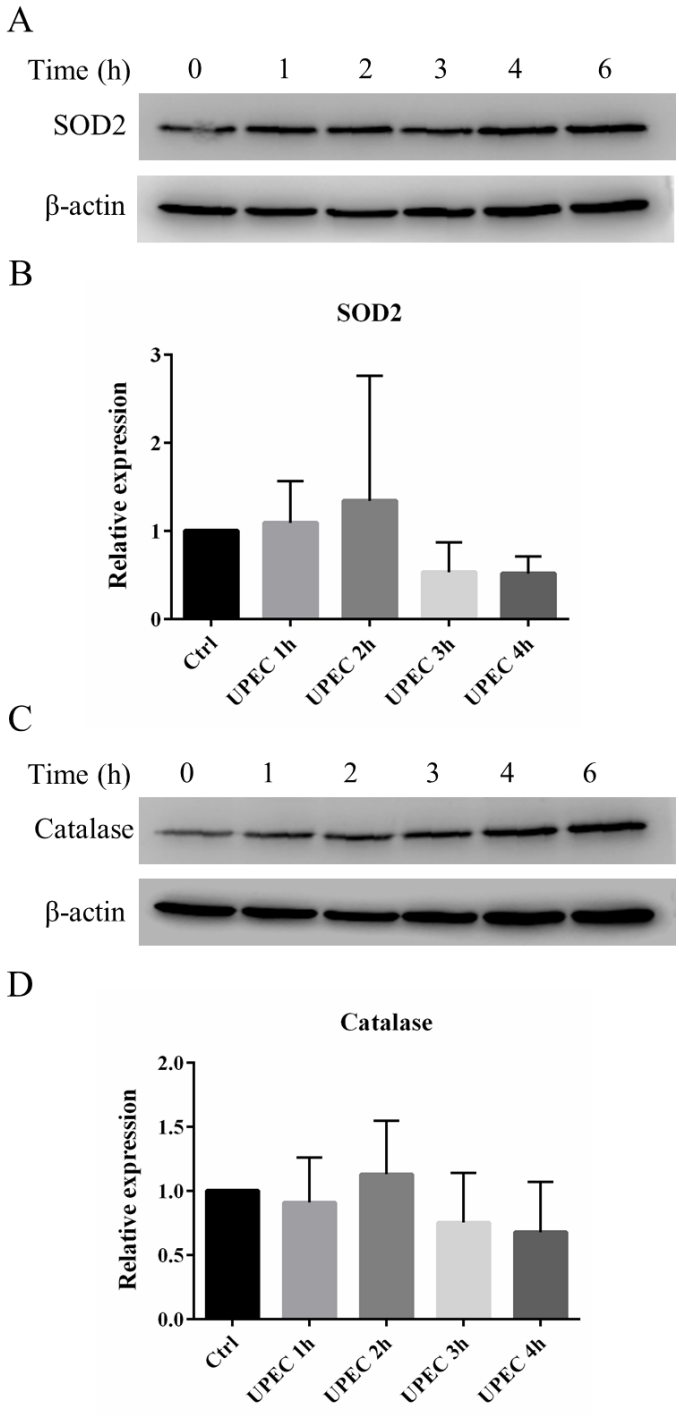

Figure 15: FOXO dependent genes SOD2 and catalase are not upregulated after UPEC treatment. SOD2 (A, B) and catalase (C, D) are not upregulated both at protein and mRNA level. Sertoli cells were infected with UPEC (MOI: 0.01) for the indicated time periods. Whole cell lysates (20 µg) were immunoblotted for SOD2, catalase, and β-actin. β-actin used as loading control. The total RNA was isolated from cells treated with UPEC (MOI: 0.01) at the indicated time periods. The amounts of SOD2 and catalase mRNA were quantified by qRT-PCR. Results were normalized to expression levels of β-2-microglobulin. All data are shown as mean ± SD of at least three independent experiments. Statistical analysis was performed using one-way ANOVA to determine the significance of the differences. Differences were considered to be significant when $p<0.05$.

3.10 FOXO dependent genes involved in cell cycle arrest and DNA repair are not regulated after UPEC treatment

It has also been demonstrated that FOXOs are associated with cell cycle arrest by regulating a set of genes involved in cell cycle progression. However, mediators of cell cycle arrest such as p27kip1, p15INK4B, cyclin D1 and cyclin D3 were not regulated in Sertoli cells after UPEC treatment as demonstrated by Western blot analysis (Figure 16A). Similarly, another FOXO target gene Gadd45α, involved in DNA repair, also did not show any significant change at the mRNA level (Figure 16B).

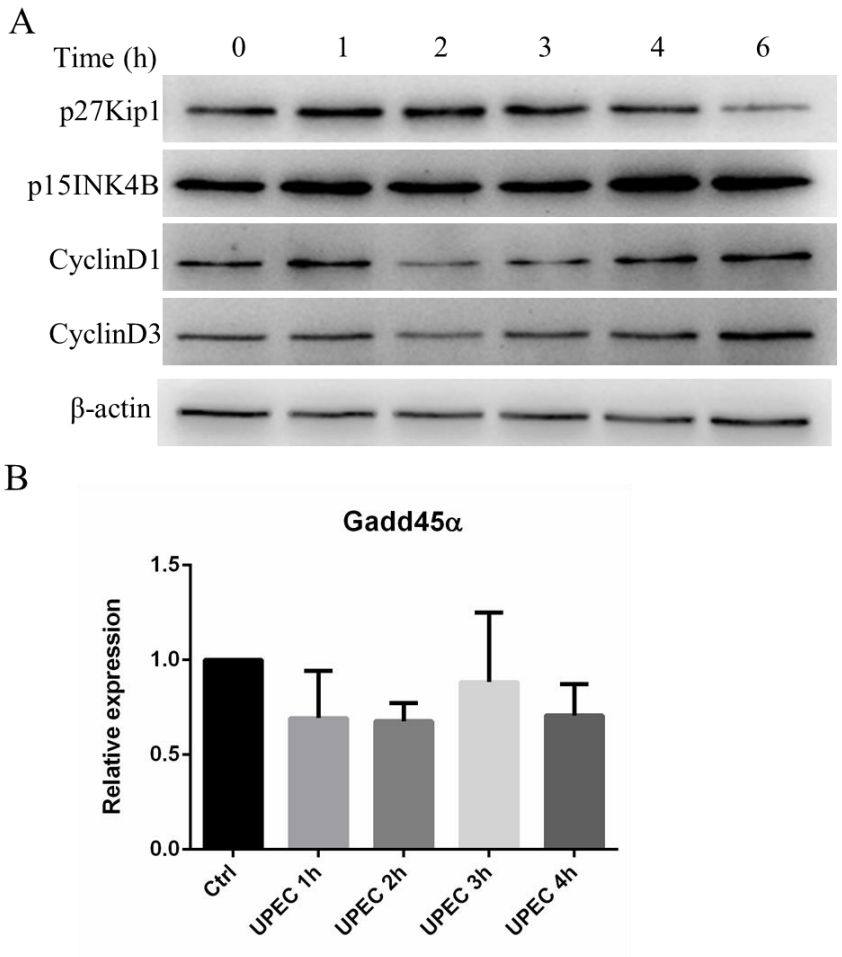

Figure 16: FOXO target genes involved in cell cycle arrest and DNA repair were not regulated at the expression level. (A) Sertoli cells were infected with UPEC (MOI: 0.01) for the indicated time periods. Extracts of whole cell lysates were separated by SDS-PAGE and immunoblots were probed

with antibodies directed against p27Kip1, p15INK4B, cyclin D1 and cyclin D3. β-actin detection served as loading control. (B) Sertoli cells were infected with UPEC (MOI: 0.01) for the indicated time periods. mRNA levels of Gadd45α were assessed by qRT-PCR. Results were normalized to expression levels of β-2-microglobulin. Presented data are shown as mean ± SD of at least three independent experiments. One-way ANOVA was performed to determine the significance of the differences. Differences were considered to be significant when $p<0.05$.

3.11 Expression of the pro-apoptotic gene *BIM* is not increased after UPEC treatment

We hypothesized that FOXOs could induce BIM to induce apoptosis in Sertoli cells. Yet, Western blot data did not show any significant change of BIM at the protein level (Figure 17A). However, the mRNA level somewhat reduced, albeit not statistically significant (Figure 17B).

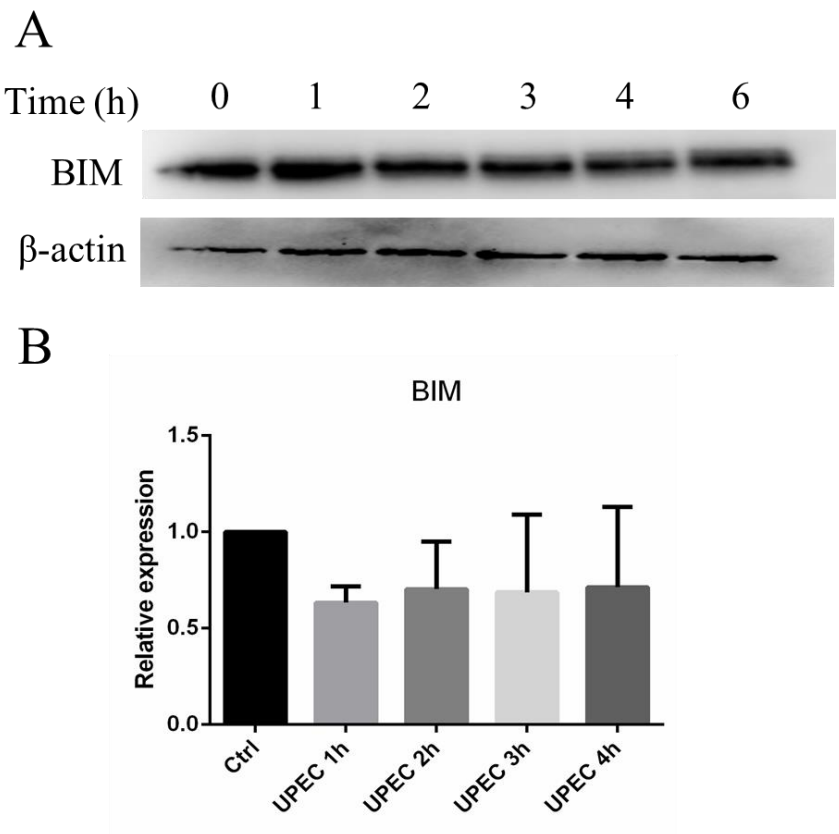

Figure 17: Expression of the pro-apoptotic gene *BIM* was not regulated after UPEC treatment. (A, B) BIM is not upregulated both at the protein and mRNA levels. Sertoli cells were infected with

UPEC MOI: 0.01 at the indicated time periods. Protein extracts were immunoblotted for BIM and β-actin. β-actin was used to ensure equal protein loading. The mRNA level of BIM was assessed by qRT-PCR. Results were normalized to expression levels of β-2-microglobulin. Presented data are shown as mean ± SD of at least three independent experiments. Statistical analysis was performed using one-way ANOVA to determine the significance of the differences. Differences were considered to be significant when $p<0.05$.

3.12 FOXOs were activated by the PI_3K inhibitor

In spite of the nuclear translocation of FOXO and enhanced DNA binding activity following UPEC infection, no significant increase in the expression of FOXO target genes was evident. Hence, it was investigated determine whether this phenomenon was specific to the investigated cell type or can be attributed to the pathogen independent of the infected cell type. Therefore, Sertoli cells were treated with the PI3-kinase/AKT inhibitor LY249002 and subsequently analyzed for AKT phosphorylation. As shown in Figure 18A, levels of phosphorylated AKT were prominent at 0 h, but were undetectable at 16 and 24 h after treatment. Concomitantly, FOXO1 and FOXO3 were found to be dephosphorylated (Figure 18B).

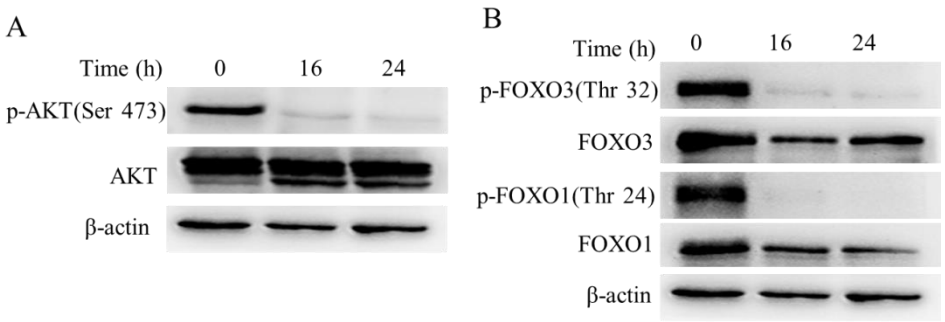

Figure 18: FOXOs are activated following AKT inhibition by PI3K inhibitor in Sertoli cells. (A, B) Sertoli cells were treated with the PI3K inhibitor LY249002 (50 μM) at the indicated time points. Protein extracts were subjected for Western blot analysis using antibodies against p-AKT (Ser 473), AKT, β-actin, p-FOXO1 (Thr 24), p-FOXO3 (Thr 32), FOXO1, FOXO3 and β-actin. β-actin was probed to ensure equal protein loading.

3.13 BIM is upregulated by the PI_3K inhibitor, but suppressed by UPEC infection

Of note, the protein levels of the FOXO target genes *SOD2*, *Catalase*, and *p27KIP1* remained unchanged as examined by Western blot analysis (Figure 19A). In contrast, protein and mRNA expression levels of BIM were significantly increased 16 and 24 h after LY249002 treatment (Figure 19B, C). To investigate this further, Sertoli cells were treated with LY249002 for 12 h followed by treatment with UPEC for 4 h. Remarkably, UPEC significantly suppressed LY249002-induced expression of BIM (Figure 19C). Because Sertoli cells are resistant to apoptosis (unpublished data from Dr. Sudhanshu Bhushan), the uroepithelial cell line 5637 was challenged with LY249002 for 13 h followed by treatment with UPEC for 3 h. Intriguingly, UPEC significantly suppressed LY249002 induced apoptosis as shown in Figure 19D.

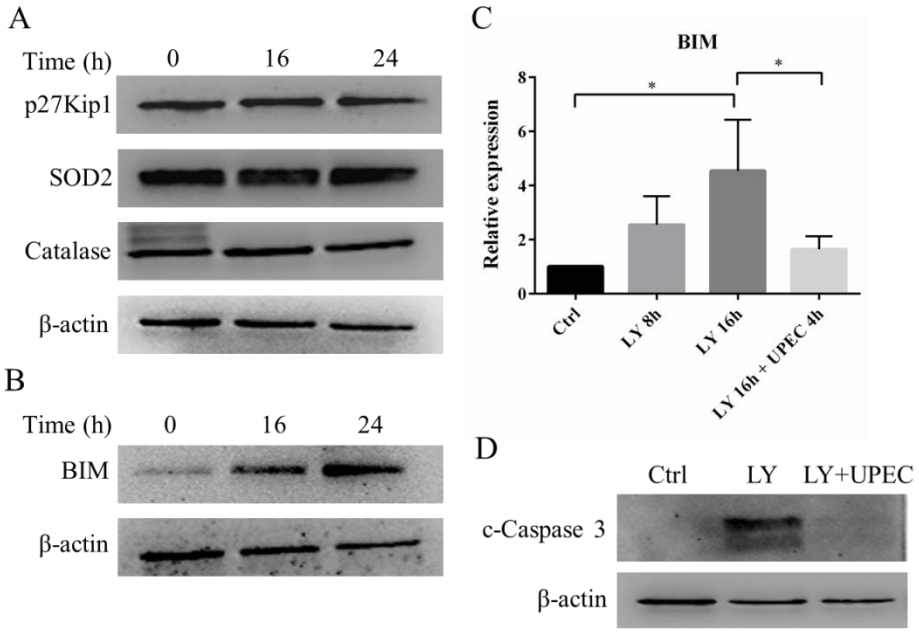

Figure 19: BIM is unregulated by the PI3K inhibitor in Sertoli cells. (A, B) Sertoli cells were treated with the PI3K inhibitor LY249002 (50 µM) at the indicated time points. Protein extracts were subjected to Western blot analysis using antibodies against SOD2, p27kip1, catalase and BIM. β-actin was probed to ensure equal protein loading. (C) Sertoli cells were treated with LY249002 (50 µM) 12 h prior to UPEC infection for another 4 h (MOI: 0.01). The amount of BIM mRNA was quantified by

qRT-PCR. Results were normalized to expression levels of β-2-microglobulin. Data are shown as mean ± SD. Presented data are representative for three independent experiments. Statistical analysis was performed using one-way ANOVA to determine the significance of the differences. *$p<0.05$. (D) 5637 cells were pre-treated with LY249002 (50 μM) for 13 h followed by co-incubation with UPEC (MOI:1) for another 3 h. Cell lysates (20 μg) were subjected to Western blot analysis using antibodies against cleaved-caspase 3 and β-actin. β-actin served as loading control.

3.14 The status of CpG islands within the promoter region of BIM remains unmethylated after UPEC treatment

It has been reported that the CpG islands within the promoter region of BIM can be methylated in order to silence BIM expression as a survival strategy utilized by viruses or cancer cells(Bachmann et al., 2010; Paschos et al., 2009; Piazza et al., 2013). Similarly, Tolg et al have shown that UPEC infection provokes down-regulation of *CDKN2A* (p16INK4A) by inducing CpG island methylation (Tolg et al., 2011). As the expression level of BIM mRNA was down-regulated after UPEC exposure, the methylation status was analyzed at various sites at the BIM promoter region as a possible mechanism using bisulphite sequencing (Figure 20A). The performance of all used primer pairs was validated prior testing. A representative analysis of CpG1 primers is shown (Figure 20B). The methylation profile at the BIM promoter region in Sertoli cells did not change after UPEC infection (Figure 20C). As a positive control *in vitro* methylated rat genomic DNA was used.

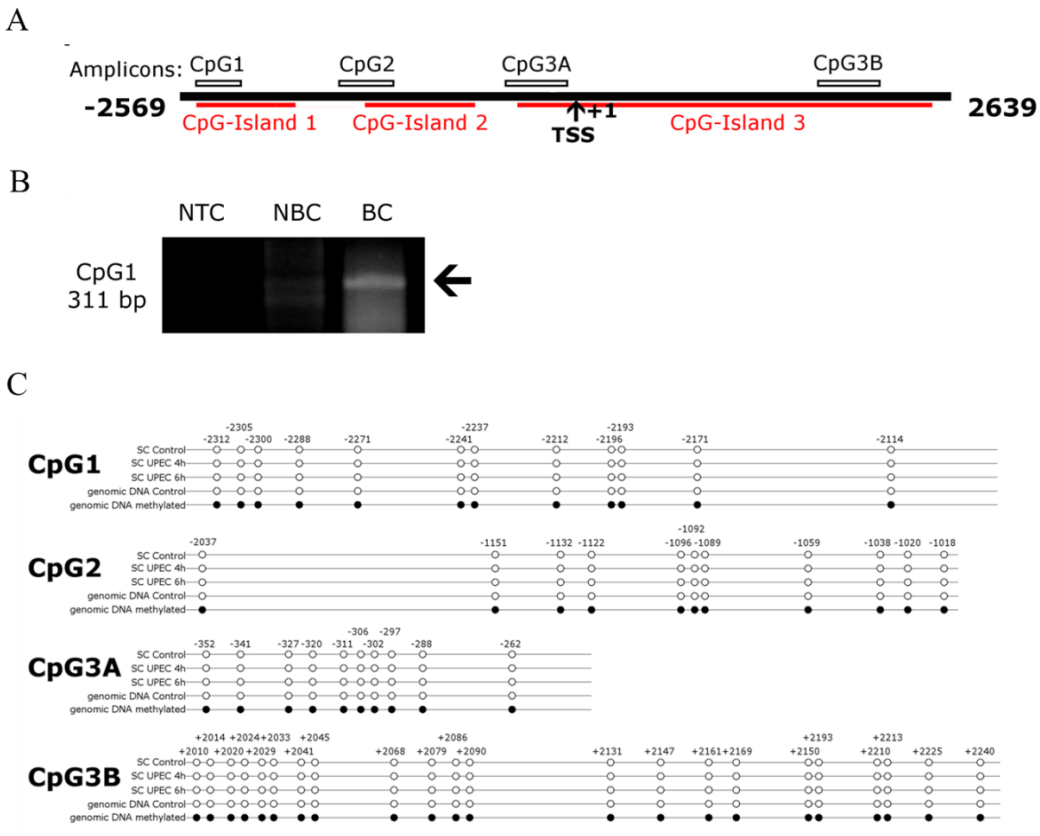

Figure 20: Infection of Sertoli cells with UPEC has no effect on the methylation status of the BIM-promoter. Sertoli cells were treated with UPEC for 4 and 6 h (MOI: 0.01). After harvesting the cells, genomic DNA was isolated following bisulfite conversion of non-methylated CpGs. Four areas of the BIM promoter in those converted samples were analyzed by sequencing. (A) A schematic overview of the CpG-Islands (defined by http://cpgislands.usc.edu/) within the BIM promoter relative to the transcription start site (TSS) is shown. Amplified and analyzed regions are indicated as CpG1, CpG2, CpG3A and CpG3B. (B) The performance of all used primer pairs was verified. A representative analysis of CpG1-fw + CpG1-rv is shown. The expected 311 bp product is only visible for bisulfite converted DNA (BC). The "no template control" (NTC) and the "non bisulfite control" (NBC) do not show this product. (C) Methylation status and distance from TSS for tested CpGs is shown for different treatments. Filled (black) circles correspond to methylated CpGs, unfilled (white) circles correspond to unmethylated CpGs. Experiments and analysis were performed 3 times. To show method´s competence of detecting methylated CpGs (positive control) untreated testicular rat DNA was analyzed and compared to *in vitro* methylated testicular rat DNA.

3.15 UPEC, but not HDM deacetylate both histone 3 and 4

Next, we evaluated the changes of global histone acetylation by Western blotting. Of note, UPEC infection completely abrogated global histone 3 (H3) and histone (H4)

acetylation in Sertoli cell extracts 4 h post-treatment. In contrast, challenge with HDM did not cause any changes in the global acetylation status of histone 3 and histone 4 (Figure 21A, B).

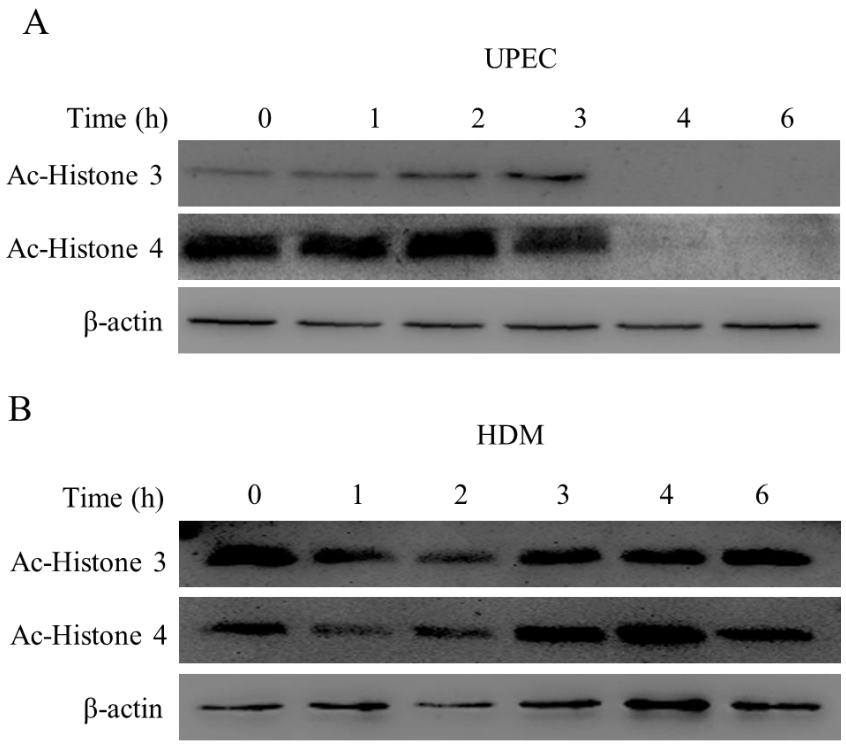

Figure 21: Infection with UPEC, but not HDM caused global deacetylation of both histone 3 and 4. (A, B). Sertoli cells were treated with UPEC or HDM (MOI: 0.01) for the indicated time periods. Protein extracts (20 µg) were separated by SDS-PAGE and immunoblots were probed with antibodies against acetylated histone 3 and acetylated histone 4. Detection of β-actin served as loading control.

3.16 Acetylation of histone 3 and 4 decreased in UPEC infected testis

The acetylation status of histone 3 and 4 were further investigated in UPEC elicited orchitis. The immunofluorescence data using acetylated histone 3 and histone 4 antibodies indicated that a decrease in UPEC infected testis in comparison to mock infected testis. These results confirmed that UPEC can deacetylate histone 3 and

histone 4 *in vitro* as well as *in vivo*.

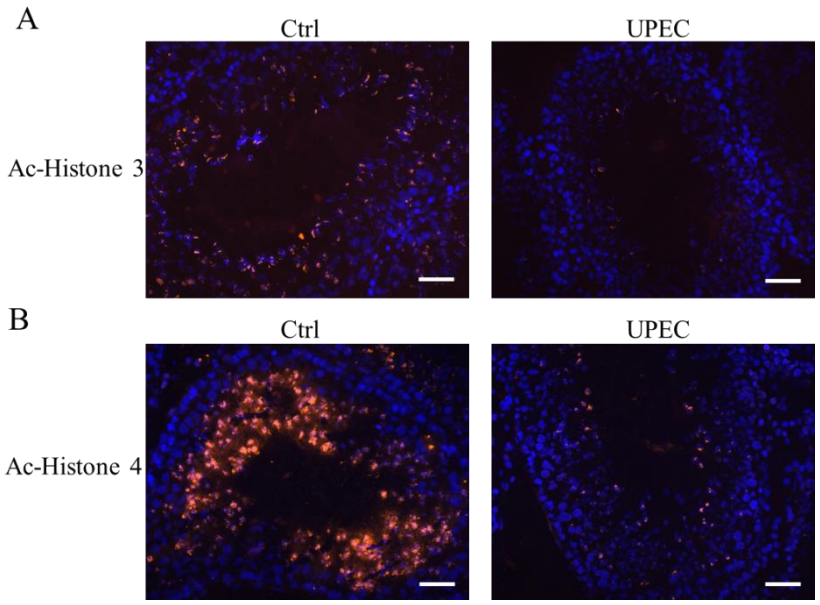

Figure 22: UPEC infection caused a global decrease of histone 3 and histone 4 acetylation. (A, B) Cryosections of sham control testis (Crtl) and testis collected 7 d after UPEC infection were probed with antibodies direct against acetylated histone 3 and acetylated histone 4. Primary antibodies were visualized with Cy3-labeled secondary antibodies and nuclei were counterstained with DAPI. Micrographs were taken using an Axioplan 2 fluorescence microscope (Carl Zeiss, ×20 objective lens). The representative images are shown. Scale bars= 50 µm.

3.17 The decrease of histone 4 acetylation at the BIM promoter region is associated with a suppression of BIM expression after UPEC infection

In order to unravel the underlying mechanism how UPEC suppress the expression of BIM – in spite of activated FOXOs -ChIP analysis was performed using acetylated histone 3 and histone 4 antibodies. The acetylation status of histone 4 was decreased after UPEC treatment in comparison with control at the BIM promoter region (Figure 23A). However, the acetylation of histone 3 did not change significantly (Figure 23B). Taken together, UPEC suppress BIM transcription by decreasing histone 4 acetylation at its promoter region.

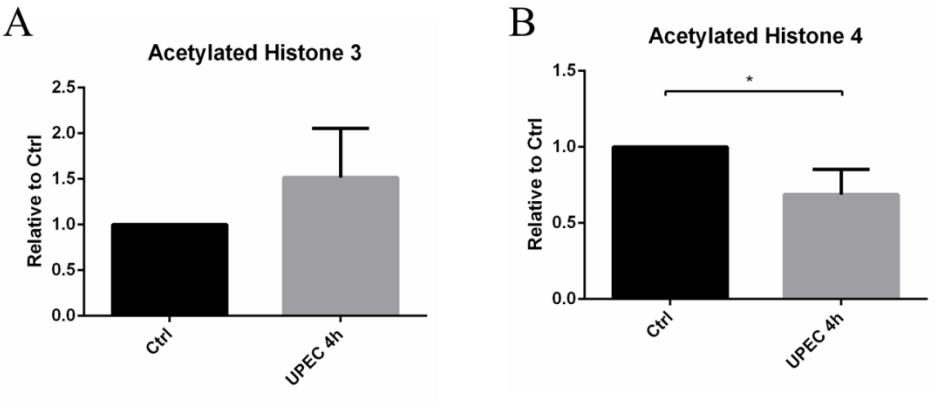

Figure 23: UPEC suppress BIM expression by deacetylation of histone 4 at the promoter region. (A, B) UPEC challenge caused deacetylation of histone 4 at the BIM promoter region. Sertoli cells were treated with UPEC (MOI: 0.01) for 4 h and then subjected to ChIP assay. Immunoprecipitated DNA associated with acetylated histone 3 and 4 were assayed by qPCR. The graphs represent percentage changes of fold enrichment relative to input chromatin for the UPEC treated group in comparison to the control group. Data are shown as mean ± SD. Presented data are representative for three independent experiments. Statistical analysis was performed using Student's t-test to determine the significance of the differences. *$p<0.05$.

3.18 Acetate partially rescues histone 3 and 4 deacetylation after UPEC infection

In the nuclei of mammalian, citrate is catalyzed to acetyl coenzyme A to provide acetyl groups for histone acetylation by an ATP-dependent-lyase (ACLY) (Choudhary et al., 2014). The activity of ACLY is controlled by AKT-dependent phosphorylation. As shown above activation of AKT was attenuated by UPEC in infected Sertoli cells. Therefore, it was hypothesized that attenuation of AKT will results in dephosphorylation of ACLY. Surprisingly, the expression of phosphorylated ACLY was not detectable in Sertoli cells. In a next step, Sertoli cells were treated with UPEC and sodium acetate (a metabolite that can be catalyzed to acetyl coenzyme A independent of AKT activity). Western blot results showed that the deacetylation of histone 3 and histone 4 were rescued 4 h and 6 h post UPEC infection by adding acetate (Figure 24). Taken together, these results indicate that UPEC can decrease

acetyl coenzyme A level to cause deacetylation of histone 3 and histone 4.

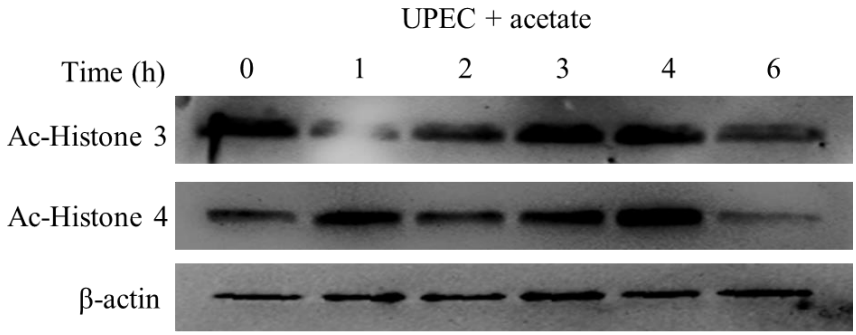

Figure 24: Supplement of acetate rescued histone 3 and histone 4 deacetylation after UPEC infection. Sertoli cells were treated with UPEC (MOI: 0.01) and sodium acetate (5 mM) for the indicated time periods. Protein extracts (20 µg) were prepared in SDS lysis buffer and equal amounts of protein were separated by electrophoresis on SDS-PAGE. Immunoblots were probed with antibodies recognizing acetylated histone 3, acetylated histone 4 and β-actin. β-actin detection served as general loading control.

3.19 UPEC inhibit ACLY activity thus inducing deacetylation of histone 3 and 4

In order to test the hypothesis that suppression of AKT/ACLY signaling pathways by UPEC can result in histone 3 and histone 4 deacetylation, uroepithelial cells (5637) were treated with UPEC. The immunoblotting data demonstrated that the phosphorylation of ACLY was completely abrogated 2 h after UPEC infection (Figure 25A). Similar to Sertoli cells, addition of acetate rescued histone 3 and histone 4 deacetylation in 5637 cells after UPEC infection (Figure 25B).

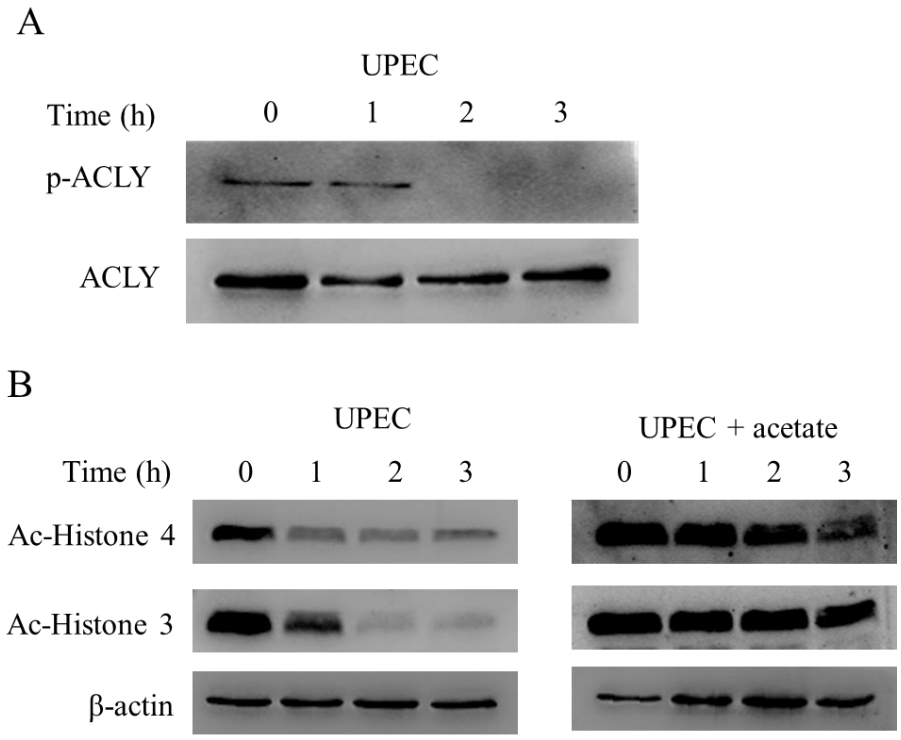

Figure 25: UPEC inhibit ACLY activity and acetylation of histone 3 and histone 4 partially maintained by adding with acetate. (A) Uroepithelia cells (5637) were treated with UPEC (MOI: 1) for the indicated time periods. Protein extracts (20 µg) were separated by SDS-PAGE. Immunoblots were probed with antibodies direct against p-ACLY (Ser 455) and ACLY. Detection of ACLY served as loading control. (B) 5637 cells were treated with UPEC MOI: 1 with/out sodium acetate (5mM) for the indicated time periods. Protein extracts (20µg) were subjected to Western blot analysis using antibodies against acetylated histone 3 and acetylated histone 4. β-actin detection was probed to ensure equal protein loading.

4 DISCUSSION

Death of host cells is a well established and obvious consequence of host-pathogen interaction during infection. Emerging data demonstrate that cell death caused by microbial infection often does not constitute an ancillary phenomenon, but is a controlled and adjustable process by the host to eliminate pathogens, clear damaged cells, and limit the spread and magnitude of inflammation. In this regard, apoptosis is an immunologically silent death mode, whereas necrosis represents an inflammatory mode of death (Lamkanfi and Dixit, 2010). During evolution, pathogens have enhanced their ability to persist by developing multiple strategies to manipulate the cell death pathways, primarily to propagate inside the host cell and to avoid host innate immune responses. In this study, it has been demonstrated that the UPEC virulence factor HlyA could manipulate host cell death pathways to facilitate pathogen survival and dissemination. UPEC can suppress the expression of the pro-apoptotic FOXO target gene *BIM* in isolated rat Sertoli cells, although the AKT/FOXO signaling pathway usually leading to BIM synthesis is activated at the same time. Moreover, it has also been confirmed that UPEC-mediated histone deacetylation is associated with BIM suppression, a molecular switch which drives Sertoli cells in necrosis, but prevents apoptosis. Preventing programmed cell death in Sertoli cells as obligatory “nurse cells” for the developing germ cells is essential to maintain or recover spermatogenic potential during or after infectious episodes. This gains particular importance as one Sertoli cell supports a large number of adjacent germ cells.

4.1 UPEC inhibit the AKT signaling pathway *in vivo* and *in vitro*

AKT is comprised of an N-terminal pleckstrin homology (PH) domain, a kinase

domain and a C-terminal regulatory tail, and is activated by many stimuli such as growth factors and cytokines (Hers et al., 2011; Staal, 1987). Following the stimulation by growth factors, the lipid enzyme PI3 kinase signaling pathway is activated, which further causes the generation of phosphatidylinositol-3, 4, 5-phosphate (PIP3) and recruits AKT as well as 3-phosphoinositide-dependent protein kinase 1 (PDK1) to the cell membrane. PIP3 can elicit a conformational change in AKT via binding to the PH domain, consequently enabling the co-recruited PDK1 to access the activation loop of AKT and phosphorylate threonine 308 (Hers et al., 2011). Activated AKT contributes to phosphorylation of a large number of downstream substrates including FOXOs and GSK3β, and is thereby involved in metabolism, growth, cell proliferation, and cell survival (Manning and Cantley, 2007). Data shown in this study demonstrate that UPEC can induce dephosphorylation of AKT serine 473 in isolated rat Sertoli cells 4 h post infection. Similar results are also observed in UPEC-infected rat testes. It has been shown that for maximal activity AKT needs the phosphorylation of serine 473 catalyzed by the mTOR complex 2 (mTORC2) (Zhang et al., 2011). In contrast, the AKT signaling pathway is terminated or inhibited by dephosphorylation of threonine 308 or serine 473. Therefore, in the present study UPEC can abrogate the pro-survival AKT signaling pathway both *in vitro* (isolated rat Sertoli cells) and *in vivo* (UPEC-elicited rat epididymo-orchitis model).

It has been shown that pore formation on cell membranes caused by the UPEC virulence factor HlyA is required for AKT dephosphorylation (Wiles et al., 2008; Wiles and Mulvey, 2013). Besides HlyA from UPEC, other bacterial pore-forming toxins such as aerolysin from *Aeromonas* species and toxin from *Staphylococcus aureus* attenuate the AKT signaling pathway. Therefore, whether AKT is a general target for these pore-forming toxins or a coinciding ‘casualty’ of their toxic effects needs to be further investigated. In general, the pore formation on cell membranes could induce Ca^{2+} influx and decrease cytosolic K^{+}. However, neither chelation of intracellular Ca^{2+} nor supplementation of KCl into cell culture media (preventing K^{+}

leakage) could block UPEC-induced AKT dephosphorylation (Wiles et al., 2008). Therefore, the underlying molecular mechanism still remains elusive. In the same study, it has been shown that protein phosphatase 2A (PP2A) or protein phosphatase 1 (PP1) inhibitors such as calyculin A, tautomycin or okadaic acid, could rescue HlyA-mediated AKT dephosphorylation, suggesting a role for both PP2A and PP1 in this process (Wiles et al., 2008). In agreement with these studies, the results from our study confirmed that UPEC could suppress the AKT signaling pathway 4 h post infection in isolated Sertoli cells. In contast, infection with HDM (hemolysin double mutant) resulted in marked increase of AKT phosphorylation at 6 h post infection. Strikingly, AKT is constitutively active in mock-infected testis in comparison with UPEC-infected testis, indicating that the AKT signaling pathway plays an essential role in testis. As shown by Ostalaza and Goni, HlyA needs to bind to extracellular calcium in order to permeabilize cell membranes (Ostolaza and Goni, 1995). Similarly, we have demonstrated that HlyA requires extracellular calcium to inactivate the AKT signaling pathway. In addition, the ablation of the AKT signaling pathway is more of a general phenomenon, as it has been shown that AKT inhibition by UPEC is not restricted to Sertoli cells. The same phenomenon was also observed in peritubular myoid cells as well as uroepithelial cells (5637 cells). Taken together, these results indicate that the AKT survival signaling pathway was inhibited by UPEC infection.

4.2 FOXOs are activated by UPEC infection

FOXOs function as transcription factor by binding to the conserved consensus core recognition motif TTGTTTAC to regulate specific gene expression programs (Furuyama et al., 2000; Obsil and Obsilova, 2011). FOXOs are negatively regulated by the AKT signaling pathway, whereas they could be activated through the JNK signaling pathway (Essers et al., 2004; Oh et al., 2005; van der Horst and Burgering, 2007; Wang et al., 2005). The phosphorylation of FOXOs by AKT at conserved

threonine and serine sites leads to cytoplasm sequestration and further degradation (Tzivion et al., 2011). Growth factor withdrawal or other factors inhibit AKT signaling, which consequently results in FOXOs nuclear accumulation and activation. In the present study, it has been shown that the UPEC virulence factor HlyA inhibits the AKT signaling pathway, consequently activating downstream FOXO proteins. Moreover, in the UPEC-elicited rat orchitis model, activation of FOXO1 and FOXO3 was documented by their dephosphorylation. The immunofluorescence data further confirmed that the expression of FOXO1 and FOXO3 was observed in the nuclei of testicular cells in the infected testis (Figure 7B, C). Additionally, in this experimental orchitis model, FOXOs are shown to be located in Sertoli cells, which are one of the most important somatic cell types in seminiferous tubules, playing an essential role in both supporting spermatogenesis and maintaining immune tolerance (Kaur et al., 2014). In the mock-infected testis, both FOXO1 and FOXO3 are barely detectable, likely due to the constitutive activation of the AKT signaling pathway. This observation is similar to the study by Goertz and colleagues, in which they demonstrated that FOXO1 was only detectable in undifferentiated spermatogonia, but not in the Sertoli cells or any other somatic cells of the mouse testis, suggesting FOXO1 plays an essential role in maintenance of spermatogonial stem cells and initiation of spermatogenesis (Goertz et al., 2011). The same group further showed that FOXO1 was expressed in undifferentiated spermatogonia in other mammals including humans (Tarnawa et al., 2013). Similar to the UPEC-infected testis, FOXOs are also activated after UPEC infection in isolated Sertoli cells, which has been further confirmed by an increase in DNA binding activity (shown in Figure 13). In addition, HDM did not activate FOXOs due to the lack of the virulence factor HlyA. These results are in agreement with a previous study, which showed that following AKT inhibition by the UPEC virulence factor HlyA, the phosphorylation of FOXO1 was decreased (Wiles et al., 2008).

Besides UPEC, other pathogens such as nontypeable *H. influenzae* (NTHi) activate FOXO transcription factors, e.g. in cultured human respiratory epithelial cells and in

alveolar and bronchial epithelial cells of infected mice *in vivo*. The increased expression of antimicrobial peptides and proinflammatory cytokines suggests that FOXOs transcription factors play an important role in innate immune responses against invading pathogens (Seiler et al., 2013). Moreover, the study by Becker et al. demonstrated a link between metabolism and FOXO driven innate immune response. In this regard, the activation of FOXO transcription factors by starvation using insulin signaling mutants or by applying small molecule inhibitors could induce antimicrobial peptides expression(Becker et al., 2010). Recently, a study by Lee and colleagues shed new light on understanding the mechanism of how the FOXO3 signaling pathway influences the outcomes of inflammatory and infectious disease. They identified a non-coding polymorphism in FOXO3 (rs12212067: T > G), at which the minor (G) allele is associated with a milder course of Crohn's disease and rheumatoid arthritis, yet at the cost of an elevated risk of severe malaria. They further demonstrated that FOXO3 nuclear accumulation and activation was faster in the minor (G) allele homozygotes than in major (T) allele homozygotes following LPS stimulation in monocytes. FOXO3 could transcriptionally upregulate TGFβ expression, which reduces proinflammatory cytokine production including TNFα and increases anti-inflammatory cytokine production such as IL-10 (Lee et al., 2013). All these studies indicate the important role of FOXOs in inflammatory and infectious diseases. Similarly, in our study FOXOs were activated by UPEC infection indicating the involvement in this specific host immune response. Collectively, in the present study, AKT inhibition by the UPEC virulence factor HlyA leads to activation of FOXOs *in vivo* (experimental UPEC-elicited orchitis in rat) and *in vitro* (isolated rat Sertoli cells).

Upon activation, FOXOs accumulate in the nucleus and regulate the expression of an array of genes which play a critical role in cell survival, ROS detoxification as well as cell cycle arrest (Eijkelenboom and Burgering, 2013). The transcriptional output of FOXOs is highly context-dependent, a fact which has been documented in numerous reports (van der Vos and Coffer, 2011). In this regard, FOXOs could promote

oxidative stress resistance via transcriptional upregulation of two key ROS scavenger proteins, namely SOD2 and catalase (Kops et al., 2002; Nemoto and Finkel, 2002; Storz, 2011). ROS production is one of the early responses against bacterial infection to facilitate pathogen clearance and to activate signaling pathways related to inflammatary and immune responses (Spooner and Yilmaz, 2011). However, excessive production of ROS also leads to host cell apoptosis and tissue damage. Hence, ROS production needs to be stringently controlled during bacterial infection. UPEC infection could increase ROS production, considering that FOXOs play an important role in detoxifying ROS after UPEC infection. Therefore the first hypothesis was that FOXOs may induce catalase and SOD2 expression to control ROS production. Surprisingly, expression of catalase and SOD2 remains unchanged both at the mRNA and protein level in any of the investigated time periods. These results suggest that FOXOs may be involved in functions other than ROS detoxification.

4.3 UPEC inhibit apoptosis by suppression of BIM expression

Archetypically, activation of FOXO triggers apoptosis in different cell types by increasing the levels of the pro-apoptotic protein BIM. It has been reported that FOXO3 upregulates BIM expression to induce neuron apoptosis in the context of growth factor deprivation (Gilley et al., 2003). In addition, Essafi and colleagues have shown that ST1571, a drug for chronic leukemia treatment, induces FOXO3 activation and promotes apoptosis by upregulation of BIM. They further demonstrated that FOXO3 activated by ST1571 could bind to the FOXO binding site in the BIM promoter region to up-regulate BIM expression and trigger apoptosis, indicating FOXO3 is a key regulator for BIM expression and apoptosis (Essafi et al., 2005). Interestingly, the human T-cell leukemia virus type 1 (HTLV-1) virus encodes HTLV-1 bZIP factor (HBZ), which could not only attenuate FOXO3 DNA binding, but also

sequestered the inactive form of FOXO3 in the nucleus. Consequently, the expression of the FOXO target gene BIM and FasL was inhibited. Therefore, HBZ-mediated BIM and FasL silencing is associated with apoptosis resistance of HTLV-1-infected T cells (Tanaka-Nakanishi et al., 2014). This study implicates that pathogen infection could manipulate host cell death pathways by affecting FOXO/BIM signaling. Similarly, in our study the data suggest that despite the activation of FOXOs following UPEC challenge, the mRNA expression level of BIM in Sertoli cells did not increase. UPEC-mediated BIM suppression was further confirmed by a co-incubation experiment of UPEC with the PI3K inhibitor LY294002. Here, UPEC significantly inhibited LY294002-induced mRNA expression of BIM. Of note, suppression of BIM expression resulted in inhibition of apoptosis by blocking caspase 3 activation (Figure 19D). This mechanism is in agreement with other reports including *E. coli* pathovars, which suggest that bacterial pathogens hijack host cell apoptosis signaling by targeting the intrinsic mitochondrial pathway (Rudel et al., 2010). For instance, enteropathogenic *Escherichia coli* (EPEC) secrete NieH effectors interacting with the Bax inhibitor 1 to inhibit caspase 3 activation and apoptosis, whilst *C. trachomatis* inhibits caspase 3 activation by upregulating the expression of the anti-apoptotic genes cIAP1, cIAP2, XIAP and MCL1. As other examples, *Yersinia pestis* prevent host cell apoptosis via Pla (a member of the omptin family of bacterial outer membrane proteases) mediated Fas ligand (FasL) degradation and *E. faecalis* protects macrophages from apoptosis again by inhibiting caspase 3 activation as seen in our study (Caulfield et al., 2014; Hemrajani et al., 2010; Rajalingam et al., 2008; Rajalingam et al., 2006; Zou and Shankar, 2014). Taken together, in light of the literature our findings strongly propose that UPEC can hijack the host cell apoptosis pathway by suppressing BIM expression. In consequence, apoptosis is inhibited by attenuating caspase 3 activation. Additionally, the results also point towards a possible epigenetic regulation of BIM expression following UPEC infection.

4.4 UPEC epigenetically suppress the expression of the FOXO target gene BIM

In the recent past, a growing body of evidence indicates that bacteria and viruses can modulate the host gene expression pattern to escape the innate immune response of the host cells by epigenetic mechanisms such as DNA methylation, histone modifications, and chromatin complexes (Bierne et al., 2012; Gomez-Diaz et al., 2012; Hamon and Cossart, 2008; Paschos and Allday, 2010).

DNA methylation is often associated with decreased gene expression, which could be used by pathogens to manipulate the host gene expression pattern. For instance, *Helicobacter pylori* infection could promote DNA methylation in the Trefoil factor (TFF) 2 promoter region and suppress TFF2 expression, consequently resulting in gastric tumor development (Peterson et al., 2010). In addition, UPEC infection could significantly increase the *de novo* DNA methyltransferases (DNMT) activity as well as DNMT1 RNA expression in uroepithelial cells. In consequence, UPEC suppress *CDKN2A* (p16INK4A) gene expression, involved in cell cycle arrest, by increasing DNA methylation in exon 1 region (Tolg et al., 2011). Recently, it has been demonstrated that a diversity of bacteria and viruses induce DNA methylation to manipulate host gene expression, such as *Helicobacter pylori*, *Epstein-Barr virus*, and *Human papillomavirus E7* (Bierne et al., 2012; Paschos et al., 2009; Peterson et al., 2010). Based on the observation that BIM expression is unchanged in spite of activated FOXOs, we investigated a possible epigenetic mechanism underlying this phenomenon. The epigenetic suppression of BIM expression has been documented in many tumor types, including leukemia, lymphoma, and lung cancer. The aberrant hypermethylation of a CpG island in the BIM promoter region has been demonstrated as a strategy to suppress BIM expression in cancer cells (Bachmann et al., 2010; Paschos et al., 2009; Piazza et al., 2013). It has also been demonstrated that Epstein-Barr virus (EBV) could induce DNA methylation in the BIM promoter region which

is involved in suppression of BIM expression and enhance the infected cell survival (Paschos et al., 2009). As the first step, the DNA methylation profile of the BIM promoter region has been examined by bisulfide sequencing. However, DNA methylation in the BIM promoter region did not change following UPEC infection in Sertoli cells (Figure 20), excluding the possibility that DNA methylation plays a role in BIM suppression.

Apart from DNA methylation, bacteria such as *Listeria monocytogenes*, *Clostridium perfringens* and *Streptococcus pneumonia* and their secreted toxins modulate the host cell transcription profile through histone modifications (Hamon et al., 2007). Histone acetylation is an active histone marker associated with actively transcribed genes. Histone acetylation facilitates transcription factor binding to the DNA elements by increasing DNA accessibility. The acetyl groups could neutralize the positive charge of lysine residues in histones, thereby weakening charge-dependent interaction between histones and nucleosomal DNA as well as linker DNA or adjacent histones. Pore-forming toxins from *Listeria monocytogenes*, *Clostridium perfringens* and *Streptococcus pneumonia* induce a dramatic dephosphorylation of histone 3 and deacetylation of histone 4, which correlates with a reduced transcriptional activity of a subset of host genes, including key immunity genes(Hamon et al., 2007). It has been further demonstrated that dephosphorylation of histone 3 induced by the *Listeria monocytogenes* toxin listeriolysin O (LLO) and other pore-forming toxins is K^+ efflux-dependent (Hamon and Cossart, 2011). In our study, it has been shown that UPEC dramatically deacetylate histone 3 and histone 4 in Sertoli cells (Figure 21), and in the uroepithelial cell line 5637 (Figure 25B), suggesting that UPEC infection might modulate the gene expression profile through histone modifications. Moreover, the acetylation of histone 3 and 4 also decreased in the UPEC-elicited orchitis model (Figure 22), which strongly indicates that UPEC could manipulate host gene expression by histone deacetylation. Furthermore, ChIP analysis data demonstrate that deacetylation of histone 4 in the BIM promoter region is associated with the suppression of BIM expression after UPEC infection. Therefore, UPEC can induce

global deacetylation of histone 3 and 4 in addition to specific deacetylation of histone 4 in the BIM promoter region, the latter being the mechanism for UPEC-mediated BIM suppression.

In spite of this progress, the underlying mechanism by which UPEC change the global histone acetylation status still remains elusive. Histone acetylation was catalyzed by histone acetyltransferases (HATs) utilizing acetyl-coenzyme A (acetyl-CoA) as an essential cofactor to provide an acetyl group to the target lysine residue (Choudhary et al., 2014). Opposite, histones are deacetylated by histone acetyltransferases (HDACs). One possible explanation of UPEC-mediated global histone deacetylation is that UPEC could activate HATs or inhibit activity of HDACs, a hypothesis which needs further investigation. Furthermore, it has been shown that the increase of histone acetylation in response to growth factor stimulation is dependent on ATP-citrate lyase (ACLY), which could convert glucose-derived citrate into acetyl-CoA (Wellen et al., 2009). Moreover, recently Lee and coworkers have reported that histone acetylation levels are determined in part by changes in acetyl-CoA availability, and glucose restriction could induce a decrease of histone acetylation (Lee et al., 2014). In this context, AKT-mediated ACLY activation could promote histone acetylation and UPEC-mediated AKT inhibition could be another underlying reason for the observed global histone deacetylation in this study. It has been further confirmed that UPEC-mediated AKT inhibition consequently leads to ACLY suppression in 5637 cells (Figure 25A). Moreover, HDM (do not inhibit AKT activity) are unable to decrease acetylation of histones as shown in Figure 21B. Taken together, these results suggest that UPEC-mediated AKT/ACLY inhibition is required to induce deacetylation of histone 3 and 4. Acetate can be catalyzed in acetyl coenzyme A independent of ACLY activity. It therefore has been hypothesized that acetate could rescue histone deacetylation following UPEC infection. As it is shown in Figure 25B, UPEC-mediated deacetylation of histone 3 and 4 was rescued by adding acetate 2 h post infection. Moreover, it has been demonstrated recently that acetate could promote histone acetylation in a dose-dependent manner via an increase

in the acetyl-CoA level, which influences early differentiation of embryonic stem cells (Moussaieff et al., 2015). Collectively, UPEC-mediated inhibition of AKT/ACLY activity, which may further lead to a decrease in the acetyl-CoA level, induces deacetylation of histone 3 and 4. Of note, deacetylation of histones can be rescued by adding acetate to the culture media.

In conclusion, the present study demonstrates that UPEC could suppress the AKT survival signaling pathway both *in vivo* (in a UPEC-elicited rat epididymo-orchitis model) and *in vitro* (in isolated rat Sertoli cells), consequently resulting in activation of FOXO transcription factors. In parallel, UPEC-mediated AKT/ACLY inhibition could induce global deacetylation of histone 3 and histone 4 leading to an epigenetic suppression of expression of the FOXO target gene *BIM* by histone modifications in the Bim promoter region. This explains why BIM expression is inhibited, whilst paradoxically the AKT/FOXO signaling pathway is active at the same time (Figure 26). Systemically, during infection UPEC induces BIM suppression to prevent apoptosis as a default response of the host to remove infected cells in a controlled fashion. Hence, UPEC epigenetically manipulate host cell gene expression involved in death pathways to facilitate its survival and dissemination.

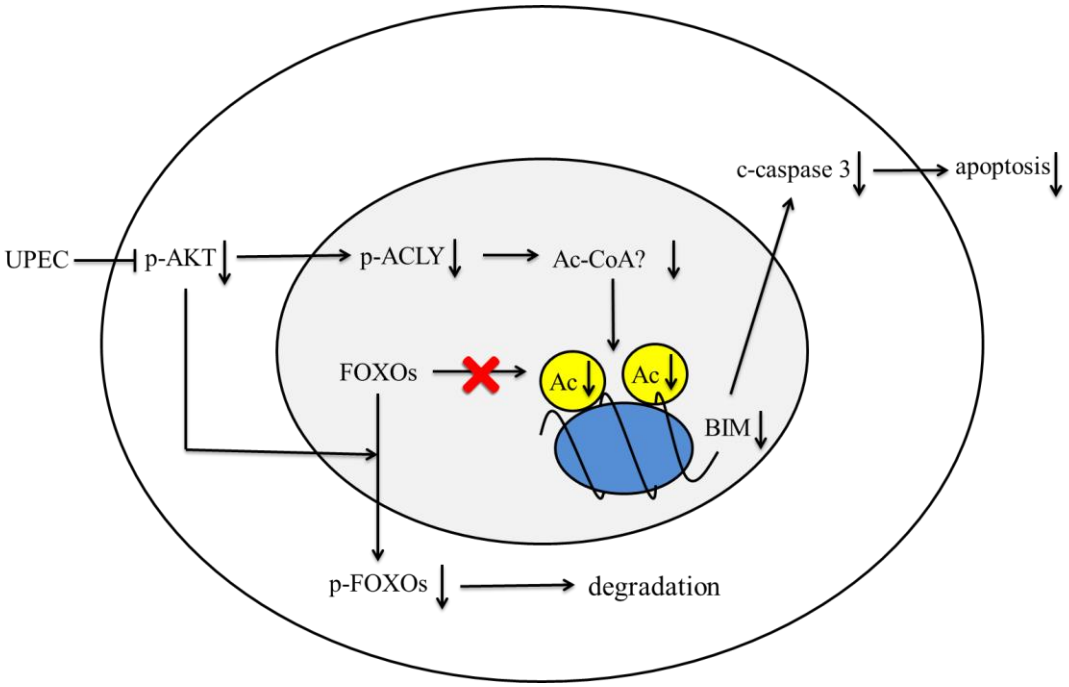

Figure 26: UPEC epigenetically suppress the FOXO target gene *BIM* expression associated with apoptosis resistance of infected cells.

5 SUMMARY

Urinary tract infections caused by uropathogenic *Escherichia coli* (UPEC) pathovars belong to the most frequent infections in humans. In men, pathogens can also spread to the genital tract via the continuous ductal system, eliciting bacterial prostatitis and/or epididymo-orchitis. Upon infection, activation of host cell death pathways is an intrinsic mechanism to eliminate the invading pathogens, conversely pathogens have evolved multiple strategies to manipulate host cell death pathways to propagate, replicate, and evade the host innate immune response. In light of the established observation that UPEC can manipulate intracellular signaling pathways to subvert innate immune responses, we sought to uncover if this pathogen is also able to interfere with the host cell death pathways. Here, it has been shown that the UPEC virulence factor alpha-hemolysin abrogates activation of the host cell pro-survival AKT signaling pathway depending on extracellular calcium. Inactivation of the AKT signaling pathway is further characterized by activation of the AKT-dependent FOXO family signaling pathway. Activation of FOXO1 and FOXO3 transcription factors were documented by their dephosphorylation and nuclear accumulation in testicular Sertoli cells. Although dephosphorylated FOXO was localized in the nuclei of Sertoli cells and showed increased DNA-binding activity following UPEC infection, no change in the expression levels of FOXO target genes such as BIM were observed. UPEC can suppress BIM expression induced by LY249002, a potent inhibitor of PI3Ks, which results in attenuation of caspase 3 activation and blockage of apoptosis. Mechanistically, UPEC-mediated AKT/ACLY inhibition could induce global deacetylation of histone 3 and histone 4, leading to an epigenetic suppression of expression of the FOXO target gene *BIM* by histone modifications in the Bim promoter region. In addition, no alteration was documented in the DNA methylation status. Taken together, these results suggest that UPEC can epigenetically silence BIM expression, a molecular switch that prevents apoptosis.

6 ZUSAMMENFASSUNG

Durch uropathogene *Escherichia coli* (UPEC) verursachte Harnwegsinfektionen gehören zu den häufigsten Infektionen beim Menschen. Bei Männern können die Erreger über das kontinuierliche Gangsystem auch auf den Genitaltrakt übergreifen und eine bakterielle Prostatitis und/oder Epididymoorchitis auslösen. Dabei stellt ein kontrollierter Zelltod durch Apoptose einen Mechanismus des Wirts dar eindringende Pathogene zu eliminieren. Umgekehrt haben die Mikroben Überlebensstrategien entwickelt, sich einer gegen sie gerichteten Immunantwort durch Manipulation intrazellulärer Signalwege zu entziehen. Aufgrund dessen war es das Ziel dieser Arbeit zu klären, ob UPEC auch in der Lage sind, die Zelltodwege des Wirts auf molekularer Ebene zu beeinflussen. Dabei hat sich gezeigt, dass der UPEC Virulenzfaktor alpha-Hämolysin die zum Überleben der Wirtszelle notwendige Aktivierung des AKT Signalwegs in Abhängigkeit von extrazellulärem Calcium aufhebt. Die Inaktivierung des AKT-Signalwegs ist durch eine Aktivierung des AKT-abhängigen Signalwegs der FOXO Transkriptionsfamilie gekennzeichnet. Eine Aktivierung von FOXO1 und FOXO3 wurde anhand einer Dephosphorylierung der FOXOs und folgender Akkumulation der Transkriptionsfaktoren im Zellkern von Sertoli-Zellen des Hodens gezeigt. Obwohl FOXO nach Infektion neben der nukleären Translokation auch eine erhöhte DNA-Bindungsaktivität in den Kernen der Sertoli-Zellen aufwies, konnte keine Änderung der Expression von FOXO-Zielgenen, wie z. Bsp. BIM, gefunden werden. Zudem kann UPEC die durch den potenten PI3K Inhibitor LY249002 induzierte BIM Expression unterdrücken. Daraus resultiert eine abgeschwächte Caspase-3-Aktivierung und folglich Blockade des Zelltods durch Apoptose. Mechanistisch kann die UPEC-vermittelte AKT/ACLY-Hemmung eine globale Deacetylierung von Histon 3 und Histon 4 hervorrufen, was durch Histon-Modifikationen in der Bim-Promotorregion zu einer epigenetischen Unterdrückung der Expression des FOXO Zielgens BIM führt. Darüber hinaus wurde keine Veränderung im DNA-Methylierungsstatus dokumentiert. Zusammengenommen

legen diese Ergebnisse nahe, dass UPEC epigenetisch die Expression von BIM unterdrücken kann. Durch diese molekulare Manipulation der infizierten Wirtszelle wird ein Zelltod durch Apoptose verhindert.

7 REFERENCES

Akhter, R., Sanphui, P., and Biswas, S.C. (2014). The essential role of p53-up-regulated modulator of apoptosis (Puma) and its regulation by FoxO3a transcription factor in beta-amyloid-induced neuron death. J Biol Chem *289*, 10812-10822.

Albrecht, M. (2009). Insights into the nature of human testicular peritubular cells. Ann Anat *191*, 532-540.

Allfrey, V.G., Faulkner, R., and Mirsky, A.E. (1964). ACETYLATION AND METHYLATION OF HISTONES AND THEIR POSSIBLE ROLE IN THE REGULATION OF RNA SYNTHESIS. Proc Natl Acad Sci U S A *51*, 786-794.

Antequera, F. (2003). Structure, function and evolution of CpG island promoters. Cell MolL Life Sci *60*, 1647-1658.

Arck, P., Solano, M.E., Walecki, M., and Meinhardt, A. (2014). The immune privilege of testis and gravid uterus: same difference? Mol Cell Endocrinol *382*, 509-520.

Bachir, B.G., and Jarvi, K. (2014). Infectious, inflammatory, and immunologic conditions resulting in male infertility. Urol Clin North Am *41*, 67-81.

Bachmann, P.S., Piazza, R.G., Janes, M.E., Wong, N.C., Davies, C., Mogavero, A., Bhadri, V.A., Szymanska, B., Geninson, G., Magistroni, V.*, et al.* (2010). Epigenetic silencing of BIM in glucocorticoid poor-responsive pediatric acute lymphoblastic leukemia, and its reversal by histone deacetylase inhibition. Blood *116*, 3013-3022.

Barber, A.E., Norton, J.P., Spivak, A.M., and Mulvey, M.A. (2013). Urinary tract infections: current and emerging management strategies. Clin Infect Dis *57*, 719-724.

Barneda-Zahonero, B., and Parra, M. (2012). Histone deacetylases and cancer. Mol Oncol *6*, 579-589.

Barski, A., Cuddapah, S., Cui, K., Roh, T.Y., Schones, D.E., Wang, Z., Wei, G., Chepelev, I., and Zhao, K. (2007). High-resolution profiling of histone methylations in the human genome. Cell *129*, 823-837.

Becker, T., Loch, G., Beyer, M., Zinke, I., Aschenbrenner, A.C., Carrera, P., Inhester, T., Schultze, J.L., and Hoch, M. (2010). FOXO-dependent regulation of innate immune homeostasis. Nature *463*, 369-373.

Bergsbaken, T., Fink, S.L., and Cookson, B.T. (2009). Pyroptosis: host cell death and inflammation. Nat Rev Microbiol *7*, 99-109.

Berndsen, C.E., and Denu, J.M. (2008). Catalysis and substrate selection by histone/protein lysine acetyltransferases. Curr Opin Struct Biol *18*, 682-689.

Bhushan, S., Schuppe, H.C., Fijak, M., and Meinhardt, A. (2009a). Testicular infection: microorganisms, clinical implications and host-pathogen interaction. J Reprod Immunol *83*, 164-167.

Bhushan, S., Schuppe, H.C., Tchatalbachev, S., Fijak, M., Weidner, W., Chakraborty, T., and Meinhardt, A. (2009b). Testicular innate immune defense against bacteria. Mol Cell Endocrinol *306*, 37-44.

Bhushan, S., Tchatalbachev, S., Klug, J., Fijak, M., Pineau, C., Chakraborty, T., and Meinhardt, A. (2008). Uropathogenic Escherichia coli block MyD88-dependent and activate MyD88-independent signaling pathways in rat testicular cells. J Immunol *180*, 5537-5547.

Bierne, H., Hamon, M., and Cossart, P. (2012). Epigenetics and bacterial infections. Cold Spring Harb Perspect Med *2*, a010272.

Bobzien, B., Yasunami, Y., Majercik, M., Lacy, P.E., and Davie, J.M. (1983). Intratesticular transplants

of islet xenografts (rat to mouse). Diabetes *32*, 213-216.

Bombieri, C., Claustres, M., De Boeck, K., Derichs, N., Dodge, J., Girodon, E., Sermet, I., Schwarz, M., Tzetis, M., Wilschanski, M.*, et al.* (2011). Recommendations for the classification of diseases as CFTR-related disorders. J Cyst Fibros *10 Suppl 2*, S86-102.

Brennan, M.A., and Cookson, B.T. (2000). Salmonella induces macrophage death by caspase-1-dependent necrosis. Mol Microbiol *38*, 31-40.

Broz, P., Ruby, T., Belhocine, K., Bouley, D.M., Kayagaki, N., Dixit, V.M., and Monack, D.M. (2012). Caspase-11 increases susceptibility to Salmonella infection in the absence of caspase-1. Nature *490*, 288-291.

Brunet, A., Bonni, A., Zigmond, M.J., Lin, M.Z., Juo, P., Hu, L.S., Anderson, M.J., Arden, K.C., Blenis, J., and Greenberg, M.E. (1999). Akt promotes cell survival by phosphorylating and inhibiting a Forkhead transcription factor. Cell *96*, 857-868.

Brunet, A., Sweeney, L.B., Sturgill, J.F., Chua, K.F., Greer, P.L., Lin, Y., Tran, H., Ross, S.E., Mostoslavsky, R., Cohen, H.Y.*, et al.* (2004). Stress-dependent regulation of FOXO transcription factors by the SIRT1 deacetylase. Science *303*, 2011-2015.

Calnan, D.R., and Brunet, A. (2008). The FoxO code. Oncogene *27*, 2276-2288.

Case, C.L., Kohler, L.J., Lima, J.B., Strowig, T., de Zoete, M.R., Flavell, R.A., Zamboni, D.S., and Roy, C.R. (2013). Caspase-11 stimulates rapid flagellin-independent pyroptosis in response to Legionella pneumophila. Proc Natl Acad Sci U S A *110*, 1851-1856.

Casson, C.N., Copenhaver, A.M., Zwack, E.E., Nguyen, H.T., Strowig, T., Javdan, B., Bradley, W.P., Fung, T.C., Flavell, R.A., Brodsky, I.E.*, et al.* (2013). Caspase-11 activation in response to bacterial secretion systems that access the host cytosol. PLoS Pathog *9*, e1003400.

Caulfield, A.J., Walker, M.E., Gielda, L.M., and Lathem, W.W. (2014). The Pla protease of Yersinia pestis degrades fas ligand to manipulate host cell death and inflammation. Cell Host Microbe *15*, 424-434.

Chan, H.C., Ruan, Y.C., He, Q., Chen, M.H., Chen, H., Xu, W.M., Chen, W.Y., Xie, C., Zhang, X.H., and Zhou, Z. (2009). The cystic fibrosis transmembrane conductance regulator in reproductive health and disease. J Physiol *587*, 2187-2195.

Chen, J., Yusuf, I., Andersen, H.M., and Fruman, D.A. (2006). FOXO transcription factors cooperate with delta EF1 to activate growth suppressive genes in B lymphocytes. J Immunol *176*, 2711-2721.

Chen, S.R., and Liu, Y.X. (2015). Regulation of spermatogonial stem cell self-renewal and spermatocyte meiosis by Sertoli cell signaling. Reproduction (Cambridge, England) *149*, R159-r167.

Choudhary, C., Weinert, B.T., Nishida, Y., Verdin, E., and Mann, M. (2014). The growing landscape of lysine acetylation links metabolism and cell signalling. Nat Rev Mol Cell Biol *15*, 536-550.

Claustres, M. (2005). Molecular pathology of the CFTR locus in male infertility. Reprod Biomed Online *10*, 14-41.

Daitoku, H., Hatta, M., Matsuzaki, H., Aratani, S., Ohshima, T., Miyagishi, M., Nakajima, T., and Fukamizu, A. (2004). Silent information regulator 2 potentiates Foxo1-mediated transcription through its deacetylase activity. Proc Natl Acad Sci U S A *101*, 10042-10047.

Daitoku, H., Sakamaki, J., and Fukamizu, A. (2011). Regulation of FoxO transcription factors by acetylation and protein-protein interactions. Biochim Biophys Acta *1813*, 1954-1960.

Dal Secco, V., Riccioli, A., Padula, F., Ziparo, E., and Filippini, A. (2008). Mouse Sertoli cells display phenotypical and functional traits of antigen-presenting cells in response to interferon gamma. Biol Reprod *78*, 234-242.

Demir, A., Turker, P., Onol, F.F., Sirvanci, S., Findik, A., and Tarcan, T. (2007). Effect of experimentally induced Escherichia coli epididymo-orchitis and ciprofloxacin treatment on rat spermatogenesis. Int J Urol *14*, 268-272.

Dhakal, B.K., and Mulvey, M.A. (2012). The UPEC pore-forming toxin alpha-hemolysin triggers proteolysis of host proteins to disrupt cell adhesion, inflammatory, and survival pathways. Cell Host Microbe *11*, 58-69.

Dijkers, P.F., Medema, R.H., Lammers, J.W., Koenderman, L., and Coffer, P.J. (2000a). Expression of the pro-apoptotic Bcl-2 family member Bim is regulated by the forkhead transcription factor FKHR-L1. Curr Biol *10*, 1201-1204.

Dijkers, P.F., Medema, R.H., Pals, C., Banerji, L., Thomas, N.S., Lam, E.W., Burgering, B.M., Raaijmakers, J.A., Lammers, J.W., Koenderman, L.*, et al.* (2000b). Forkhead transcription factor FKHR-L1 modulates cytokine-dependent transcriptional regulation of p27(KIP1). Mol Cell Biol *20*, 9138-9148.

Doyle, T.J., Kaur, G., Putrevu, S.M., Dyson, E.L., Dyson, M., McCunniff, W.T., Pasham, M.R., Kim, K.H., and Dufour, J.M. (2012). Immunoprotective properties of primary Sertoli cells in mice: potential functional pathways that confer immune privilege. Biol Reprod *86*, 1-14.

Droge, W., and Kinscherf, R. (2008). Aberrant insulin receptor signaling and amino acid homeostasis as a major cause of oxidative stress in aging. Antioxid Redox Signal *10*, 661-678.

Eddy, E.M., Vernon, R.B., Muller, C.H., Hahnel, A.C., and Fenderson, B.A. (1985). Immunodissection of sperm surface modifications during epididymal maturation. Am J Anat *174*, 225-237.

Eijkelenboom, A., and Burgering, B.M. (2013). FOXOs: signalling integrators for homeostasis maintenance. Nat Rev Mol Cell Biol *14*, 83-97.

Emody, L., Kerenyi, M., and Nagy, G. (2003). Virulence factors of uropathogenic Escherichia coli. Int J Antimicrob Agents *22 Suppl 2*, 29-33.

Essafi, A., Fernandez de Mattos, S., Hassen, Y.A., Soeiro, I., Mufti, G.J., Thomas, N.S., Medema, R.H., and Lam, E.W. (2005). Direct transcriptional regulation of Bim by FoxO3a mediates STI571-induced apoptosis in Bcr-Abl-expressing cells. Oncogene *24*, 2317-2329.

Essers, M.A., Weijzen, S., de Vries-Smits, A.M., Saarloos, I., de Ruiter, N.D., Bos, J.L., and Burgering, B.M. (2004). FOXO transcription factor activation by oxidative stress mediated by the small GTPase Ral and JNK. EMBO J *23*, 4802-4812.

Evans, R.M. (1988). The steroid and thyroid hormone receptor superfamily. Science *240*, 889-895.

Fadok, V.A., Bratton, D.L., Konowal, A., Freed, P.W., Westcott, J.Y., and Henson, P.M. (1998). Macrophages that have ingested apoptotic cells in vitro inhibit proinflammatory cytokine production through autocrine/paracrine mechanisms involving TGF-beta, PGE2, and PAF. J Clin Invest *101*, 890-898.

Fallarino, F., Luca, G., Calvitti, M., Mancuso, F., Nastruzzi, C., Fioretti, M.C., Grohmann, U., Becchetti, E., Burgevin, A., Kratzer, R.*, et al.* (2009). Therapy of experimental type 1 diabetes by isolated Sertoli cell xenografts alone. J Exp Med *206*, 2511-2526.

Favaloro, B., Allocati, N., Graziano, V., Di Ilio, C., and De Laurenzi, V. (2012). Role of apoptosis in disease. Aging *4*, 330-349.

Fischle, W., Wang, Y., Jacobs, S.A., Kim, Y., Allis, C.D., and Khorasanizadeh, S. (2003). Molecular basis for the discrimination of repressive methyl-lysine marks in histone H3 by Polycomb and HP1 chromodomains. Genes Dev *17*, 1870-1881.

Furuyama, T., Nakazawa, T., Nakano, I., and Mori, N. (2000). Identification of the differential

distribution patterns of mRNAs and consensus binding sequences for mouse DAF-16 homologues. Biochem J *349*, 629-634.

Galluzzi, L., Bravo-San Pedro, J.M., Vitale, I., Aaronson, S.A., Abrams, J.M., Adam, D., Alnemri, E.S., Altucci, L., Andrews, D., Annicchiarico-Petruzzelli, M.*, et al.* (2015). Essential versus accessory aspects of cell death: recommendations of the NCCD 2015. Cell Death Differ *22*, 58-73.

Gilley, J., Coffer, P.J., and Ham, J. (2003). FOXO transcription factors directly activate bim gene expression and promote apoptosis in sympathetic neurons. J Cell Biol *162*, 613-622.

Goertz, M.J., Wu, Z., Gallardo, T.D., Hamra, F.K., and Castrillon, D.H. (2011). Foxo1 is required in mouse spermatogonial stem cells for their maintenance and the initiation of spermatogenesis. J Clin Invest *121*, 3456-3466.

Gomez-Diaz, E., Jorda, M., Peinado, M.A., and Rivero, A. (2012). Epigenetics of host-pathogen interactions: the road ahead and the road behind. PLoS Pathog *8*, e1003007.

Greer, E.L., Oskoui, P.R., Banko, M.R., Maniar, J.M., Gygi, M.P., Gygi, S.P., and Brunet, A. (2007). The energy sensor AMP-activated protein kinase directly regulates the mammalian FOXO3 transcription factor. J Biol Chem *282*, 30107-30119.

Griswold, M.D. (1998). The central role of Sertoli cells in spermatogenesis. Semin Cell Dev Biol *9*, 411-416.

Grunstein, M. (1997). Histone acetylation in chromatin structure and transcription. Nature *389*, 349-352.

Guertin, M.J., and Lis, J.T. (2013). Mechanisms by which transcription factors gain access to target sequence elements in chromatin. Curr Opin Genet Dev *23*, 116-123.

Gur, C., Coppenhagen-Glazer, S., Rosenberg, S., Yamin, R., Enk, J., Glasner, A., Bar-On, Y., Fleissig, O., Naor, R., Abed, J.*, et al.* (2013). Natural killer cell-mediated host defense against uropathogenic E. coli is counteracted by bacterial hemolysinA-dependent killing of NK cells. Cell Host Microbe *14*, 664-674.

Hagar, J.A., Powell, D.A., Aachoui, Y., Ernst, R.K., and Miao, E.A. (2013). Cytoplasmic LPS activates caspase-11: implications in TLR4-independent endotoxic shock. Science *341*, 1250-1253.

Hamon, M.A., Batsche, E., Regnault, B., Tham, T.N., Seveau, S., Muchardt, C., and Cossart, P. (2007). Histone modifications induced by a family of bacterial toxins. Proc Natl Acad Sci U S A *104*, 13467-13472.

Hamon, M.A., and Cossart, P. (2008). Histone modifications and chromatin remodeling during bacterial infections. Cell Host Microbe *4*, 100-109.

Hamon, M.A., and Cossart, P. (2011). K+ efflux is required for histone H3 dephosphorylation by Listeria monocytogenes listeriolysin O and other pore-forming toxins. Infect Immun *79*, 2839-2846.

Head, J.R., and Billingham, R.E. (1985). Immunologically privileged sites in transplantation immunology and oncology. Perspect Biol Med *29*, 115-131.

Head, J.R., Neaves, W.B., and Billingham, R.E. (1983). Immune privilege in the testis. I. Basic parameters of allograft survival. Transplantation *36*, 423-431.

Heintzman, N.D., Stuart, R.K., Hon, G., Fu, Y., Ching, C.W., Hawkins, R.D., Barrera, L.O., Van Calcar, S., Qu, C., Ching, K.A.*, et al.* (2007). Distinct and predictive chromatin signatures of transcriptional promoters and enhancers in the human genome. Nat Genet *39*, 311-318.

Hemrajani, C., Berger, C.N., Robinson, K.S., Marches, O., Mousnier, A., and Frankel, G. (2010). NleH effectors interact with Bax inhibitor-1 to block apoptosis during enteropathogenic Escherichia coli infection. Proc Natl Acad Sci U S A *107*, 3129-3134.

Hermann, A., Goyal, R., and Jeltsch, A. (2004). The Dnmt1 DNA-(cytosine-C5)-methyltransferase methylates DNA processively with high preference for hemimethylated target sites. J Biol Chem *279*, 48350-48359.

Hers, I., Vincent, E.E., and Tavare, J.M. (2011). Akt signalling in health and disease. Cell Signal *23*, 1515-1527.

Hilbert, D.W., Paulish-Miller, T.E., Tan, C.K., Carey, A.J., Ulett, G.C., Mordechai, E., Adelson, M.E., Gygax, S.E., and Trama, J.P. (2012). Clinical Escherichia coli isolates utilize alpha-hemolysin to inhibit in vitro epithelial cytokine production. Microbes Infect *14*, 628-638.

Hinton, B.T., and Palladino, M.A. (1995). Epididymal epithelium: its contribution to the formation of a luminal fluid microenvironment. Microsc Res Tech *30*, 67-81.

Hon, G.C., Hawkins, R.D., and Ren, B. (2009). Predictive chromatin signatures in the mammalian genome. Hum Mol Genet *18*, R195-201.

Huang, H., Muddiman, D.C., and Tindall, D.J. (2004). Androgens negatively regulate forkhead transcription factor FKHR (FOXO1) through a proteolytic mechanism in prostate cancer cells. J Biol Chem *279*, 13866-13877.

Huang, H., Regan, K.M., Wang, F., Wang, D., Smith, D.I., van Deursen, J.M., and Tindall, D.J. (2005). Skp2 inhibits FOXO1 in tumor suppression through ubiquitin-mediated degradation. Proc Natl Acad Sci U S A *102*, 1649-1654.

Hviid, A., Rubin, S., and Muhlemann, K. (2008). Mumps. Lancet *371*, 932-944.

Jiang, X.H., Bukhari, I., Zheng, W., Yin, S., Wang, Z., Cooke, H.J., and Shi, Q.H. (2014). Blood-testis barrier and spermatogenesis: lessons from genetically-modified mice. Asian J Androl *16*, 572-580.

Johnson, L., Thompson, D.L., Jr., and Varner, D.D. (2008). Role of Sertoli cell number and function on regulation of spermatogenesis. Anim Reprod Sci *105*, 23-51.

Jones, P.A. (2012). Functions of DNA methylation: islands, start sites, gene bodies and beyond. Nat Rev Genet *13*, 484-492.

Jungwirth, A., Giwercman, A., Tournaye, H., Diemer, T., Kopa, Z., Dohle, G., and Krausz, C. (2012). European Association of Urology guidelines on Male Infertility: the 2012 update. Eur Urol *62*, 324-332.

Katayama, K., Nakamura, A., Sugimoto, Y., Tsuruo, T., and Fujita, N. (2008). FOXO transcription factor-dependent p15(INK4b) and p19(INK4d) expression. Oncogene *27*, 1677-1686.

Kaur, G., Thompson, L.A., and Dufour, J.M. (2014). Sertoli cells--immunological sentinels of spermatogenesis. Semin Cell Dev Biol *30*, 36-44.

Kayagaki, N., Wong, M.T., Stowe, I.B., Ramani, S.R., Gonzalez, L.C., Akashi-Takamura, S., Miyake, K., Zhang, J., Lee, W.P., Muszynski, A.*, et al.* (2013). Noncanonical inflammasome activation by intracellular LPS independent of TLR4. Science *341*, 1246-1249.

Keck, C., Gerber-Schafer, C., Clad, A., Wilhelm, C., and Breckwoldt, M. (1998). Seminal tract infections: impact on male fertility and treatment options. Hum Reprod Update *4*, 891-903.

Kenyon, C., Chang, J., Gensch, E., Rudner, A., and Tabtiang, R. (1993). A C. elegans mutant that lives twice as long as wild type. Nature *366*, 461-464.

Kerr, J.F., Wyllie, A.H., and Currie, A.R. (1972). Apoptosis: a basic biological phenomenon with wide-ranging implications in tissue kinetics. Br J Cancer *26*, 239-257.

Khan, S.N., and Khan, A.U. (2010). Role of histone acetylation in cell physiology and diseases: An update. Clin Chim Acta *411*, 1401-1411.

Koch, C.M., Andrews, R.M., Flicek, P., Dillon, S.C., Karaoz, U., Clelland, G.K., Wilcox, S., Beare,

D.M., Fowler, J.C., Couttet, P*., et al.* (2007). The landscape of histone modifications across 1% of the human genome in five human cell lines. Genome Res *17*, 691-707.

Kolasinska-Zwierz, P., Down, T., Latorre, I., Liu, T., Liu, X.S., and Ahringer, J. (2009). Differential chromatin marking of introns and expressed exons by H3K36me3. Nat Genet *41*, 376-381.

Kooistra, S.M., and Helin, K. (2012). Molecular mechanisms and potential functions of histone demethylases. Nat Rev Mol Cell Biol *13*, 297-311.

Kops, G.J., Dansen, T.B., Polderman, P.E., Saarloos, I., Wirtz, K.W., Coffer, P.J., Huang, T.T., Bos, J.L., Medema, R.H., and Burgering, B.M. (2002). Forkhead transcription factor FOXO3a protects quiescent cells from oxidative stress. Nature *419*, 316-321.

Korbutt, G.S., Elliott, J.F., and Rajotte, R.V. (1997). Cotransplantation of allogeneic islets with allogeneic testicular cell aggregates allows long-term graft survival without systemic immunosuppression. Diabetes *46*, 317-322.

Kornberg, R.D., and Lorch, Y. (1999). Twenty-five years of the nucleosome, fundamental particle of the eukaryote chromosome. Cell *98*, 285-294.

Kraemer, B.F., Campbell, R.A., Schwertz, H., Franks, Z.G., Vieira de Abreu, A., Grundler, K., Kile, B.T., Dhakal, B.K., Rondina, M.T., Kahr, W.H.A*., et al.* (2012). Bacteria differentially induce degradation of Bcl-xL, a survival protein, by human platelets. Blood *120*, 5014-5020.

Kroemer, G., Galluzzi, L., Vandenabeele, P., Abrams, J., Alnemri, E.S., Baehrecke, E.H., Blagosklonny, M.V., El-Deiry, W.S., Golstein, P., Green, D.R*., et al.* (2009). Classification of cell death: recommendations of the Nomenclature Committee on Cell Death 2009. Cell Death Differ *16*, 3-11.

Lamkanfi, M., and Dixit, V.M. (2010). Manipulation of host cell death pathways during microbial infections. Cell Host Microbe *8*, 44-54.

Lamkanfi, M., and Dixit, V.M. (2014). Mechanisms and functions of inflammasomes. Cell *157*, 1013-1022.

Lang, T., Dechant, M., Sanchez, V., Wistuba, J., Boiani, M., Pilatz, A., Stammler, A., Middendorff, R., Schuler, G., Bhushan, S*., et al.* (2013). Structural and functional integrity of spermatozoa is compromised as a consequence of acute uropathogenic E. coli-associated epididymitis. Biol Reprod *89*, 59.

Lee, H.M., Oh, B.C., Lim, D.P., Lee, D.S., Cho, J., Lee, G., and Lee, J.R. (2007). Role of complement regulatory proteins in the survival of murine allo-transplanted Sertoli cells. J Korean Med Sci *22*, 277-282.

Lee, J.C., Espeli, M., Anderson, C.A., Linterman, M.A., Pocock, J.M., Williams, N.J., Roberts, R., Viatte, S., Fu, B., Peshu, N*., et al.* (2013). Human SNP Links Differential Outcomes in Inflammatory and Infectious Disease to a FOXO3-Regulated Pathway. Cell *155*, 57-69.

Lee, J.V., Carrer, A., Shah, S., Snyder, N.W., Wei, S., Venneti, S., Worth, A.J., Yuan, Z.F., Lim, H.W., Liu, S*., et al.* (2014). Akt-dependent metabolic reprogramming regulates tumor cell histone acetylation. Cell Metab *20*, 306-319.

Lee, K.K., and Workman, J.L. (2007). Histone acetyltransferase complexes: one size doesn't fit all. Nat Rev Mol Cell Biol *8*, 284-295.

Li, P., Lee, H., Guo, S., Unterman, T.G., Jenster, G., and Bai, W. (2003). AKT-independent protection of prostate cancer cells from apoptosis mediated through complex formation between the androgen receptor and FKHR. Mol Cell Biol *23*, 104-118.

Lim, H.G., Lee, H.M., Oh, B.C., and Lee, J.R. (2009). Cell-mediated immunomodulation of chemokine receptor 7-expressing porcine sertoli cells in murine heterotopic heart transplantation. J Heart Lung

Transplant *28*, 72-78.

Linkermann, A., Stockwell, B.R., Krautwald, S., and Anders, H.J. (2014). Regulated cell death and inflammation: an auto-amplification loop causes organ failure. Nat Rev Immunol *14*, 759-767.

Lu, Y., Bhushan, S., Tchatalbachev, S., Marconi, M., Bergmann, M., Weidner, W., Chakraborty, T., and Meinhardt, A. (2013). Necrosis is the dominant cell death pathway in uropathogenic Escherichia coli elicited epididymo-orchitis and is responsible for damage of rat testis. PLoS One *8*, e52919.

Ludwig, M. (2008). Diagnosis and therapy of acute prostatitis, epididymitis and orchitis. Andrologia *40*, 76-80.

Ludwig, M., Johannes, S., Bergmann, M., Failing, K., Schiefer, H.G., and Weidner, W. (2002). Experimental Escherichia coli epididymitis in rats: a model to assess the outcome of antibiotic treatment. BJU international *90*, 933-938.

Luger, K., Mader, A.W., Richmond, R.K., Sargent, D.F., and Richmond, T.J. (1997). Crystal structure of the nucleosome core particle at 2.8 A resolution. Nature *389*, 251-260.

Ma, Q., Fu, W., Li, P., Nicosia, S.V., Jenster, G., Zhang, X., and Bai, W. (2009). FoxO1 mediates PTEN suppression of androgen receptor N- and C-terminal interactions and coactivator recruitment. Mol Endocrinol (Baltimore, Md) *23*, 213-225.

Malumbres, M., and Barbacid, M. (2009). Cell cycle, CDKs and cancer: a changing paradigm. Nat Rev Cancer *9*, 153-166.

Manning, B.D., and Cantley, L.C. (2007). AKT/PKB signaling: navigating downstream. Cell *129*, 1261-1274.

Margueron, R., and Reinberg, D. (2011). The Polycomb complex PRC2 and its mark in life. Nature *469*, 343-349.

Marks, P.A., and Xu, W.S. (2009). Histone deacetylase inhibitors: Potential in cancer therapy. J Cell Biochem *107*, 600-608.

Matsumoto, T., Sakari, M., Okada, M., Yokoyama, A., Takahashi, S., Kouzmenko, A., and Kato, S. (2013). The androgen receptor in health and disease. Annu Rev Physiol *75*, 201-224.

Mayerhofer, A. (2013). Human testicular peritubular cells: more than meets the eye. Reproduction (Cambridge, England) *145*, R107-116.

McComb, S., Cheung, H.H., Korneluk, R.G., Wang, S., Krishnan, L., and Sad, S. (2012). cIAP1 and cIAP2 limit macrophage necroptosis by inhibiting Rip1 and Rip3 activation. Cell Death Differ *19*, 1791-1801.

McIlwain, D.R., Berger, T., and Mak, T.W. (2013). Caspase functions in cell death and disease. Cold Spring Harbor Perspect Biol *5*, a008656.

Medema, R.H., Kops, G.J., Bos, J.L., and Burgering, B.M. (2000). AFX-like Forkhead transcription factors mediate cell-cycle regulation by Ras and PKB through p27kip1. Nature *404*, 782-787.

Meinhardt, A., and Hedger, M.P. (2011). Immunological, paracrine and endocrine aspects of testicular immune privilege. Mol Cell Endocrinol *335*, 60-68.

Mital, P., Hinton, B.T., and Dufour, J.M. (2011). The blood-testis and blood-epididymis barriers are more than just their tight junctions. Biol Reprod *84*, 851-858.

Mital, P., Kaur, G., and Dufour, J.M. (2010). Immunoprotective sertoli cells: making allogeneic and xenogeneic transplantation feasible. Reproduction (Cambridge, England) *139*, 495-504.

Modur, V., Nagarajan, R., Evers, B.M., and Milbrandt, J. (2002). FOXO proteins regulate tumor necrosis factor-related apoptosis inducing ligand expression. Implications for PTEN mutation in prostate cancer. J Biol Chem *277*, 47928-47937.

Moldoveanu, T., Follis, A.V., Kriwacki, R.W., and Green, D.R. (2014). Many players in BCL-2 family affairs. Trends Biochem Sci *39*, 101-111.

Moussaieff, A., Rouleau, M., Kitsberg, D., Cohen, M., Levy, G., Barasch, D., Nemirovski, A., Shen-Orr, S., Laevsky, I., Amit, M*., et al.* (2015). Glycolysis-mediated changes in acetyl-CoA and histone acetylation control the early differentiation of embryonic stem cells. Cell Metab *21*, 392-402.

Murphy, J.M., Czabotar, P.E., Hildebrand, J.M., Lucet, I.S., Zhang, J.G., Alvarez-Diaz, S., Lewis, R., Lalaoui, N., Metcalf, D., Webb, A.I*., et al.* (2013). The pseudokinase MLKL mediates necroptosis via a molecular switch mechanism. Immunity *39*, 443-453.

Naber, K.G., and Weidner, W. (2000). Chronic prostatitis-an infectious disease? J Antimicrob Chemother *46*, 157-161.

Nagamatsu, K., Hannan, T.J., Guest, R.L., Kostakioti, M., Hadjifrangiskou, M., Binkley, J., Dodson, K., Raivio, T.L., and Hultgren, S.J. (2015). Dysregulation of Escherichia coli alpha-hemolysin expression alters the course of acute and persistent urinary tract infection. Proc Natl Acad Sci U S A *112*, E871-880.

Nemoto, S., and Finkel, T. (2002). Redox regulation of forkhead proteins through a p66shc-dependent signaling pathway. Science *295*, 2450-2452.

Nielubowicz, G.R., and Mobley, H.L. (2010). Host-pathogen interactions in urinary tract infection. Nat Rev Urol *7*, 430-441.

O'Bryan, M.K., Gerdprasert, O., Nikolic-Paterson, D.J., Meinhardt, A., Muir, J.A., Foulds, L.M., Phillips, D.J., de Kretser, D.M., and Hedger, M.P. (2005). Cytokine profiles in the testes of rats treated with lipopolysaccharide reveal localized suppression of inflammatory responses. Am J Physiol Regul Integr Comp Physiol *288*, R1744-1755.

O'Donnell, M.A., Perez-Jimenez, E., Oberst, A., Ng, A., Massoumi, R., Xavier, R., Green, D.R., and Ting, A.T. (2011). Caspase 8 inhibits programmed necrosis by processing CYLD. Nat Cell Biol *13*, 1437-1442.

Obsil, T., and Obsilova, V. (2011). Structural basis for DNA recognition by FOXO proteins. Biochim Biophys Acta *1813*, 1946-1953.

Obsilova, V., Vecer, J., Herman, P., Pabianova, A., Sulc, M., Teisinger, J., Boura, E., and Obsil, T. (2005). 14-3-3 Protein interacts with nuclear localization sequence of forkhead transcription factor FoxO4. Biochemistry *44*, 11608-11617.

Ochsendorf, F.R. (2008). Sexually transmitted infections: impact on male fertility. Andrologia *40*, 72-75.

Oh, S.W., Mukhopadhyay, A., Svrzikapa, N., Jiang, F., Davis, R.J., and Tissenbaum, H.A. (2005). JNK regulates lifespan in Caenorhabditis elegans by modulating nuclear translocation of forkhead transcription factor/DAF-16. Proc Natl Acad Sci U S A *102*, 4494-4499.

Okano, M., Bell, D.W., Haber, D.A., and Li, E. (1999). DNA methyltransferases Dnmt3a and Dnmt3b are essential for de novo methylation and mammalian development. Cell *99*, 247-257.

World Health Organization. (2000). WHO Manual for the Standardized Investigation, Diagnosis and Management of the Infertile Couple. Cambridge: Cambridge Universality Press.

Osegbe, D.N. (1991). Testicular function after unilateral bacterial epididymo-orchitis. Eur Urol *19*, 204-208.

Ostolaza, H., and Goni, F.M. (1995). Interaction of the bacterial protein toxin alpha-haemolysin with model membranes: protein binding does not always lead to lytic activity. FEBS letters *371*, 303-306.

Paschos, K., and Allday, M.J. (2010). Epigenetic reprogramming of host genes in viral and microbial

pathogenesis. Trends Microbiol *18*, 439-447.

Paschos, K., Smith, P., Anderton, E., Middeldorp, J.M., White, R.E., and Allday, M.J. (2009). Epstein-barr virus latency in B cells leads to epigenetic repression and CpG methylation of the tumour suppressor gene Bim. PLoS Pathog *5*, e1000492.

Pasparakis, M., and Vandenabeele, P. (2015). Necroptosis and its role in inflammation. Nature *517*, 311-320.

Peterson, A.J., Menheniott, T.R., O'Connor, L., Walduck, A.K., Fox, J.G., Kawakami, K., Minamoto, T., Ong, E.K., Wang, T.C., Judd, L.M*., et al.* (2010). Helicobacter pylori infection promotes methylation and silencing of trefoil factor 2, leading to gastric tumor development in mice and humans. Gastroenterology *139*, 2005-2017.

Piazza, R., Magistroni, V., Mogavero, A., Andreoni, F., Ambrogio, C., Chiarle, R., Mologni, L., Bachmann, P.S., Lock, R.B., Collini, P*., et al.* (2013). Epigenetic silencing of the proapoptotic gene BIM in anaplastic large cell lymphoma through an MeCP2/SIN3a deacetylating complex. Neoplasia *15*, 511-522.

Pilatz, A., Ceylan, I., Schuppe, H.C., Ludwig, M., Fijak, M., Chakraborty, T., Weidner, W., Bergmann, M., and Wagenlehner, F. (2015). Experimental Escherichia coli epididymitis in rats: assessment of testicular involvement in a long-term follow-up. Andrologia *47*, 160-167.

Pilatz, A., Hossain, H., Kaiser, R., Mankertz, A., Schuttler, C.G., Domann, E., Schuppe, H.C., Chakraborty, T., Weidner, W., and Wagenlehner, F. (2015). Acute Epididymitis Revisited: Impact of Molecular Diagnostics on Etiology and Contemporary Guideline Recommendations. Eur Urol *68*, 428-435.

Rajalingam, K., Sharma, M., Lohmann, C., Oswald, M., Thieck, O., Froelich, C.J., and Rudel, T. (2008). Mcl-1 is a key regulator of apoptosis resistance in Chlamydia trachomatis-infected cells. PLoS One *3*, e3102.

Rajalingam, K., Sharma, M., Paland, N., Hurwitz, R., Thieck, O., Oswald, M., Machuy, N., and Rudel, T. (2006). IAP-IAP complexes required for apoptosis resistance of C. trachomatis-infected cells. PLoS Pathog *2*, e114.

Rathinam, V.A., Vanaja, S.K., Waggoner, L., Sokolovska, A., Becker, C., Stuart, L.M., Leong, J.M., and Fitzgerald, K.A. (2012). TRIF licenses caspase-11-dependent NLRP3 inflammasome activation by gram-negative bacteria. Cell *150*, 606-619.

Relton, C.L., and Davey Smith, G. (2010). Epigenetic epidemiology of common complex disease: prospects for prediction, prevention, and treatment. PLoS medicine *7*, e1000356.

Riccioli, A., Starace, D., Galli, R., Fuso, A., Scarpa, S., Palombi, F., De Cesaris, P., Ziparo, E., and Filippini, A. (2006). Sertoli cells initiate testicular innate immune responses through TLR activation. J Immunol *177*, 7122-7130.

Rubin, S., Eckhaus, M., Rennick, L.J., Bamford, C.G., and Duprex, W.P. (2015). Molecular biology, pathogenesis and pathology of mumps virus. J Pathol *235*, 242-252.

Rudel, T., Kepp, O., and Kozjak-Pavlovic, V. (2010). Interactions between bacterial pathogens and mitochondrial cell death pathways. Nat Rev Microbiol *8*, 693-705.

Rusz, A., Pilatz, A., Wagenlehner, F., Linn, T., Diemer, T., Schuppe, H.C., Lohmeyer, J., Hossain, H., and Weidner, W. (2012). Influence of urogenital infections and inflammation on semen quality and male fertility. World J Urol *30*, 23-30.

Sanberg, P.R., Borlongan, C.V., Saporta, S., and Cameron, D.F. (1996). Testis-derived Sertoli cells survive and provide localized immunoprotection for xenografts in rat brain. Nat Biotechnol *14*, 1692-

1695.

Sarosiek, K.A., Chi, X., Bachman, J.A., Sims, J.J., Montero, J., Patel, L., Flanagan, A., Andrews, D.W., Sorger, P., and Letai, A. (2013). BID preferentially activates BAK while BIM preferentially activates BAX, affecting chemotherapy response. Mol Cell *51*, 751-765.

Schiefer, H.G. (1998). Microbiology of male urethroadnexitis: diagnostic procedures and criteria for aetiologic classification. Andrologia *30 Suppl 1*, 7-13.

Schmidt, M., Fernandez de Mattos, S., van der Horst, A., Klompmaker, R., Kops, G.J., Lam, E.W., Burgering, B.M., and Medema, R.H. (2002). Cell cycle inhibition by FoxO forkhead transcription factors involves downregulation of cyclin D. Mol Cell Biol *22*, 7842-7852.

Schuppe, H.C., and Meinhardt, A. (2005). Immune privilege and inflammation of the testis. Chem Immunol Allergy *88*, 1-14.

Schuppe, H.C., Meinhardt, A., Allam, J.P., Bergmann, M., Weidner, W., and Haidl, G. (2008). Chronic orchitis: a neglected cause of male infertility? Andrologia *40*, 84-91.

Seiler, F., Hellberg, J., Lepper, P.M., Kamyschnikow, A., Herr, C., Bischoff, M., Langer, F., Schafers, H.J., Lammert, F., Menger, M.D.*, et al.* (2013). FOXO Transcription Factors Regulate Innate Immune Mechanisms in Respiratory Epithelial Cells. J Immunol *190*, 1603-1613.

Selawry, H.P., and Cameron, D.F. (1993). Sertoli cell-enriched fractions in successful islet cell transplantation. Cell Transplant *2*, 123-129.

Seoane, J., Le, H.V., Shen, L., Anderson, S.A., and Massague, J. (2004). Integration of Smad and forkhead pathways in the control of neuroepithelial and glioblastoma cell proliferation. Cell *117*, 211-223.

Setchell, B.P. (1990). The testis and tissue transplantation: historical aspects. J Reprod Immunol *18*, 1-8.

Shahbazian, M.D., and Grunstein, M. (2007). Functions of site-specific histone acetylation and deacetylation. Annu Rev Biochem *76*, 75-100.

Shamas-Din, A., Kale, J., Leber, B., and Andrews, D.W. (2013). Mechanisms of action of Bcl-2 family proteins. Cold Spring Harb Perspect Biol *5*, a008714.

Sipione, S., Simmen, K.C., Lord, S.J., Motyka, B., Ewen, C., Shostak, I., Rayat, G.R., Dufour, J.M., Korbutt, G.S., Rajotte, R.V.*, et al.* (2006). Identification of a novel human granzyme B inhibitor secreted by cultured sertoli cells. J Immunol *177*, 5051-5058.

Spooner, R., and Yilmaz, O. (2011). The role of reactive-oxygen-species in microbial persistence and inflammation. Int J Mol Sci *12*, 334-352.

Staal, S.P. (1987). Molecular cloning of the akt oncogene and its human homologues AKT1 and AKT2: amplification of AKT1 in a primary human gastric adenocarcinoma. Proc Natl Acad Sci U S A *84*, 5034-5037.

Storz, P. (2011). Forkhead homeobox type O transcription factors in the responses to oxidative stress. Antioxid Redox Signal *14*, 593-605.

Strasser, A., O'Connor, L., and Dixit, V.M. (2000). Apoptosis signaling. Annu Rev Biochem *69*, 217-245.

Suarez-Pinzon, W., Korbutt, G.S., Power, R., Hooton, J., Rajotte, R.V., and Rabinovitch, A. (2000). Testicular sertoli cells protect islet beta-cells from autoimmune destruction in NOD mice by a transforming growth factor-beta1-dependent mechanism. Diabetes *49*, 1810-1818.

Sun, L., Wang, H., Wang, Z., He, S., Chen, S., Liao, D., Wang, L., Yan, J., Liu, W., Lei, X.*, et al.* (2012). Mixed lineage kinase domain-like protein mediates necrosis signaling downstream of RIP3

kinase. Cell *148*, 213-227.

Tait, S.W., and Green, D.R. (2012). Mitochondria and cell signalling. J Cell Sci *125*, 807-815.

Tanaka-Nakanishi, A., Yasunaga, J., Takai, K., and Matsuoka, M. (2014). HTLV-1 bZIP factor suppresses apoptosis by attenuating the function of FoxO3a and altering its localization. Cancer Res *74*, 188-200.

Tarnawa, E.D., Baker, M.D., Aloisio, G., Carr, B.R., and Castrillon, D.H. (2013). Gonadal Expression of Foxo1, but Not Foxo3, Is Conserved in Diverse Mammalian Species. Biol Reprod *88*, 103.

Tolg, C., Sabha, N., Cortese, R., Panchal, T., Ahsan, A., Soliman, A., Aitken, K.J., Petronis, A., and Bagli, D.J. (2011). Uropathogenic E. coli infection provokes epigenetic downregulation of CDKN2A (p16INK4A) in uroepithelial cells. Lab Invest *91*, 825-836.

Tran, H., Brunet, A., Grenier, J.M., Datta, S.R., Fornace, A.J., Jr., DiStefano, P.S., Chiang, L.W., and Greenberg, M.E. (2002). DNA repair pathway stimulated by the forkhead transcription factor FOXO3a through the Gadd45 protein. Science *296*, 530-534.

Tucker, K.L. (2001). Methylated cytosine and the brain: a new base for neuroscience. Neuron *30*, 649-652.

Tzivion, G., Dobson, M., and Ramakrishnan, G. (2011). FoxO transcription factors; Regulation by AKT and 14-3-3 proteins. Biochim Biophys Acta *1813*, 1938-1945.

Ulett, G.C., Totsika, M., Schaale, K., Carey, A.J., Sweet, M.J., and Schembri, M.A. (2013). Uropathogenic Escherichia coli virulence and innate immune responses during urinary tract infection. Curr Opin Microbiol *16*, 100-107.

van der Heide, L.P., and Smidt, M.P. (2005). Regulation of FoxO activity by CBP/p300-mediated acetylation. Trends Biochem Sci *30*, 81-86.

van der Horst, A., and Burgering, B.M. (2007). Stressing the role of FoxO proteins in lifespan and disease. Nat Rev Mol Cell Biol *8*, 440-450.

van der Horst, A., de Vries-Smits, A.M., Brenkman, A.B., van Triest, M.H., van den Broek, N., Colland, F., Maurice, M.M., and Burgering, B.M. (2006). FOXO4 transcriptional activity is regulated by monoubiquitination and USP7/HAUSP. Nat Cell Biol *8*, 1064-1073.

van der Vos, K.E., and Coffer, P.J. (2008). FOXO-binding partners: it takes two to tango. Oncogene *27*, 2289-2299.

van der Vos, K.E., and Coffer, P.J. (2011). The extending network of FOXO transcriptional target genes. Antioxid Redox Signal *14*, 579-592.

Vanden Berghe, T., Linkermann, A., Jouan-Lanhouet, S., Walczak, H., and Vandenabeele, P. (2014). Regulated necrosis: the expanding network of non-apoptotic cell death pathways. Nat Rev Mol Cell Biol *15*, 135-147.

Verdin, E., and Ott, M. (2014). 50 years of protein acetylation: from gene regulation to epigenetics, metabolism and beyond. Nat Rev Mol Cell Biol *16*, 258-264.

Volkmann, N., Marassi, F.M., Newmeyer, D.D., and Hanein, D. (2014). The rheostat in the membrane: BCL-2 family proteins and apoptosis. Cell Death Differ *21*, 206-215.

Voll, R.E., Herrmann, M., Roth, E.A., Stach, C., Kalden, J.R., and Girkontaite, I. (1997). Immunosuppressive effects of apoptotic cells. Nature *390*, 350-351.

Wajant, H. (2002). The Fas signaling pathway: more than a paradigm. Science *296*, 1635-1636.

Wang, F., Chan, C.H., Chen, K., Guan, X., Lin, H.K., and Tong, Q. (2011). Deacetylation of FOXO3 by SIRT1 or SIRT2 leads to Skp2-mediated FOXO3 ubiquitination and degradation. Oncogene *31*, 1546-1557.

Wang, M.C., Bohmann, D., and Jasper, H. (2005). JNK extends life span and limits growth by antagonizing cellular and organism-wide responses to insulin signaling. Cell *121*, 115-125.

Wang, Q., Sztukowska, M., Ojo, A., Scott, D.A., Wang, H., and Lamont, R.J. (2015). FOXO responses to Porphyromonas gingivalis in epithelial cells. Cell Microbiol. doi: 10.1111/cmi.12459.

Weidner, W., Krause, W., and Ludwig, M. (1999). Relevance of male accessory gland infection for subsequent fertility with special focus on prostatitis. Hum Reprod Update *5*, 421-432.

Weidner, W., Pilatz, A., Diemer, T., Schuppe, H.C., Rusz, A., and Wagenlehner, F. (2013). Male urogenital infections: impact of infection and inflammation on ejaculate parameters. World J Urol *31*, 717-723.

Weigel, D., Jurgens, G., Kuttner, F., Seifert, E., and Jackle, H. (1989). The homeotic gene fork head encodes a nuclear protein and is expressed in the terminal regions of the Drosophila embryo. Cell *57*, 645-658.

Wellen, K.E., Hatzivassiliou, G., Sachdeva, U.M., Bui, T.V., Cross, J.R., and Thompson, C.B. (2009). ATP-citrate lyase links cellular metabolism to histone acetylation. Science *324*, 1076-1080.

Westphal, D., Kluck, R.M., and Dewson, G. (2014). Building blocks of the apoptotic pore: how Bax and Bak are activated and oligomerize during apoptosis. Cell Death Differ *21*, 196-205.

Wiles, T.J., Dhakal, B.K., Eto, D.S., and Mulvey, M.A. (2008). Inactivation of host Akt/protein kinase B signaling by bacterial pore-forming toxins. Mol Biol Cell *19*, 1427-1438.

Wiles, T.J., and Mulvey, M.A. (2013). The RTX pore-forming toxin alpha-hemolysin of uropathogenic Escherichia coli: progress and perspectives. Future Microbiol *8*, 73-84.

Xie, Q., Hao, Y., Tao, L., Peng, S., Rao, C., Chen, H., You, H., Dong, M.Q., and Yuan, Z. (2012). Lysine methylation of FOXO3 regulates oxidative stress-induced neuronal cell death. EMBO Rep *13*, 371-377.

Yamagata, K., Daitoku, H., Takahashi, Y., Namiki, K., Hisatake, K., Kako, K., Mukai, H., Kasuya, Y., and Fukamizu, A. (2008). Arginine methylation of FOXO transcription factors inhibits their phosphorylation by Akt. Mol Cell *32*, 221-231.

Yang, J.Y., Zong, C.S., Xia, W., Yamaguchi, H., Ding, Q., Xie, X., Lang, J.Y., Lai, C.C., Chang, C.J., Huang, W.C*., et al.* (2008). ERK promotes tumorigenesis by inhibiting FOXO3a via MDM2-mediated degradation. Nat Cell Biol *10*, 138-148.

You, H., Pellegrini, M., Tsuchihara, K., Yamamoto, K., Hacker, G., Erlacher, M., Villunger, A., and Mak, T.W. (2006). FOXO3a-dependent regulation of Puma in response to cytokine/growth factor withdrawal. J Exp Med *203*, 1657-1663.

Yu, J., Chen, Z., Ni, Y., and Li, Z. (2012). CFTR mutations in men with congenital bilateral absence of the vas deferens (CBAVD): a systemic review and meta-analysis. Hum Reprod (Oxford, England) *27*, 25-35.

Zentner, G.E., and Henikoff, S. (2013). Regulation of nucleosome dynamics by histone modifications. Nat Struct Mol Biol *20*, 259-266.

Zhang, X., Tang, N., Hadden, T.J., and Rishi, A.K. (2011). Akt, FoxO and regulation of apoptosis. Biochim Biophys Acta *1813*, 1978-1986.

Zhao, J., Jitkaew, S., Cai, Z., Choksi, S., Li, Q., Luo, J., and Liu, Z.G. (2012). Mixed lineage kinase domain-like is a key receptor interacting protein 3 downstream component of TNF-induced necrosis. Proc Natl Acad Sci U S A *109*, 5322-5327.

Zou, J., and Shankar, N. (2014). Enterococcus faecalis infection activates phosphatidylinositol 3-kinase signaling to block apoptotic cell death in macrophages. Infect Immun *82*, 5132-5142.

8 ACKNOWLEDGEMENTS

The experimental work of this dissertation was performed in the Department of Anatomy and Cell Biology at Justus-Liebig University Giessen, Germany, under the supervision of Prof. Dr. Andreas Meinhardt.

First and foremost, I would like to express my deepest gratitude to my mentor and supervisor Prof. Dr. Andreas Meinhardt for giving me the chance to work on this interesting and challenging project. In particular, I would like to thank my supervisor for his excellent guidance, enormous support, caring, patience, motivation and the independent research atmosphere, which is vital for me to grow as an independent researcher. I would like to thank Dr. Sudhanshu Bhushan, who provided me both scientific and technical guidance, patiently corrected my writing and financially supported my research.

I thank Dr Florian Eisel and Dr. Agnieszka Paradowska for their help with bisulfite sequencing and Chip assay experiments. I also thank Dr Vera Michel for proofreading my thesis and helping me to translate the summary part into German.

I would like to extend my sincere thanks to Prof. Dr. Trinad Chakraborty, Dr. Svetlin Tchatalbachev and Juri Schklarenko for providing bacteria for my experiments on time, without which I could not have accomplished this project so smoothly.

I also thank Dr. Jörg Klug for asking critical questions during lab meetings and Dr. Monika Fijak for teaching me immunofluorescence microscopy and flow cytometry. I would like to thank Ming Wang and Tao Lei, who as good friends, were always willing to help and give their best suggestions. It would have been a lonely lab

without them. I thoroughly appreciate the kind help from all my other colleagues: Dr Ferial Aslani, Dr Magdalena Walecki, Pawel Szczesniak, Farhad Khosravi, Nour Nicolas, Pradeep Kudipudi, Jan-Per Wenzel, Vera Stadler, Tim Sebastian and Elke Stoschek. I would like to acknowledge Eva Wewel for administrative help.

I also much appreciate the generous help from Vijith Vijayan, Jiangping Chen, and Shan Wang.

This is a great opportunity to express my deepest gratitude to my parents, who were always supporting me and encouraging me with their best wishes.

In the end, I owe my thanks to my motherland and the China Scholarship Council, which has provided me with the great opportunity and financial support to study in Germany.

Der Lebenslauf wurde aus der elektronischen Version der Arbeit entfernt.

The curriculum vitae was removed from the electronic version of the paper.

10 LIST OF OWN PUBLICATION

1. Publication originally from this thesis

- Sudhanshu Bhushan, Ferial Aslani, Zhengguo Zhang, Tim Sebastian, Hans-Peter Elsässer and Jörg Klug. Isolation of Sertoli Cells and Peritubular Cells from Rat Testes. Journal of Visualized Experiments, 2015. (Accepted)
- Zhengguo Zhang, Ming Wang, Florian Eisel, Svetlin Tchatalbachev, Trinad Chakraborty, Andreas Meinhardt and Sudhanshu Bhushan. Uropathogenic *Escherichia coli* epigenetically manipulate host cell death pathways. Journal of infectious Diseases. (**Under Review**).

2. Other publications

- Zhang Zheng-guo, Chen Bin, Yang Hao, et al. One case of misdiagnosed 46, XX male syndrome and literature review. Chinese Journal of Misdiagnostics, 2010,10(33) [Article in Chinese]
- Zhang Zhengguo, Chen Bin, Yang Hao, et al. One case report of prune-belly syndrome. Journal of Shanghai Jiaotong University (Medical Science), 2010, 30(11) [Article in Chinese]
- Chen Bin, Zhang Zheng-guo, Wang Hong-xiang, et al. The experience of standardized diagnosis and treatment of azoospermia (a report of 1027 cases). Journal of Peking University (Health Sciences), 2010, 42(4) [Article in Chinese]
- Zhang Zhengguo, Chen Bin. Genetic Causes of Male Infertility. Chinese Journal of Andrology, 2010, 24(10) [Article in Chinese]
- Zhang Zhengguo, Chen Bin. New concepts in Klinefelter syndrome. Chinese Journal of Birth Health & Heredity, 2010, 18(10) [Article in Chinese]

Conference Abstracts:

- 8th European Congress of Andrology (Oct. 2014), Barcelona, Spain. In experimental epididymo-orchitis uropathogenic E.coli determine damage by controlling host cell death pathways.[Poster Presentation]
- Syposium Urologische Forschung der Deutschen Gesellschaft für Urologie (Nov. 2013).Giessen, Germany. Uropathogenic E.coli activates FOXO transcription factors in isolated rat Sertoli cells. [Poster Presentation]
- 6th International Giessen Graduate Centre for the Life Sciences (GGL) Annual Conference (Sep. 2013), Giessen, Germany. Uropathogenic *E. coli* Inactivate Host Survival AKT Signalling Pathway in Sertoli Cells. [Oral Presentation]
- 7th European Congress of Andrology (Dec. 2012), Berlin, Germany. Uropathogenic E.coli inactivate host survival AKT signalling pathway in testicular cells.[Poster Presentation]
- 17th Chinese Urological Association (CUA) Annual Meeting (Oct, 2010), Xi An China. The clinical features of 50 cases CBAVD patients. [Oral Presentation]

11 EHRENWÖRTLICHE ERKLÄRUNG

Ich erkläre: Ich habe die vorgelegte Dissertation selbständig und ohne unerlaubte fremde Hilfe und nur mit den Hilfen angefertigt, die ich in der Dissertation angegeben habe. Alle Textstellen, die wörtlich oder sinngemäß aus veröffentlichten oder nicht veröffentlichten Schriften entnommen sind, und alle Angaben, die auf mündlichen Auskünften beruhen, sind als solche kenntlich gemacht. Bei den von mir durchgeführten und in der Dissertation erwähnten Untersuchungen habe ich die Grundsätze guter wissenschaftlicher Praxis, wie sie in der „Satzung der Justus-Liebig-Universität Giessen zur Sicherung guter wissenschaftlicher Praxis“ niedergelegt sind, eingehalten.

I declare that I have completed this dissertation single-handedly without the unauthorized help of a second party and only with the assistance acknowledged therein. I have appropriately acknowledged and referenced all text passages that are derived literally from or are based on the content of published or unpublished work of others, and all information that relates to verbal communications. I have abided by the principles of good scientific conduct laid down in the charter of the Justus Liebig University of Giessen in carrying out the investigations described in the dissertation.

Giessen, den

_____

Zhengguo Zhang